Aus der Medizinische Klinik und Poliklinik IV
(Direktor Prof. Dr. med. Martin Reincke)
Ludwig-Maximilians-Universität München
Sektion für Rheumatologie und Klinische Immunologie
Leiter: Prof. Dr. med. Hendrik Schulze-Koops

miRNA regulation of Treg function and phenotype in autoimmunity

Dissertation
zum Erwerb des Doktorgrades der Naturwissenschaften (Dr. rer. nat.)
an der Medizinischen Fakultät
der Ludwig-Maximilians-Universität München

vorgelegt von
Qihui Zhou
aus Yantai (China)

2014

Gedruckt mit Genehmigung der Medizinischen Fakultät der Ludwig-Maximilians-Universität München

Erstgutachter:	PD Dr. rer. nat. Alla Skapenko
Zweitgutachter:	Prof. Dr. rer. nat. Ludger Klein
Dekan:	Prof. Dr. med. Dr. h. c. M. Reiser, FACR, FRCR
Tag der mündlichen Prüfung:	22.07.2014

Diese Dissertation wurde im Rahmen des Promotionsstudienganges „ Oligonukleotide in Zellbiologie und Therapie“ des Graduiertenkolleg 1202 der DFG unterstützt.

Teile dieser Arbeit wurden in folgenden Orginalpublikationen veröffentlicht:

1. **Qihui Zhou**, Sonja Haupt, Iryna Prots, Katja Thümmler, Elisabeth Kremmer, Peter E. Lipsky, Hendrik Schulze-Koops, and Alla Skapenko

miR-142-3p is involved in CD25+ CD4 T cell proliferation by targeting the expression of glycoprotein A repetitions predominant.

J Immunol 2013 190:6579-6588; doi:10.4049/jimmunol.1202993

2. **Qihui Zhou***, Sonja Haupt*, Johannes T. Kreuzer, Ariane Hammitzsch, Fabian Proft, Carla Neumann, Jan Leipe, Matthias Witt, Hendrik Schulze-Koops, and Alla Skapenko

Decreased expression of miR-146a and miR-155 contributes to an abnormal Treg phenotype in patients with rheumatoid arthritis.

Ann Rheum Dis 2014 in press; doi:10.1136/annrheumdis-2013-204377

Eidesstattliche Versicherung

Zhou, Qihui

Name, Vorname

Ich erkläre hiermit an Eides statt,
dass ich die vorliegende Dissertation mit dem Thema

miRNA regulation of Treg function and phenotype in autoimmunity

selbständig verfasst, mich außer der angegebenen keiner weiteren Hilfsmittel bedient und alle Erkenntnisse, die aus dem Schrifttum ganz oder annähernd übernommen sind, als solche kenntlich gemacht und nach ihrer Herkunft unter Bezeichnung der Fundstelle einzeln nachgewiesen habe.

Ich erkläre des Weiteren, dass die hier vorgelegte Dissertation nicht in gleicher oder in ähnlicher Form bei einer anderen Stelle zur Erlangung eines akademischen Grades eingereicht wurde.

Ort, Datum

Unterschrift Doktorandin

Table of Contents

Abbreviations

Ab	Antibody
ACR	American College of Rheumatology
AMV	Avian myoblastosis virus
ANOVA	Analysis of variance
Anti-CCP	Anti-cyclic citrullinated protein
APC	Antigen presenting cell
ATP	Adenosine triphosphate
bp	Base pair
CD	Cluster of differentiation
cDNA	Complementary DNA
CRP	C-reactive protein
DAS28	Disease activity score 28
DDT	Dichlorodiphenyltrichloroethane
DMARD	Disease-modifying anti-rheumatic drug
DMSO	Dimethyl sulfoxide
DNA	Deoxyribonucleic acid
dNTP	Deoxyribonucleotide triphosphate
E.coli	*Escherichia coli*
EDTA	Ethylenediaminetetraacetic acid
ESR	Erythrocyte sedimentation rate
EULAR	European League Against Rheumatism
FACS	Fluorescence activated cell sorting
FCS	Fetal calf serum
FITC	Fluorescein isothiocyanate
FOXP3	Forkhead box P3
GARP	Glycoprotein A repetitions predominant
gDNA	Genomic DNA
HC	Healthy control
IL	Interleukin
IPTG	Isopropyl β-D-1-thiogalactopyranoside
iTreg	Induced regulatory T cells
LB	Lysogeny broth
MACS	Magnetic activated cell sorting

MHC	Major histocompatibility complex
mRNA	messenger RNA
MTX	Methotrexat
NHS	Normal human serum
NK cells	Natural killer cells
NSAID	Non-steroidal anti-inflammatory drug
nTreg	Natural regulatory T cells
OD	Optical density
PCR	Polymerase chain reaction
PBMC	Peripheral blood mononuclear cells
PBS	Phosphate buffered saline
PE	Phycoerythrin
PEG	Polyethylene glycol
PFA	Paraformaldehyde
RA	Rheumatoid arthritis
RF	Rheumafactor
RNA	Ribonucleic acid
RT	Reverse transcriptase
RT	Real time
SD	Standard deviation
SEM	Standard error of the mean
SNP	Single nucleotide polymorphism
S.O.C medium	Super Optimal Broth medium
TAE	TRIS-Acetate-EDTA
Taq polymerase	*Thermus aquaticus* polymerase
TCR	T cell receptor
TGF	Transforming growth factor
Th-cell	T helper-cell
TNF	Tumor necrosis factor
Treg cells	Regulatory T cells
X-Gal	5-bromo-4-chloro-indolyl-β-D-galactopyranoside

Summary

Regulatory T cells (Tregs) have been implicated in the maintenance of peripheral tolerance and controlling of autoimmune disease development. Rheumatoid arthritis (RA) is a chronic inflammatory autoimmune disease characterized by development of bone erosions and severe joint destructions. The importance of Tregs in RA has been proven in both patients and animal models. Glycoprotein A repetitions predominant (GARP) has been recently identified to be specifically expressed on human Tregs and is important for the suppressive capacity of Tregs. Recent studies have highlighted the important role of miRNA-mediated post-transcriptional regulation in many immunological processes including their involvement in regulating the function of human Tregs. During my PhD study I therefore investigated the involvement of miRNA-regulated GARP in Treg function and moreover miRNA regulation of Treg function in RA.

GARP possesses a 2 kb long 3'UTR. In the first part of my PhD study I could demonstrate that the distal part of GAPR 3'UTR was capable to down-modulate GARP protein expression via a microRNA recognition element (MRE) of miR-142-3p. The attenuation of GARP expression by miR-142-3p led to the diminution of Treg proliferation and their regulatory capacity, indicating the important role of miR-142-3p in Treg homeostasis and function. Thereafter the expression levels of miR-142-3p and GARP in Tregs of patients with RA were further analyzed. The up-regulation of miR-142-3p upon TCR stimulation was more prominent in RA Tregs than healthy individuals (HC). Accordingly reduced level of GARP expression upon TCR stimulation was observed in Tregs of RA as compared to HC Tregs. Genotyping analysis of GARP 3'UTR region revealed that two single nucleotide polymorphisms (SNPs), rs1320645 and rs1320646, presented differently in RA patients. Furthermore, two haplotypes of the 3'UTR of GARP also distributed variously in RA patients.

Two additional miRNAs, miR-146a and miR-155 have been implicated in RA pathogenesis. In the next part of my PhD study, I analyzed their expression in Tregs of RA and their influence on Treg phenotype. Both miRNAs, miR-146a and miR-155, demonstrated diminished expression in Tregs of RA patients. The Treg-specific diminution of miR-146a expression was observed in particular in patients with active disease and correlated with joint inflammation. Analysis of the expression of their putative targets that are involved in NF-κB

signaling pathway suggested impaired mRNA expression of IRAK1, TRAF6 and IKKε. NF-κB activity was however comparable between RA patients and healthy individuals. Yet, mRNA expression levels of other targets, STAT1 and SOCS1, which are the regulators of cytokine signaling, were elevated in patients with RA. The expression level of STAT1 mRNA correlated with the expression level of miR-146a but not of SOCS1 with miR-155. Interference with miR-146a altered the expression and phosphorylation of STAT1. In this regard, Tregs of active RA patients demonstrated pro-inflammatory phenotype characterized by increased IL-2, IFNγ, IL-17 and TNF expression although the suppressive capacity of these Tregs was not interfered. Moreover, diminished levels of miR-146a and miR-155 were observed in serum from patients with RA.

In summary, in my PhD study, I identified and characterized miR-142-3p regulation of GARP expression in Tregs. Delineation of miR-142-3p expression and the linked GARP expression in RA provides an important hint for the impaired Treg proliferation and function in RA. Analysis of SNPs and haplotypes of the 3'UTR of GARP bring an additional concept for decreased GARP expression in RA. Further analysis of the expression levels of miR-146a and miR-155, which interfere with cytokine signaling pathway, illuminated further fact of RA Treg. Thus in RA miRNAs control different specific aspects of Treg function by regulating the expression of their target genes and thereby might contribute critically to RA pathogenesis.

Zusammenfassung

Regulatorische T-Zellen (Tregs) sind mit der Aufrechterhaltung der peripheren Toleranz und der Kontrolle der Entstehung von Autoimmunerkrankung in Verbindung gebracht worden. Die rheumatoide Arthritis (RA) ist eine chronisch-entzündliche Autoimmunerkrankung, die durch die Entwicklung von Knochenerosionen und schweren Gelenkzerstörungen charakterisiert ist. Die Bedeutung von Tregs für die RA ist sowohl bei Patienten als auch in Tiermodellen nachgewiesen worden. *Glycoprotein A repetitions predominant* (GARP) wird spezifisch auf menschlichen Tregs exprimiert. Dessen Expression ist von kritischer Bedeutung für die regulatorische Kapazität von Tregs. Jüngste Studien haben die wichtige Rolle der miRNA-vermittelten posttranskriptionellen Regulation bei vielen immunologischen Vorgängen nachgewiesen, unter anderem ihre Beteiligung an der Funktion von Tregs. Im Rahmen meiner Doktorarbeit habe ich daher den Einfluss der durch miRNA-regulierten GARP-Expression auf die Treg-Funktion analysiert. Darüber hinaus habe ich die miRNA-Regulation der Treg-Funktion in der RA untersucht.

Ich habe zeigen können, dass der distale Teil der 2 kb langen 3'-UTR des GARP die GARP-Protein-Expression herunter reguliert. Dies geschah über ein miR-142-3p Erkennungselement (*microRNA recognition element*, MRE). Die Abschwächung der GARP-Expression durch miR-142-3p führte zur Verringerung der Proliferation und der regulatorischen Funktion von Tregs. Dies weist auf die wichtige Rolle der miR-142-3p in der Homöostase und Funktion von Tregs hin. Anschließend analysierten wir die Expression von miR-142-3p und GARP bei Patienten mit RA. Die Hochregulation von miR-142-3p nach TCR-Stimulation war in Tregs von RA-Patienten ausgeprägter als bei gesunden Personen (*healthy controls,* HC). Dementsprechend wurde eine verringerte Expression von GARP nach TCR-Stimulation in Tregs von RA-Patienten im Vergleich zu HC beobachtet. Die genetische Analyse der GARP-3'-UTR-Region offenbarte zwei Einzel-Nukleotid-Polymorphismen (*single nucleotide polymorphisms*, SNPs), rs1320645 und rs1320646, die in RA-Patienten signifikant häufiger vorkommen. Des weiteren wurden in RA-Patienten häufiger zwei verschiedene Haplotypen in der 3'-UTR von GARP gefunden.

Zwei weitere miRNAs, miR-146a und miR-155, sind in der Literatur im Zusammenhang mit der RA-Pathogenese beschrieben worden. In meiner Doktorarbeit analysierte ich daher ihre Expression in Tregs von RA-Patienten und ihren Einfluss auf Tregs. Beide miRNAs, miR-146a und miR-155, zeigten eine verminderte Expression in Tregs von RA-Patienten. Die

Treg-spezifische Abnahme der miR-146a-Expression wurde insbesondere bei Patienten mit aktiver Erkrankung beobachtet und korrelierte mit der Gelenkentzündung. Die Analyse der Expression ihrer putativen Ziele, die an der NF-κB-Signalkaskade beteiligt sind, ließ auf eingeschränkte mRNA-Expression von IRAK1, TRAF6 und IKKε schließen. NF-κB-Aktivität war jedoch vergleichbar bei Patienten und gesunden Personen. Dennoch war die mRNA Expression von zwei anderen putativen Ziele, STAT1 und SOCS1, welche Regulatoren der Zytokin-Signalwege sind, bei Patienten mit RA erhöht. Der Expressionslevel von STAT1 mRNA korrelierte mit dem Niveau der Expression von miR-146a. Der Expressionslevel korrelierte jedoch nicht mit dem der miR-155. Manipulation von miR-146a beeinflusste die Expression und Phosphorylierung von STAT1. In dieser Hinsicht wiesen die Tregs der aktiven RA-Patienten einen proinflammatorischen Phänotyp charakterisiert durch eine erhöhte IL-2-, IFNγ-, IL-17- und TNF-Produktion auf. Die suppressive Kapazität dieser Tregs war jedoch nicht beeinträchtigt. Darüber hinaus wurden reduzierte Mengen an miR-146a und miR-155 im Serum von Patienten mit RA beobachtet.

Zusammenfassend identifizierte und charakterisierte ich in meiner Doktorarbeit die posttranskriptionelle Regulierung der GARP-Expression in Tregs durch miR-142-3p. Ich habe zeigen können, dass miR142-3p entscheidend für hohe GARP-Expression auf Tregs und damit für die Treg-Funktion ist. Die Analyse der miR-142-3p-Expression und der damit verbunden GARP-Expression bei der RA lieferte darüber hinaus einen wichtigen Hinweis auf die Beeinträchtigung der Treg-Proliferation und -Funktion in der RA. SNPs- und Haplotypen-Verteilung in der 3'-UTR von GARP könnten eine weitere Ursache für die verringerte GARP-Expression bei der RA sein. Desweiteren habe ich gezeigt, dass die Expression von miR-146a und miR-155 in Patienten dereguliert ist. Dies beeinflusst direkt Zytokin-Signalwege. Tregs von RA-Patienten wiesen ein verändertes Zytokinproduktionsprofil auf. Es lässt sich aufgrund meiner Daten schlussfolgern, dass bei der RA miRNAs für die Treg-Funktion verantwortlich sind durch Regulierung ihrer Zielgene. Dadurch könnten miRNAs entscheidend zur Pathogenese der RA beitragen.

Introduction

I.1 CD4 T cells

I.1.1 General properties of immune systems

The immune system protects the human body against infections, such as viral, bacterial, fungal and parasitic. Two types of immune defense are involved in the process: innate and adaptive immune responses. The innate immune response, which is driven by granulocytes and macrophages, acts immediately after infection entry and is short-lasting and non-specific to the pathogens. The adaptive immune response, which is driven by lymphocytes, acts later during infection and is highly specific and powerful against pathogens (Murphy et al. 2012).

Lymphocytes can be further divided into two main subtypes: T lymphocytes (T cells), which mediate cellular and initiate humoral immunity; and B lymphocytes (B cells), which are essential for humoral immunity. Upon infection, naive lymphocytes recognize specific pathogen motifs (antigens) presented by antigen-presenting cells (APCs), get activated and start to proliferate and differentiate into antigen-specific effectors cells. By producing antibodies or by activating other cells within the immune system, effector lymphocytes therefore are able to drive the clearance of the infections. Some effector cells further differentiate into memory lymphocytes that persist long-term memory to expand quickly upon re-exposure to their specific antigens (Murphy et al. 2012).

I.1.2 CD4 T effector cell subsets

Upon infection, naive CD4 T lymphocytes, which have no previous contact with their specific antigen, get activated and start to proliferate and differentiate into antigen-specific effectors cells. The sufficient activation of naive T cells requires two signals: firstly, the binding of T cell receptors (TCRs) with antigens presented by the MHC II and, secondly, a co-stimulatory signal, comprising the binding of CD28 to the molecules on the APCs such as CD80, CD86 (Schwartz 1990, Schwartz 1992). The nature of the antigen, the strength of the MHC-antigen-TCR interaction and co-stimulation, as well as the surrounding cytokine milieu influence the activation of CD4 T cells and drive the expression of lineage specific signal transduction molecules and transcription factors. This results in the differentiation of naive CD4 T cells towards specific effector CD4 T cell subsets with the secretion of lineage specific cytokines (Smith et al. 1986).

I.1.2.1 Th1/Th2 effector cells

The first described and most-well-studied effector CD4 T cell subtypes are type 1 T helper (Th1) and type 2 T helper (Th2) cells, which were discovered by Coffman and Mosman in 1986 (Mosmann et al. 1986). Th1 cells develop preferentially under the influence of interleukin (IL)-12 and IL-18. IL-12 and IL-18 activate the signal transducer and activator of transcription 4 (STAT4) and induce the expression of the Th1 master transcription factor T-box transcription factor (T-bet). They are characterized by the production of Th1 signature cytokine interferon (IFN)-γ as well as other pro-inflammatory cytokines such as IL-2, lymphotoxin-α (LTA), and tumor necrosis factor (TNF) (Romagnani 2006). They are of great importance for defense against intracellular pathogens such as bacteria and protozoa (Delprete et al. 1991, Annunziato and Romagnani 2009).

Th2 cells are generated under the induction of IL-4. IL-4 signals through the activation of STAT6 and induce the expression of the Th2 master transcription factors GATA binding protein 3 (GATA-3) and c-Maf (Skapenko et al. 2001, Skapenko et al. 2004). Th2 cells are characterized by the production of Th2-signature cytokines IL-4 as well as IL-5 and IL-13 (Mosmann et al. 1986, Abbas et al. 1996, Annunziato and Romagnani 2009). Th2 cells are important for parasite clearance by functioning as a helper of B cells to drive the humoral immune response (Annunziato and Romagnani 2009).

I.1.2.2 Th17 effector cells

In the last decade, a distinct T helper cell subset characterized by the production of IL-17 was identified (Infante-Duarte et al. 2000, Harrington et al. 2005, Park et al. 2005). They are induced from naive CD4 T cells by pro-inflammatory cytokines IL-1β, IL-6 (Acosta-Rodriguez et al. 2007), IL-21 (Yang et al. 2008) and IL-23 (Volpe et al. 2008) and characterized by the expression of master transcription factor, retinoic acid receptor related orphan receptor C (RORC). Besides the production of the Th17-signature cytokines IL-17A and IL-17F, Th17 cells also secrete IL-22, IL-26 and chemokine ligand 20 (CCL20) (Wilson et al. 2007). They may involve in mediating host defense against certain bacteria and fungi (Korn et al. 2009).

I.1.2.3 Th22 and Th9 effector cell

Recently a new subtype of effector CD4 T cells that produce IL-22 has been identified as Th22 cells. Th22 cells produce IL-22 without the co-secretion of IL-17 and IFNγ (Duhen et

al. 2009, Trifari et al. 2009). The differentiation of Th22 cells occurs under the influence of IL-6 and TNF (Duhen et al. 2009) and is dependent on expression of the aryl hydrocarbon receptor (AHR). Many reports have suggested that Th22 cells are skin-homing T cells therefore it acts on the induction of keratinocyte hyperplasia and the induction of tissue repair and wound healing (Zenewicz et al. 2007).

Another newly identified effector CD4 T cells subtype is Th9 cells, characterized by their primary capacity to secrete IL-9 but lacking the production of other lineage specific cytokines (Locksley 2009). Th9 cell differentiation requires IL-4 and TGFβ (Dardalhon et al. 2008, Veldhoen et al. 2008). IL-4 and TGFβ induce the expression of the Th9 master transcription factor, PU.1 and interferon regulator factor 4 (IRF4) (Staudt et al. 2010, Ramming et al. 2012). Th9 cells promote cell proliferation and therefore contribute to tissue inflammation (Townsend et al. 2000, Nowak et al. 2009).

I.1.3 Regulatory T cells

I.1.3.1 General properties of regulatory T cells

To tightly control destructive immune response against pathogens and to sustain immunological self-tolerance and homeostasis, another subtype of CD4 T cells, the so called regulatory T cells (Tregs) exists. Depending on ontogeny and phenotype, two main subtypes of Tregs are well accepted: thymus derived naturally occurring regulatory T cells (nTregs) and regulatory T cells induced in the periphery (iTregs) (Ohkura et al. 2013).

Tregs, first described by Sakaguchi in 1995, composite 5-10% of peripheral CD4 T cells. They constitutively express the Treg master transcription factor, forkhead box P3 (Foxp3), and are highly positive for the IL-2 receptor α-chain (CD25) (Fontenot et al. 2005). Tregs are anergic and important for maintaining of self-tolerance. Adaptive transfer of $CD25^{+}$-depleted CD4 T cells into immune-deficient mice results in the development of severe autoimmune disease (Sakaguchi et al. 1995, Vignali et al. 2008). Mice lacking Foxp3, the so-called "scurfy mice", are characterized by a lymphoproliferative disease resulting in early death within three to four weeks of age (Brunkow et al. 2001). Induced depletion of Tregs by diphtheria toxin in depletion of regulatory T cell (DEREG) mice model reveals similar "scurfy-like" symptom. This further confirms the importance of Tregs in the controlling of effector T cell proliferation and homeostasis (Lahl et al. 2007).

Whereas nTregs represent a homogeneous population, there is a high diversity within total

Treg population. Thus Tregs are now accepted as a heterogenic cell population, comprising several subtypes (Schmidt et al. 2012). For example, Sakaguchi's group has performed a detailed characterization of human Foxp3^{+} Tregs and suggested a composition of naive CD45RA^{+}Foxp3^{low} resting Tregs, memory CD45RA^{-}Foxp3^{high} activated Tregs, and CD45RA^{-}Foxp3^{low} cytokine-secreting Tregs. The first two groups maintain Treg phenotype and function, whereas the latter is non-suppressive (Miyara et al. 2009). In mice, several Tregs subtypes carrying distinct transcriptional signatures have been identified as well (Feuerer et al. 2009, Feuerer et al. 2010). These diverse Treg subtypes might recruit different suppression mechanism, depending on location and type of immune response. For instance, Tregs can suppress the proliferation of effector T cells through a contact depend mechanism or through the IL-2 deprivation (Thornton and Shevach 1998, Pandiyan et al. 2007). They can produce inhibitory cytokines, for example IL-10, TGF-β and IL-35 (Asseman et al. 1999, Li et al. 2006, Collison et al. 2007). They can also induce cytolysis of effector cells by presenting granzyme and perforin. Furthermore, Tregs can suppress effector T cells by targeting on dendritic cells (Grossman et al. 2004).

I.1.3.2 GARP as a specific marker of regulatory T cells

Despite the expression of Foxp3 and high level of CD25, Tregs are also characterized by other cell surface receptors, including glucocorticoid-induced tumor necrosis factor receptor (GITR), cytotoxic T lymphocyte-associated antigen 4 (CTLA-4), latency associated peptide (LAP) and lymphocyte-activation gene 3 (LAG-3) (Annunziato et al. 2002, Shimizu et al. 2002). Besides, down-regulated expression of IL-7 α chain CD127 has also been described to be characteristic for nTregs (Seddiki et al. 2006). However, most of these markers are problematic to be Treg specific markers in human. For instance, upon the immune activation, non-regulatory effector T cells up-regulate CD25 and express Foxp3 transiently. CD127 is down-regulated in effector T cells in response to activation. Therefore, identifying unique and specific cell surface markers expressed on Tregs are of great interest.

Recently, a surface receptor, Glycoprotein A repetitions predominant precursor (GARP; or leucine rich repeat containing protein 32, LRRC32), has been identified as a molecule specially expressed on Tregs. Human *GARP* or *LRRC32* gene (ID: 2615) locates in the chromosomal region 11q13-11q14. It consists of three exons although only the last two exons are protein coding (Ollendorff et al. 1994). The protein coding sequence of *GARP* gene is highly conserved cross species. It shares over 80% identity between human and mouse (Ollendorff et al. 1992). The mature 80kD GARP protein consists of 662 amino acids,

containing 20 leucine-rich repeats in the extracellular region, followed by a hydrophobic transmembrane domain and a 15-residue C-terminal cytoplasmic domain (Ollendorff et al. 1994). The N-terminal of GARP contains a 17-residue signal peptide, which guides the native GARP to its surface location (Chan et al. 2011).

The expression of GARP on Tregs was firstly reported by analysis of microarray to identify genes specifically expressed in human $CD25^+$ CD4 T cells after TCR stimulation (Wang et al. 2008, Probst-Kepper et al. 2009). GARP expression is detected on activated Tregs as well as on expanded Treg clones (Wang et al. 2008, Stockis et al. 2009). GARP can be induced by IL-2 and IL-4, but not by TGF-β and retinoic acid *in vitro* (Edwards et al. 2013, Haupt et al. under preparation). Using of specific small interfering RNA (siRNA) to knock down GARP expression in Tregs results in impaired Treg suppressive function (Tran et al. 2009, Probst-Kepper et al. 2010). Interestingly, TGF-β-induced iTreg lacks the expression of GARP (Tran et al. 2007). These findings have implied that GARP is a specific marker of activated Treg cells and is important for Treg suppressive function.

GARP has been characterized as a potential receptor of latent TGF-β (Stockis et al. 2009, Chan et al. 2011). TGF-β is a pleiotropic cytokine that are essential for preventing autoimmunity (Wan and Flavell 2008). It is firstly secreted as pro-TGF-β precursor homodimers. The pro-TGF-β is then cleaved by a pro-protein convertase Furin to generate latent-TGF-β which consists of two noncovalently associated domains: C-terminal domain ~110-residue mature TGF-β and N-terminal domain ~250-residue latency-associated peptide (LAP) (Dubois et al. 1995, Pesu et al. 2008). LAP prevents the binding of mature TGF-β to its receptor, therefore the release of mature TGF-β from latent TGF-β complex is of great importance for Tregs (Stockis et al. 2009). Wang and colleagues have shown that GARP captures and presents latent TGF-β on the cell surface. The integrin $\alpha_v\beta_6$ and $\alpha_v\beta_8$ on the surface of the target cells then release mature TGF-β from GARP-latent TGF-β complex (Wang et al. 2012). Furthermore, conditional knockout of GARP in CD4 T cells leads to failure of expressing latent TGF-β on Tregs (Edwards et al. 2013). These observations suggest the function of GARP as a receptor and activator for latent TGF-β on Tregs.

I.2 Rheumatoid arthritis

I.2.1 General characteristics of rheumatoid arthritis

An immune response can be a double-edged sword. Besides its protective function by fighting against pathogens, the immune system can become harmful to the body if being insufficiently

controlled. Good examples for that are allergic reactions, host tissues damage and autoimmune processes. Allergies are caused by hypersensitivity in response to environmental antigens. Host tissue damage may occur as a result of uncontrolled response against pathogens (Murphy et al. 2012). In addition, it is of great importance for the immune system to distinguish between host- (self or auto) and foreign- (non-self) antigens. Usually, the so-called autoreactive T cells (T cells that recognized self-antigens) are eliminated during maturation of T cells in thymus. However, some of them can escape from the selection step and enter into the periphery. These cells may react to APCs which present self-antigens. Thus a process termed as autoimmunity is initiated (Romagnani 2006). Uncontrolled autoimmunity may lead to autoimmune diseases. The occurrence of the diseases may be restricted to either local organs (e.g. in autoimmune thyroiditis) (Dayan and Daniels 1996) or involve a systemic range (e.g. systemic lupus erythematosus [SLE] and Rheumatoid arthritis [RA]) (Majithia and Geraci 2007, Rahman and Isenberg 2008).

RA is a chronic inflammatory autoimmune disease which affects approximately 0.5-1% of adult population in the industrialized countries, with two to three times more women than men (Firestein 2003). The average age where disease commonly occurs is about 30 to 50 years old (Crowston et al. 1997, Smolen et al. 2007, Choy 2012). RA is a systemic disease characterized by the involvement of tender and swollen joints, the development of bone erosions and severe joint destructions (Aletaha et al. 2010). The usage of 2010 American College of Rheumatology (ACR) and the European League Against Rheumatism (EULAR) classification criteria is accepted as a standard mean for early RA diagnosis. The criteria can be applied to patients who have at least one swollen joint and the synovitis can not be better explained by another disorder like SLE, psoriatic arthritis (PsA), and gout, etc. A score system is included in the criteria covering four categories: joint involvement (0-5 points), serology (0-3 points), acute-phase reactants (0-1 point) and duration of symptoms (0-1 point). Patients with total points ≥ 6 are termed as with definite RA. Any tender or swollen joints are included in order to identify joint involvement. The serological markers refer to rheumatoid factor (RF) and antibodies to cyclic citrullinated proteins. The acute-phase reactants refer to the level of C-reactive protein (CRP) and erythrocyte sedimentation rate (ESR) (Aletaha et al. 2010).

Once patients are defined, the progression of disease can be evaluated based on the disease activity score for 28 joints (DAS28). The counts of both tender joints (TJC28) and swollen joints (SJC28) are recorded and markers for acute-phase reactants (ESR or CRP) are

measured (Prevoo et al. 1995). Besides, a subjective assessment (SA) of disease activity is made by patients based on a visual analogue scale between 0 and 100, where 0 stands for no activity and 100 stands for highest activity. The final value of DAS28 is calculated from all of the four parameters and covers between 0 and 10 points. Patients therefore can be stratified according to DAS28 score into four groups: patients who have DAS28 higher than 5.1 are termed as patients with high disease activity; patients who have DAS28 in between 3.2 and 5.1 are termed as patients with moderate disease activity; patients who have DAS28 in between 2.6 and 3.2 are termed as patients with low disease activity; patients who have DAS28 below 2.6 are termed as patients in remission (Aletaha et al. 2010).

I.2.2 RA etiology

RA is regarded as an autoimmune disease, due to the existence of autoantibodies such as RF and anti-CCP antibodies (Firestein 2003, Choy 2012). However, the cause of the disease is not yet fully understood. In general, the disease is triggered by self-antigens of unknown origin presented by professional APCs (Burkhardt et al. 2001, Smolen et al. 2007). Autoreactive CD4 T cells recognize the self-antigen presenting cells via MHC II, which results in the activation and expansion of antigen-specific effector T cells. As a consequence, activated effector T cells secrete pro-inflammatory cytokines such as IFNγ, IL-17 and TNFα (Ehrenstein et al. 2004). The cytokines produced by T cells lead to the activation of B cells to promote the production of autoantibodies and the activation of macrophages to promote the production of pro-inflammatory cytokines such as TNF, IL-1, and IL-6 (Debets et al. 1988, Rodriguez-Pinto 2005). These pro-inflammatory cytokines in turn stimulate the differentiation of fibroblast and osteoclast, which play an important role in the destruction of cartilage and bone tissue in the affected joints (McInnes and Schett 2007). In addition, the functional activity of Treg cells is severely impaired in RA. This may lead to a break down of Treg-mediated tolerance. Thereafter, the expansion of effector T cells is uncontrolled and the initial autoimmune response develops into persistent inflammation (Ehrenstein et al. 2004).

Environmental factor such as smoking may also contribute to RA pathogenesis (Choy 2012). In addition, about 60% occurrence of the disease is associated with heritability (MacGregor et al. 2000). Genotyping studies to investigate single nucleotide polymorphisms (SNPs) provide powerful tools to study the possible genetic factors that may associate with RA. Several genetic factors have therefore been identified. For instance, the alleles of *human leukocyte antigen* (HLA) gene which locates at chromosome 6 (6p21.3) and encodes human MHC II molecules contribute to three times higher susceptibility of RA. They encode a conserved

amino acid motif in peptide binding domain to allow the presentation of self-antigens. Thereby APCs that express MHC II encoded by these RA-associated alleles can activate autoreactive effector CD4 T cells to initiate autoimmunity (Patil et al. 2001). Besides, *protein tyrosine phosphatase non-receptor type 22* (*PTPN22)* gene which locates at chromosome 1 (1p13 region) is reported to inhibit TCR signaling and T cell activation (Vang et al. 2005). A missense nonsynonymous SNP which introduces a R620W substitution (arginine substitution for tryptophan [W] at amino acid position 620) interferes the protein function and is verified as a RA-associated allele by different research groups (Plenge et al. 2005, Orozco et al. 2006, Lee et al. 2007). Furthermore, two SNPs, which are located within the functionally important IL-4- and STAT6-binding regions of the IL-4 receptor gene (*IL-4R*), are identified to associate with RA susceptibility and severity. In particular, the I50V SNP (amino acid substitutions of isoleucine [I] to valine [V] at position 50) is identified as a novel genetic marker for early severe RA as a result of its high association with aggressive bone erosions (Prots et al. 2006, Leipe et al. 2014).

I.2.3 Central role of CD4 T cells in RA

Although the mechanisms behind the pathogenesis of RA is not fully understood, the important role CD4 T cells played in the process has been highlighted (Choy 2012). Many evidences suggest that impaired frequencies and functions of T cell subsets including effector T cells and Tregs contribute to uncontrolled inflammation and disease development (Cope et al. 2007). Elevated frequency of Th1 cells and reduced frequency of Th2 cells in RA are correlated with disease activity (van der Graaff et al. 1999). Increased levels of IL-2 and IFNγ, but not of IL-4 are secreted by activated CD4 T cells in RA peripheral blood and inflamed synovial tissues (Schulze-Koops and Kalden 2001). Moreover, the differentiation capacity of uncommitted CD4 T cells towards Th2 cells is badly impaired (Skapenko et al. 1999). These findings suggest that Th1 cells are more associated with autoimmune diseases while Th2 cells in this respect have a more protective effect. Recent studies have brought a new sight for understanding the pathogenesis of RA by focusing on IL-17 producing Th17 cells. IL-17 induces the production of IL- 6, which leads to the activation of monocytes and macrophages resulting in osteoclastogenesis and cartilage destruction (Chabaud et al. 2001, Kotake and Kamatani 2002, Yago et al. 2007). The serum level of IL-17, as well as the frequencies of Th17 cells are elevated in patients with early RA and highly correlated with disease activity (Leipe et al. 2010). IL-17-defficient mice show their resistance to collagen-induced arthritis (CIA) (Nakae et al. 2003). Moreover, the blockage of IL-6, a Th17 inducing

cytokine neutralizes the development of CIA in mice (Fujimoto et al. 2008). In addition to IL-17, IL-22, which is secreted by Th17 cells and Th22 cells, is also involved in the disease development of RA. Elevated serum levels of IL-22 are observed in patients with early RA and are highly correlated with the development of bone erosions (Cascao et al. 2010, Leipe et al. 2011, Leipe et al. 2014).

Despite of the altered frequencies and functions of effector T cells in RA, the abnormality of Tregs also contributes to the pathogenesis of RA. Tregs have been implicated in the maintenance of peripheral tolerance and control of the disease development. Several studies have indicated that the frequency of Tregs in the peripheral blood is decreased from patients with RA and is negatively correlated with disease activity score 28 (DAS28), C-reactive protein (CRP), and erythrocyte sedimentation rate (ESR) (Kawashiri et al. 2011, Matsuki et al.). On the other hands, other studies have shown a similar, even higher frequency of Tregs in patients with RA compared to healthy individuals (HC) (Bayry et al. 2007, Han et al. 2008). Regardless of this debate, the importance of Tregs in RA has been proven in both patients and animal models (Frey et al. 2010, Pesce et al. 2013). Valencia and colleagues have observed reduced suppressive capacity of Tregs isolated from patients with RA (Valencia et al. 2006). This can be negatively affected by elevated expression of multiple pro-inflammatory cytokines (Valencia et al. 2006, van Amelsfort et al. 2007), or deficient regulation of CTLA-4 (Flores-Borja et al. 2008). Studies with K/BxN mice, which spontaneously develop inflammatory arthritis induced by a $CD4^+$ T-cell response to a GPI peptide, suggest the eventual function of Treg cells is to affect disease pathogenesis and severity, but not to prevent disease occurrence (Nguyen et al. 2007, van Amelsfort et al. 2007). These findings are further confirmed by the amelioration of disease in collagen-induced arthritis model after the transfer of exogenous $CD25^+$ CD4 T cells into pre-arthritic mice (Kelchtermans et al. 2009).

Taken together, functional analysis of various CD4 T cells subsets in RA patients and animal models reveal an impaired regulation of the immune response at various levels: on the one hand, an uncontrolled effector T cells expansion and pro-inflammatory cytokine production, on the other hand a simultaneous failure in the expansion and the function of Tregs.

I.3 microRNA

I.3.1 General properties of miRNA

Recent studies have highlighted the important role of microRNA (miRNA)-mediated post-transcriptional regulation in many immunological processes. miRNAs are endogenous small (~23 nucleotide), evolutionally conserved non-coding RNAs. Human cells express around 500 to 1000 miRNAs, targeting more than half of the genes (Bentwich et al. 2005, Lewis et al. 2005, Friedman et al. 2009). The majority of miRNA genes are considered to be independent transcription units (Lee et al. 2002), based on the fact that they locate either intergenically or in a reverse direction to the neighboring genes (Lagos-Quintana et al. 2001, Mourelatos et al. 2002). Some of the miRNA genes locate in the introns of protein or non-protein coding genes, thereby can be transcribed together with the host gene (Rodriguez et al. 2004).

The biosynthesis of mature miRNAs involves four steps: transcription, nuclear processing, nuclear export and cytoplasmic processing (Figure 1) (Winter et al. 2009). miRNA genes are transcribed generally by RNA polymerase II into large primary transcripts (pri-miRNA) using a mechanism similar to protein-coding genes (Lee et al. 2004). The pri-miRNA is then cleaved by the RNase III endonuclease Drosha and DiGeorge Syndrome Critical Region 8 (DGR8) in the nucleus into a ~70-nt precursor miRNA (pre-miRNA) (Gregory et al. 2006). Afterwards, the pre-miRNA is recognized by Exportin-5 and transported into the cytoplasm (Murchison and Hannon 2004), where it is cleaved by another RNase III endonuclease, Dicer, resulting in a ~21-nt miRNA duplex (Lund and Dahlberg 2006).

In the cytoplasm, one strand of the miRNA duplex (leading strand) is loaded into an Argonaute- (Ago-) containing ribonucleoprotein (RNP) complex referred to as RNA-induced silencing complex (RISC), whereas another strand (passenger strand) is normally degraded (Rana 2007). Once incorporated into RISC, the miRNA guides the complex to its mRNA targets, binds the 3' untranslated region (3'UTR) of the target and represses translation (Huntzinger and Izaurralde 2011). The specificity for the binding of the miRNAs to their targets is determined by the miRNA seed region, which is 6-8 nucleotides in length and located in the 5' end of the miRNA (Lewis et al. 2003). When perfect or near perfect complementarity happens between the seed region and the target mRNA, this results in target mRNA cleavage and degradation. Otherwise the inhibition of translation occurs without mRNA degradation (Williams 2008, Eulalio et al. 2009). The Ago protein family plays an

important role in the function of the RISC complex. In human, four Ago proteins exist and miRNAs can be incorporated indiscriminately of their sequence into Ago1- through Ago4-containing RISC. However, only Ago2-associated RISC is exclusively associated with the mRNA degradation (Pratt and MacRae 2009). Instead of functioning as an on-off switch miRNAs modulate the expression of their target gene by impacting the gene expression from 1.2- to 4- fold (O'Neill et al. 2011, O'Connell et al. 2012).

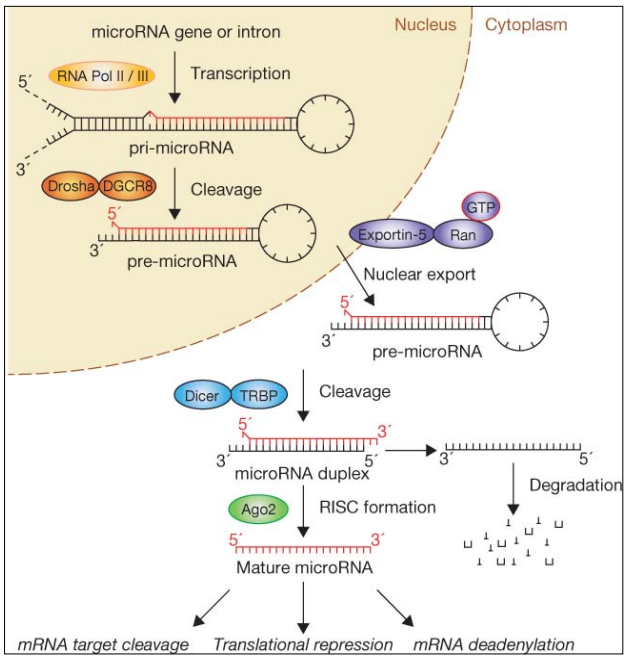

Figure 1. Schematic overview of miRNA biogenesis
The canonical biosynthesis of mature miRNAs involves four steps: transcription of pri-miRNA by RNA polymerase II, nuclear processing of pre-miRNA by Drosha, nuclear export by Exportin-5 and cytoplasmic processing by Dicer (adapted from Winter et. al, 2009)

Recent studies have shown the existence of miRNAs in the circulating system outside of the cells. The first evidence demonstrated the presence of miRNAs in exosomes (Valadi et al. 2007). Since then circulating miRNAs are confirmed in vesicles, such as apoptotic bodies (Zernecke et al. 2009), high-/low-density lipoprotein (HDL/LDL) complexes (Vickers et al. 2011), RNA-binding proteins (Arroyo et al. 2011), as well as in serum and other body fluids (Chim et al. 2008, Lawrie et al. 2008). The circulating miRNAs are important for cell-cell communications and can be used as a biomarker for disease prognosis and diagnosis (Lawrie et al. 2008).

I.3.2 miRNA as a regulator of immune response

During last few decades it becomes apparent that immune cells express miRNAs during immune response and as a consequence these miRNAs impact immune response at the cellular and organismal levels. Evidence exists in both innate immune response and adaptive

immune response. Many miRNAs are involved in controlling innate immune response, for instance miR-155, miR-146a, miR-21, miR-125b and let-7. Activation of TLR signaling pathway by various pathogens initiates innate immune response and the production of several miRNAs, such as miR-155, miR-146a and miR-21 (Kawai and Akira 2010). In turn, these miRNAs function as positive or negative regulator of the TLR signaling: miR-155 functions as a pro-inflammatory miRNA and accelerates the immune response by targeting on Src homology-2 domain-containing inositol 5-phosphatase 1 (SHIP1) and suppressor of cytokine signaling 1 (SOCS1) (Androulidaki et al. 2009, O'Connell et al. 2009). miR-146a involves in a negative feedback loop to regulate the innate immune response. It inhibits the expression of its target TNF receptor associated factor 6 (TRAF6) and interleukin-1 receptor-associated kinase 1 (IRAK1), therefore dampens the downstream nuclear factor kappa-light-chain-enhancer of activated B cells (NF-κB) activation and attenuates the expression of pro-inflammatory cytokines such as IL-6 and TNFα (Boldin et al. 2011, Zhao et al. 2011). miR-21 also serves as negative regulator of NF-κB pathway by inhibiting the expression of programmed cell death protein 4 (PDCD4) (Sheedy et al. 2010). In addition, miR-125b and let-7 restrict the expression of TNF and IL-6, respectively, resulting in repression of the production of pro-inflammatory cytokines (Tili et al. 2007, Iliopoulos et al. 2009).

In the context of adaptive immune response, miR-17 to miR-92 clusters are important for T cell lineage development by inhibiting the expression of BCL2-like 11 (BIM) and phosphatase and tensin homolog (PTEN) (Iliopoulos et al. 2009). Moreover, miR-155 and miR-182 play an important role in the clonal expansion of activated effector CD4 T cells by repressing B-cell integration cluster (BIC) and forkhead box protein O1 (Foxo1) (Rodriguez et al. 2007, Stittrich et al. 2010). miR-155 deficient mice are not capable to produce Th1 and Th17 cells in autoimmune inflammation (Kurowska-Stolarska et al. 2011, Oertli et al. 2011). miR-326 functions as a supporter in Th17 cells differentiation by targeting v-ets avian erythroblastosis virus E26 oncogene homolog 1 (Ets1) in experimental autoimmune encephalomyelitis (EAE) (Du et al. 2009). In addition to regulating the development and function of effector T cells, miRNAs are also important for the function of Tregs. Ablations of two key miRNA processing enzymes, Dicer or Drosha in Tregs result in severe even fatal autoimmunity in mice (Chong et al. 2008, Liston et al. 2008). miR-142-3p interferes Treg suppressive capacity by controlling cAMP expression (Huang et al. 2009). miR-146a is demonstrated to maintain Treg cell suppression capacity as well as prevent deflection of activated Treg cells into Th1-like cells in animal model (Lu et al. 2010).

I.3.3 miRNA and human disease

Taken into account for their important roles in regulating immune response, a number of reports have demonstrated several specific miRNAs that affect many types of autoimmune diseases both in human as well as in mouse models. Mice deficient in miR-155 expression are resistant to EAE, colitis and CIA due to their failure in producing Th1 and Th17 cells (O'Connell et al. 2010, Kurowska-Stolarska et al. 2011, Oertli et al. 2011). miR-326 provokes the development of EAE (Du et al. 2009). miR-146a deficient mice show high susceptibility in the course of CIA (Nakasa et al. 2011). In human, abnormal expression of miR-146a, miR-155 and miR-21 are associated with the development of SLE (Dai et al. 2010, Garchow et al. 2011, Luo et al. 2011). In RA, high expression level of miR-146a, miR-155 has been demonstrated in synovial tissue and synovial fibroblasts (Nakasa et al. 2008, Stanczyk et al. 2008). Peripheral monocytes and CD4 T cells from RA revealed altered expression of miR-146a (Pauley et al. 2008, Li et al. 2010).

In addition to intracellular miRNAs, many studies raised their pivotal role of miRNAs in different body fluid in disease pathogenesis (Hasuwa et al. 2013, Wang et al. 2013). Increased levels of miR-146a and miR-155 have been found in the intrarenal and urine samples from patients with IgA nephropathy (Wang et al. 2011). A recent analysis of circulating miRNA profiles in plasma from patients with SLE demonstrated increased levels of miR-142-3p and miR-181a, and decreased levels of miR-106a, miR-17, miR-20a, miR-203, and miR-92a (Carlsen et al. 2013).

Aims of the thesis

RA is a chronic inflammatory autoimmune disease characterized by development of bone erosions and severe joint destructions. Tregs are involved in maintaining of peripheral tolerance and control of the disease development. The importance of Tregs in RA has been demostrated in both patients and animal models. Recently, a surface molecule, GARP, has been identified to be specifically expressed on Tregs and is important for the suppressive capacity of Tregs. On the other hand, miRNA-mediated post-transcriptional regulation has also been reported to control many immunological processes including the involvement of regulating Treg function. Therefore, the detailed aims of my PhD thesis were:

1. to analyze whether and which miRNAs are involved in the regulation of GARP expression;
2. to dissect the functional outcome of miRNA-regulated GARP expression in Tregs;
3. to correlate the miRNA-regulated GARP expression with clinical characteristics of RA;
4. for comparison to analyze expression of other RA-associated miRNAs in Tregs.

Materials and Methods

II.1 Materials

II.1.1 Reagents

Reagents	Origin
Acetic Acid (CH_3COOH)	Merck, Darmstadt, Germany
Acetone(C_3H_6O)	Merck
Acrylamid/bis-acrylamid 30 % (37.5:1)	Merck
Agarose	Merck
Albumin fraction V from bovine serum (BSA)	Merck
Ammonium chloride (NH_4Cl)	Sigma-Aldrich, St. Louis, USA
Ammonium persulfate (APS)	Sigma-Aldrich
Ampicillin, sodium salt	Life Technologies, Carlsbad, USA
L-Arginine-HCl	Thermo Scientific, Lafayette, USA
L-Arginine-HCl, $^{13}C_6$,$^{15}N_4$	Thermo Scientific
β-Mercaptoethanol	Sigma-Aldrich
Biotin	Sigma-Aldrich
Bromophenol blue	Merck
BupH modified Dulbecco's PBS	Thermo Scientific
Carboxyfluorescein succinimidyl ester (CFSE)	Life Technologies
Chloroform ($CHCl_3$)	Merck
Complete protease inhibitor cocktail	Roche, Penzberg, Germany
Dimethylformamide (DMF)	Sigma-Aldrich
Dimethylsulfoxid (DMSO)	Merck
Dithiothreitol (DTT)	Sigma-Aldrich
Dulbecco's modified eagle medium (DMEM)	Life Technologies
dNTP set, 100 mM	Life Technologies
Dynabeads human T-activator CD3/CD28	Life Technologies
Dynabeads MyOne streptavidin C1	Life Technologies
ECL western blotting detection reagent	GE Healthcare, Munich, Germany
Ethanol (C_2H_5OH)	Merck
Ethylendinitrotetraaceticacid (EDTA)	Sigma-Aldrich

Ficoll	Biotest, Dreieich, Germany
GelCode blue stain reagent	Thermo Scientific
Geneticin (G418)	Life Technologies
L-Glutamine ($C_5H_{10}N_2O_3$)	Life Technologies
Glycerol ($C_3H_5(OH)_3$)	Merck
Glycine (NH_2CH_2COOH)	Merck
GlycoBlue	Life Technologies
Heparin-sodium salt	Ratiopharm, Ulm, Germany
Hydrochloric acid 37% (HCl)	Merck
IPTG (isopropylthio-β-galactoside)	Life Technologies
Isopropanol (C_3H_7OH)	Merck
LB agar powder (Lennox L Agar)	Life Technologies
LB Broth (1x)	Life Technologies
Lipofectamine 2000 transfection reagent	Life Technologies
L-Lysine-2HCl	Thermo Scientific
L-Lysine-2HCl, $^{13}C_6$, $^{15}N_2$	Thermo Scientific
Magnesium chloride ($MgCl_2$)	Merck
Methanol (CH_3OH)	Sigma-Aldrich
M-PER mammalian protein extraction reagent	Thermo Scientific
NP-40	Millipore, Billerica, USA
Nonfat dry milk powder	Real
NuPAGE 4-12% bis-tris gel	Life Technologies
Oligo-dT_{12-18}	GE Healthcare
Paraformaldehyde (PFA)	Merck
Penicillin G/Streptomycin	Life Technologies
Phosphatase inhibitor cocktail 3	Sigma-Aldrich
Phosphate buffered saline (PBS)	Life Technologies
Potassium chloride (KCl)	Merck
Potassium bicarbonate ($KHCO_3$)	Merck
Protein G sepharose 4 fast flow beads	GE Healthcare
Protran nitrocellulose membranes	Whatman, Dassel, Germany
rmp Protein A sepharose fast flow beads	GE Healthcare
RPMI 1640	Life Technologies

RPMI media for SILAC	Thermo Scientific
Recombinant human IL-2	Chiron, Emerville, USA
Saponin	Sigma
Sheep erythrocytes	Fiebig-Naehrstofftechnik, Idstein, Germany
Sodium azide (NaN_3)	Merck
Sodium chloride (NaCl)	Merck
Sodium dodecyl sulfate (SDS)	Merck
Sodium hydroxide (NaOH)	Merck
SYBR safe DNA gel stain (10,000x)	Life Technologies
TaqMan universal PCR master mix 2x	Life Technologies
Tetramethylethylenediamin (TEMED)	Merck
Tris (hydroxymethyl)-aminomethane ($C_4H_{11}NO_3$)	Merck
Tween 20	Sigma-Aldrich
X-Gal (5-Bromo-4-Chloro-3-Indolyl β-D-Galactopyranoside)	Life Technologies

II.1.2 Antibodies and biotinylated peptides

II.1.2.1 Antibodies for FACS analysis

Specificity	Conjugate	Clone	Provider
Anti-human CD3	FITC	UCHT1	Sigma-Aldrich
Anti-human CD3/anti-human CD4 dual Tag	FITC/PE	UCHT-1/ Q4120	Sigma-Aldrich
Anti-human CD4	FITC	Q4120	Sigma-Aldrich
Anti-human CD25	PE	M-A251	BD Pharmingen, San Jose, USA
Anti-human GARP hybridoma supernatant	Non	7H2	Helmholtz Center, Munich, Germany
Anti-human Stat1 (N-Terminus)	PE	1/Stat1	BD Phosflow, San Jose, USA
Anti-human Stat1 (pS727)	Alexa Fluor 647	K51-856	BD Phosflow
Anti-mouse CD3	PE	17A2	BD Pharmingen
Anti-mouse CD4	FITC	GK 1.5	BD Pharmingen
Anti-mouse CD25	PE	PC 6.15	BD Pharmingen
Anti-rat IgG(H+L)	PE	Polyclonal	Dianova, Hamburg, Germany

Rat IgG	Non	Polyclonal	Sigma-Aldrich
Anti-mouse IgG2b, κ	Alexa Fluor 647	MPC-11	BD Pharmingen
Anti-mouse IgG1	PE		BD Pharmingen

II.1.2.2 Antibodies for Immunoprecipitation

Specificity	Clone	Provider
Anti-Ago1 hybridoma supernatant	4B8	Dr. G. Meister, Regensburg, Germany
Anti-Ago2 hybridoma supernatant	11A9	Dr. G. Meister
Anti-GARP	Plato-1	Enzo Life Sciences, Lausen, Switzerland
Anti-Radixin	EP1862Y	Abcam, Cambridge, UK
Mouse IgG 2b, κ	IgG 2b, κ	BioLegend, San Diego, USA
Rabbit IgG	Polyclonal	Cell signaling, Danvers, USA
Rat IgG	Polyclonal	Sigma-Aldrich

II.1.2.3 Antibodies for Immunoblotting

Specificity	Clone	Provider
Anti-GARP	Plato-1	Enzo Life Sciences
Anti-goat IgG-HRP	Polyclonal	Santa Cruz
Anti-mouse IgG-HRP	Polyclonal	Cell signaling
Anti-Radixin	Polyclonal	Santa Cruz

II.1.2.4 Biotinylated Peptides

Name	Sequence	Provider
WT peptide	Desthiobiotin-SGSAILLTTLAACCCVRRQKFNQQYKA-OH	Max-Planck Institute, Munich, Germany
Scr peptide	Desthiobiotin-SGRACQCTAQRIKLQSFLACNVTAYKL-OH	Max-Planck Institute

II.1.3 Ladders/Markers

Name	Provider
Biotinylated protein ladder	Cell signaling
GeneRuler DNA ladder (100 bp)	Fermentas, Sankt Leon-Rot, Germany
GeneRuler DNA ladder (1 kb)	Fermentas
Prestained protein marker (7-175 kDa)	New England Biolabs, Ipswich, USA

II.1.4 Serum

Name	Provider
Dialyzed fetal bovine serum(FBS)	Thermo Scientific
Fetal calf serum (FCS)	Life Technologies
Mouse serum	Sigma-Aldrich
Normal human serum (NHS)	From our lab, Munich, Germany
Rat serum	Sigma-Aldrich

II.1.5 Enzymes

II.1.5.1 Restriction Endonucleases

RE Name	Recognition site	Supplied Reaction Buffer	Origin
BamHI	G´GATCC	10x NEBuffer 3+100x BSA	New England Biolabs
EcoRI	G´AATTC	Buffer EcoRI+	Fermentas
EcoRV	GAT´ATC	10x NEBuffer 3+100x BSA	New England Biolabs
HindIII	A´AGCTT	Buffer R+	Fermentas
HpaI	GTT´AAC	10x NEBuffer 4	New England Biolabs
KpnI	GGTAC´C	10x NEBuffer 1+100x BSA	New England Biolabs
NheI	G´CTAGC	10x NEBuffer 2+100x BSA	New England Biolabs
NotI	GC´GGCCGC	10x NEBuffer 3+100x BSA	New England Biolabs
PmeI	CTTT´AAAC	10x NEBuffer 4+100x BSA	New England Biolabs
SacI	GAGCT´C	10x NEBuffer 1+100x BSA	New England Biolabs
SacII	CCGC´GG	10x NEBuffer 4	New England Biolabs
SalI	G´TCGAC	10x NEBuffer 3+100x BSA	New England Biolabs
SpeI	A´CTAGT	10x NEBuffer 4	New England Biolabs
XbaI	T´CTAGA	10x NEBuffer 4+100x BSA	New England Biolabs
XhoI	C´TCGAG	10x NEBuffer 4+100x BSA	New England Biolabs

II.1.5.2 Other Enzymes

Enzymes	Supplied Reaction Buffer	Origin
AmpliTaq DNA polymerase	10x PCR Buffer II	Life Technologies
AMV reverse transcriptase	5x AMV RT Buffer	Promega, Mannheim, Germany

Protease K	1x Protease K reaction buffer	New England Biolabs
GeneAmp High Fidelity PCR Enzyme Mix	10x GeneAmp High Fidelity PCR Buffer	Life Technologies
Quick T4 DNA Ligase	2x Quick Ligation Reaction Buffer	New England Biolabs

II.1.6 MicroRNA mimics and antagomirs

All reagents were purchased from Thermo Scientific.

miRIDIAN microRNA mimics

miRNA mimics	Assay ID	Mature miRNA Sequence
miRNA negative control (cel-miR-67)	CN-00100	UCACAACCUCCUAGAAAGAGUAGA
hsa-miR-142-3p	C-300610	UGUAGUGUUUCCUACUUUAUGGA
hsa-miR-181a	C-300552	AACAUUCAACGCUGUCGGUGAGU
hsa-miR-181b	C-300554	AACAUUCAUUGCUGUCGGUGGGU
hsa-miR-181c	C-300556	AACAUUCAACCUGUCGGUGAGU
hsa-miR-381	C-300690	UAUACAAGGGCAAGCUCUCUGU
hsa-miR-424	C-300717	CAGCAGCAAUUCAUGUUUUGAA
hsa-miR-497	C-300765	CAGCAGCACACUGUGGUUUGU
hsa-miR-551a	C-300868	GCGACCCACUCUUGGUUUCCA
hsa-miR-661	C-300981	UGCCUGGGUCUCUGGCCUGCGCGU
hsa-miR-662	C-300982	UCCCACGUUGUGGCCCAGCAG

miRIDIAN microRNA hairpin inhibitors

Inhibitor	Assay ID	Targeted miRNA Sequence
Inhibitor negative control	IN-001005	UCACAACCUCCUAGAAAGAGUAGA
Inhibitor hsa-miR-142-3p	IH-300610	UGUAGUGUUUCCUACUUUAUGGA
Inhibitor hsa-miR-424	IH-300717	CAGCAGCAAUUCAUGUUUUGAA

II.1.7 TaqMan Assays

All assays were purchased from Life Technologies.

II.1.7.1 TaqMan Gene Expression Assays

TaqMan gene expression endogenous controls

Gene	Assay ID	Interrogated Sequence

β-actin	4326315E	NM_001101.2
Cyclophilin A	4310883E	NM_021130.3

TaqMan Gene Expression Assays

Gene	Assay ID	Interrogated Sequence
FoxP3	Hs01085835_m1	NM_001114377.1, NM_014009.3
GARP	Hs00194136_m1	NM_001128922.1, NM_005512.2
IFNγ	Hs00989291_m1	NM_000619.2
IKKε	Hs01063858_m1	NM_001193321.1, NM_001193322.1, NM_014002.3
IL-2	Hs00174114_m1	NM_000586.3
IL-10	Hs00961622_m1	NM_000572.2
IL-17	Hs00174383_m1	NM_002190.2
IRAK1	Hs01018347_m1	NM_001025242.1, NM_001025243.1, NM_001569.3
SOCS1	Hs00705164_s1	NM_003745.1
STAT1	Hs01013996_m1	NM_007315.3, NM_139266.2
TNF	Hs01113624_g1	NM_000594.2
TRAF6	Hs00371512_g1	NM_004620.3, NM_145803.2

II.1.7.2 TaqMan MicroRNA Assays

TaqMan control miRNA assays

Control	Assay ID	NCBI Accession#	Mature miRNA Sequence
RNU6B	001093	NR_002752	CGCAAGGATGACACGCAAATTCGTGAAG CGTTCCATATTTTT
RNU48	001006	NR_002745	ATGACCCCAGGTAACTCTGAGTGTGTCGC TGATGCCATCCCGCAGCGCTCTGACC

TaqMan MicroRNA Assays

miRNA	Assay ID	miRBase ID	Mature miRNA Sequence
cel-miR-67	000224	cel-miR-67-3p	UCACAACCUCCUAGAAAGAGUAGA
hsa-miR-142-3p	000464	hsa-miR-142-3p	UGUAGUGUUUCCUACUUUAUGGA
hsa-miR-146a	000468	hsa-miR-146a-5p	UGAGAACUGAAUUCCAUGGGUU
hsa-miR-155	002623	hsa-miR-155-5p	UUAAUGCUAAUCGUGAUAGGGGU
hsa-miR-223	002295	hsa-miR-223-3p	UGUCAGUUUGUCAAAUACCCCA
hsa-miR-424	000604	hsa-miR-424-5p	CAGCAGCAAUUCAUGUUUUGAA

II.1.7.3 SNP Genotyping Assays

SNP ID	Location	Type	Polymorphism
rs1320644	Chr.11: 76370187	3'UTR	A/G, Transition Substitution
rs1320645	Chr.11: 76370088	3'UTR	A/C, Transversion Substitution
rs1320646	Chr.11: 76370047	3'UTR	C/T, Transition Substitution
rs3781699	Chr.11: 76369785	3'UTR	G/T, Transversion Substitution
rs3781700	Chr.11: 76369709	3'UTR	A/C, Transversion Substitution
rs1803627	Chr.11: 76369344	3'UTR	A/C, Transversion Substitution
rs3197153	Chr.11: 76369072	3'UTR	C/T, Transition Substitution
rs7685	Chr.11: 76368639	3'UTR	A/C, Transversion Substitution

II.1.8 Primer list

All primers were synthesized from Eurofins MWG, Ebersberg, Germany.

II.1.8.1 Primers for gene amplification

Primer sets for cloning GARP 3'UTR[*]

Name	Sequence
GARP 3'UTR	For 5′-CTCGAGAGAAGCCGGGAGAC-3′ Rev 5′-CCGCGGACATTCAGGTAGG-3′
GARP 3'UTR-Up	For 5′-TCTAGAGGGGGACTGAAGAACATCAACC-3′ Rev 5′-CAAACTCCAGGCTCTGCTCAATAG-3′
GARP 3'UTR-Down	For 5′-GGGAATGCTGGGAAATGAGATAC-3′ Rev 5′-TGTGAAGAG TGGGAGGACGAAG-3′
GARP 3'UTR-distal	For 5′-GTTTAAACGATGGGAAACTGAGGCTTAGG-3′ Rev 5′-TCTAGAACATTCAGGTAGG -3′
GARP 3'UTR-Frag1	For 5′- GAGAGTTTAAACAGAAGCCGGGAGAC -3′ Rev 5′- CATTCCCAGTGCCCAGA -3′
GARP 3'UTR-Frag2	For 5′- GAGAGTTTAAACGGGAATGCTGGGAAATGAGATAC -3′ Rev 5′- CTTAACCAGACCCTGCTGG -3′
GARP 3'UTR-Frag3	For 5′- GAGAGTTTAAACCAGCAGGGTCTGG -3′ Rev 5′- GAGAGTCGACGAATCTCACCTATGGC -3′
GARP 3'UTR-Frag4	For 5′- GAGAGTTTAAACAGCACCGTCCCTG -3′ Rev 5′- GAGAGTCGACAGACACAAGGCTTGG -3′
GARP 3'UTR-Frag5	For 5′-GAGAGTTTAAACAAGCCTTGTGTCTGC-3′ Rev 5′-GAGAGTCGACGAATCTCACCTATGGC-3′
GARP 3'UTR-Frag6	For 5′-GAGAGTTTAAACTGCCATAGGTGAGATTC-3′ Rev 5′-GAGAGTCGACCCACAAGTTTCATTCTC-3′

GARP 3'UTR-Frag7	For	5′-GAGAGTTTAAACCTGAGGCTTAGGAAGAG-3′
	Rev	5′-GAGAGTCGACGGCCAAGCACAGGTAAG-3′
GARP 3'UTR-Frag8	For	5′-GAGAGTTTAAACACCTGTGCTTGGC-3′
	Rev	5′-GAGAGTCGACTGGGCCTTGGTGTTC-3′
GARP 3'UTR-Frag9	For	5′-GAGAGTTTAAACGAACACCAAGGCCC-3′
	Rev	5′-GAGAGTCGACGAGGAGTGTTACGTGC-3′
GARP 3'UTR-Frag10	For	5'-GAGAGTTTAAACCTACTGCACGTAAC-3′
	Rev	5'-GAGAGTCGACACATTCAGGTAGG-3′

Primer sets for cloning Radixin[§]

Name	Sequence	
Radixin-Frag1	For	5'-CACCATGCCGAAACCAATCAACG-3'
	Rev	5'-CCGCTTATTGATTCTCAGACGAGG-3'
Radixin-Frag2	For	5'-ATGATAGACTCCTACCCCAGCGTG-3'
	Rev	5'-TTTCCAAGTCTTCCTGGGCTG-3'
Radixin-Frag3	For	5'-TGCCGACCAGATGAAGAATCAG-3'
	Rev	5'-CATTTGCTTTATGCTGCTTTGGCAAGAGC-3'
Radixin	For	5'-GAGA*G*GATCCATGCCGAAACCAATCAACG-3'
	Rev	5'-GAGACTCGAGCATTTGCTTTATGCTGCTTTGGCAAGAGC-3'

*Underlined sequences indicate the inserted restriction sites.

[§]Underlined sequences indicate the restriction site of BamHI (forward primer) and XhoI (reverse primer).

II.1.8.2 Primers for sequencing

Name	Sequence	
GARP 3'UTR-5pri	For	5'-GGGAATGCTGGGAAATGAGATAC-3'
	Rev	5'-ACAAATCCTCCTGGGCTTGG -3'
GARP 3'UTR-mid	For	5'-TCATCCTTCTGTCTCCAGGGC-3'
	Rev	5'-CAAACTCCAGGCTCTGCTCAATAG-3'
GARP 3'UTR-3pri	For	5'-GATGGGGAAACTGAGGCTTAGG-3'
	Rev	5'-GTAAAATGGGGTGGAGAGAGTGG-3'
M13	For	5'-TGTAAAACGACGGCCAGT-3'
	Rev	5'-CAGGAAACA GCT ATG ACC-3'
pmirGlo	For	5'-ACACGGTAAAACCATGAC-3'
	Rev	5'-GTCCAAACTCATCAATGTA-3'

II.1.8.3 Primers for the site-directed mutagenesis*

Name	Sequence	
GARP 3'UTR-MRE-142-3p mutated	For	5'-ggtccccacgcctgatctttgaaaacaGGacagggctgctgtcac-3'
	Rev	5'-gtgacagcagccctgtCCtgttttcaaagatcaggcgtggggacc-3'
GARP 3'UTR-MRE-424 mutated	For	5'-ttgaaaacactacacagggcAAgtcacttcccagggcccagg-3'
	Rev	5'-cctgggccctgggaagtgacTTgccctgtgtagtgttttcaa-3'

GARP 3'UTR-MRE-142-3p/424 mutated	For	5'-cctgatctttgaaaacaGGacagggcAAgtcacttcccagggccc-3'
	Rev	5'-gggccctgggaagtgacTTgccctgtCCtgttttcaaagatcagg-3'

*Capital letters indicate the mutated nucleotides.

II.1.8.4 Oligonucleotides for cloning MREs*§

Name		Sequence
MRE-142-3p-Canon	For	5'-AAACTAGCGGCCGCTAGTTCCATAAAGTAGGAAACACTACAG-3'
	Rev	5'-CTAGCTGTAGTGTTTCCTACTTTATGGAACTAGCGGCCGCTAGTTT-3'
MRE-142-3p-GARP	For	5'-AAACTAGCGGCCGCTAGTCCCACGCCTGATCTTTGAAAACACTACAG-3'
	Rev	5'-CTAGCTGTAGTGTTTTCAAAGATCAGGCGTGGGACTAGCGGCCGCTAGTTT-3'
MRE-142-3p-mut	For	5'-AAACTAGCGGCCGCTAGTCCCACGCCTGATCTTTGAAAACggCAG-3'
	Rev	5'-CTAGCTGccGTTTTCAAAGATCAGGCGTGGGACTAGCGGCCGCTAGTTT-3'
MRE-181a-Canon	For	5'-AAACTAGCGGCCGCTAGTACTCACCGACAGCGTTGAATGTTG-3'
	Rev	5'-CTAGCAACATTCAACGCTGTCGGTGAGTACTAGCGGCCGCTAGTTT-3'
MRE-181b-Canon	For	5'-AAACTAGCGGCCGCTAGTACCCACCGACAGCAATGAATGTTG-3'
	Rev	5'-CTAGCAACATTCATTGCTGTCGGTGGGTACTAGCGGCCGCTAGTTT-3'
MRE-181c-Canon	For	5'-AAACTAGCGGCCGCTAGTACTCACCGACAGGTTGAATGTTG-3'
	Rev	5'-CTAGCAACATTCAACCTGTCGGTGAGTACTAGCGGCCGCTAGTTT-3'
MRE-181a/b/c-GARP	For	5'-AAACTAGCGGCCGCTAGTAACTCTTTGTATAACCTACCTGAATGTAG-3'
	Rev	5'-CTAGCTACATTCAGGTAGGTTATACAAAGAGTTACTAGCGGCCGCTAGTTT-3'
MRE-381-Canon	For	5'-AAACTAGCGGCCGCTAGTACAGAGAGCTTGCCCTTGTATAG-3'
	Rev	5'-CTAGCTATACAAGGGCAAGCTCTCTGTACTAGCGGCCGCTAGTTT-3'
MRE-381-GARP	For	5'-AAACTAGCGGCCGCTAGTCCAGGCCTCGGGACCAACTCTTTGTATAAG-3'
	Rev	5'-CTAGCTTATACAAAGAGTTGGTCCCGAGGCCTGGACTAGCGGCCGCTAGTTT-3'
MRE-424-Canon	For	5'-AAACTAGCGGCCGCTAGTTTCAAAACATGAATTGCTGCTGG-3'
	Rev	5'-CTAGCCAGCAGCAATTCATGTTTTGAAACTAGCGGCCGCTAGTTT-3'
MRE-424-GARP	For	5'-AAACTAGCGGCCGCTAGTTTTGAAAACACTACACAGGGCTGCTGG-3'
	Rev	5'-CTAGCCAGCAGCCCTGTGTAGTGTTTTCAAAACTAGCGGCCGCTAGTTT-3'
MRE-424-mut	For	5'-AAACTAGCGGCCGCTAGTTTTGAAAACACTACACAGGGCaaGG-3'
	Rev	5'-CTAGCCttGCCCTGTGTAGTGTTTTCAAAACTAGCGGCCGCTAGTTT-3'
MRE-497-Canon	For	5'-AAACTAGCGGCCGCTAGTACAAACCACAGTGTGCTGCTGG-3'
	Rev	5'-CTAGCCAGCAGCACACTGTGGTTTGTACTAGCGGCCGCTAGTTT-3'
MRE-497-GARP	For	5'-AAACTAGCGGCCGCTAGTTTTGAAAACACTACACAGGGCTGCTGG-3'
	Rev	5'-CTAGCCAGCAGCCCTGTGTAGTGTTTTCAAAACTAGCGGCCGCTAGTTT-3'
MRE-551a-Canon	For	5'-AAACTAGCGGCCGCTAGTTGGAAACCAAGAGTGGGTCG-3'
	Rev	5'-CTAGCGACCCACTCTTGGTTTCCAACTAGCGGCCGCTAGTTT-3'
MRE-551a-GARP	For	5'-AAACTAGCGGCCGCTAGTTGGAGGCCAAGGTGTGGGTCG-3'
	Rev	5'-CTAGCGACCCACACCTTGGCCTCCAACTAGCGGCCGCTAGTTT-3'
MRE-661-Canon	For	5'-AAACTAGCGGCCGCTAGTACGCGCAGGCCAGAGACCCAGGCAG-3'
	Rev	5'-CTAGCTGCCTGGGTCTCTGGCCTGCGCGTACTAGCGGCCGCTAGTTT-3'
MRE-661-GARP(3)	For	5'-AAACTAGCGGCCGCTAGTGGCTGCTGTCACTTCCCAGGGCCCAGGCCG-3'
	Rev	5'CTAGCGGCCTGGGCCCTGGGAAGTGACAGCAGCCACTAGCGGCCGCTAGTTT-3'

MRE-661-GARP(4)	For	5'-AAACTAGCGGCCGCTAGTGGCCCAGGCCTCAGCCCAGGCCG-3'
	Rev	5'-CTAGCGGCCTGGGCTGAGGCCTGGGCCACTAGCGGCCGCTAGTTT-3'

*Underlined sequences indicate the restriction site of NotI.
§Lower case indicates the mutated nucleotides.

II.1.8.5 Other Oligonucleotides*§

Name		Sequence
Stop Codon-linker	For	5'-TCGAG**TGA**C**TAA**A**TAG**TTTAAACA-3'
	Rev	5'-AGCTTGTTTAAACTATTTAGTCAC-3'

*Underlined sequences indicate the restriction site of PmeI.
§Bold font indicates the stop codons.

II.1.9 Vector list

Vector name	Inserted sequence
pCR2.1-GARP-3'UTR-Up	21676140-21673856 bp of NT_167190.1
pCR2.1-GARP-3'UTR-Down	21676571-21675120 bp of NT_167190.1
pCR2.1-GARP-3'UTR-Up&Down	21676140-21675120 bp of NT_167190.1
pCR2.1-GARP-3'UTR	GARP-3'UTR, +2128-+4182 bp of NM_001128922.1
pcDNA3.1-GARPcds	GARP cds, +139-+2127 bp of NM_001128922.1
pcDNA3.1-GARPcds-3'UTR	GARP cds, +139-+2127 bp of NM_001128922.1 and GARP-3'UTR, +2128-+4182bp of NM_001128922.1
pcDNA3.1-Radixin	Radixin cds, +311-+2125 bp of NM_001260492
pEGFP-C1*	Stop codon-linker
pEGFP-C1*-fr(1-10)	Overlapping fragments of GARP-3'UTR
pmirGlo-GARP-3'UTR-distal	Distal part of GARP-3'UTR, +3818-+4182 bp of NM_001128922.1
pmirGlo- MRE-Canon	Canonical sequence of MRE
pmirGlo- MRE-GARP	MRE sequence in the GARP-3'UTR
pmirGlo-MRE-mut	Mutated MRE sequence in the GARP-3'UTR

II.1.10 Kits

Kit name *(application)*	Origin
AffinityScript QPCR cDNA Synthesis Kit	Agilent Technologies, Santa Clara, USA
Amaxa Cell Line Nucleofector Kit V	Lonza, Cologne, Germany

Amaxa human T cell Nucleofector Kit	Lonza
Amaxa Mouse T Cell Nucleofector Kit	Lonza
Bio-Rad Protein Assay Kit	Bio-Rad, Munich, Germany
CD25 Microbeads II, human	Miltenyi Biotech, Bergisch Galdbach, Germany
CD25 MicroBead Kit, mouse	Miltenyi Biotech
Dual-Glo Luciferase Assay System	Promega
$CD4^+$ T cell isolation kit II, human	Miltenyi Biotech
$CD4^+$ T cell Isolation Kit II, mouse	Miltenyi Biotech
Human IL-17 Quantikine ELISA Kit	R&D system, Minneapolis, USA
Human IFNγ Quantikine ELISA Kit	R&D system
Human TNF Quantikine ELISA Kit	R&D system
miRNeasy Serum/Plasma Kit	Qiagen, Hilden, Germany
QIAamp DNA Blood Mini Kit	Qiagen
QIAGEN Plasmid Maxi Kit	Qiagen
QIAprep Spin Miniprep Kit	Qiagen
QIAquick Gel Extraction Kit	Qiagen
QIAquick PCR Purification Kit	Qiagen
QuikChange Lightning Site-Directed Mutagenesis Kit	Agilent Technologies
RNeasy Plus Mini Kit	Qiagen
TaqMan MicroRNA Reverse Transcription Kit	Life Technologies
TOPO TA Cloning Kit	Life Technologies

II.1.11 Buffers

Buffers and Solutions	Composition
Blotting buffer	12.5 mM Tris-HCl 86 mM Glycine 0.05 % SDS 20 % Methanol
FACS PBS	PBS 2 % FCS 0.01 % NaN_3
MACS Buffer	PBS 0.5 % BSA 2 mM EDTA
10x NH_4Cl solution	41.45 g NH_4Cl 5 g $KHCO_3$ 1 mM EDTA, H_2O ad 0.5 l

NP-40 cell lysis/wash buffer	50 mM Tris-HCl (pH8.0) 1 % NP40 2 mM EDTA 25 mM NaCl
10x Oligo annealing buffer	100 mM Tris-HCl (pH 7.5) 1 M NaCI 10 mM EDTA
1x Protease K reaction buffer	25 mM EDTA 300 mM NaCl 200 mM Tris-HCl (pH7.5) 2 % SDS
RNP-IP lysis buffer	0.5% NP-40 150 mM KCl 25 mM Tris-HCl (pH7.5) 2 mM EDTA 0.5 mM DTT (freshly added)
RNP-IP wash buffer	0.05 % NP-40 300 mM NaCl 50 mM Tris-HCl (pH7.5) 5 mM $MgCl_2$
Resolving gel (8%)	0.35 M Tris-HCl (pH8.8) 8% Acrylamid/bis-acrylamid 100 µl 10% SDS 100 µl 10% APS 10 µl TEMED, H_2O ad 10 ml
Stacking gel	126.7 mM Tris-HCl (pH6.8) 4% Acrylamid/bis-acrylamid 50 µl 10% SDS 50 µl 10% APS 5 µl TEMED, H_2O ad 5 ml
SDS running buffer	25 mM Tris-HCl 192 mM Glycine 0.1 % SDS
2x SDS sample buffer	4 % SDS 125 mM Tris-HCl 20 % Glycerol 100 mM DTT 0.02 % Bromophenol Blue
50x TAE buffer	242 g Tris-HCl 57.2 ml acetic acid 50 mM EDTA (pH8.0), H_2O ad 1 l
TBST	20 mM Tris-HCl (pH7.6) 140 mM NaCl 0.1 % Tween-20

II.2 Methods

II.2.1 Molecular Biological Methods

II.2.1.1 Genomic DNA isolation

Genomic DNA (gDNA) from whole blood was extracted using QIAamp DNA Blood Mini Kit (Qiagen) according to manufacturer's instructions. Each pulse-vortexing step was followed by snap centrifugation to collect all liquid drops from the inside of the lid. Briefly, 200 µl of whole blood sample were added to a 1.5ml Eppendorf tube containing 20 µl of QIAGEN Protease (supplied) and mixed with 200 µl of Buffer AL by pulse-vortexing for 15 sec. The mixtures were incubated at 56°C for 10 min and mixed with 200 µl of ethanol (96%-100%) by pulse-vortexing for 15 sec, then applied to QIAamp Mini spin columns and centrifuged at 8000 rpm for 1 min. Columns were washed first with 500 µl of Buffer AW1 at 8000 rpm for 1 min, then with 500 µl of Buffer AW2 at 13,000 rpm for 3 min. After the last wash, columns were placed to fresh collecting tubes and centrifuged for additional 1 min at 13,000 rpm. After transferring the columns to fresh Eppendorf tubes, 200 µl of distilled water/column were added and centrifuged at 13,000 rpm for 1 min to elute DNA. The quality and quantity of DNA were controlled by analyzing the absorbance at 260 nm/280 nm (A_{260}/A_{280}) using an Eppendorf BioPhotometer (Eppendorf, Hamburg, Germany). Genomic DNA was then stored at 4°C for immediate usage or -20°C for longer storage.

II.2.1.2 RNA isolation

II.2.1.2.a Total RNA isolation from cells

Total RNA was extracted using RNeasy Plus Mini Kit (Qiagen) following the manufacturer's instructions. After washing with PBS, 1 to 5 Mio cells were collected and lysed in 350 µl of RLT buffer containing 1 % β-mercaptoethanol. Cell lysates were then applied first to QIAShredder columns by centrifuging under 13,000 rpm for 2 min. The gDNA Eliminator Spin Columns were used afterwards by centrifuging under 10,000 rpm for 30 sec. Eluent was mixed with 350 µl of 70 % Ethanol and applied to Rneasy Minikit Spin Columns. After a short spin down for 15 sec at 10,000 rpm, columns were washed first with 700 µl of RW1 Buffer followed by two times 500 µl of RPE Buffer. After the last wash, columns were transferred to fresh collecting tubes and centrifuged for additional 2 min at 13,000 rpm. After transferring the columns to fresh Eppendorf tubes, 33 µl of RNease-free water/column were added and centrifuged at 13,000 rpm for 1 min to elute RNA. The quality and quantity of total RNA were controlled by analyzing the absorbance at 260 nm/280 nm (A_{260}/A_{280}) using an

Eppendorf BioPhotometer. RNA was then stored at 4°C for immediate usage or -20°C for longer storage.

II.2.1.2.b Serum RNA isolation

Serum RNA was extracted using miRNeasy Serum/Plasma Kit (Qiagen) based on the manufacturer's instructions. Unless stated otherwise, centrifugation was performed at room temperature. 200 µl of serum were mixed with 1 ml of QIAzol lysis Reagent and incubated at room temperature for 5 min. 5 µl of 1 nM *C.elegans* miR-67 mimic (CN-001000, Thermo Scientific) were added after incubation as spike-in control. 200 µl of chloroform were carefully added to the mixture, vortexed vigorously for 15 sec, incubated for 2 to 3 min at room temperature and followed by centrifuging for 15 min at 12,000 rpm at 4°C. The upper aqueous phase (around 600 µl) was transferred to a new tube and mixed thoroughly with 900 µl of 100 % ethanol. The mixtures were then applied to RNeasy MinElute spin. After short spin down for 15 sec at 10,000 rpm, columns were washed first with 700 µl of RWT Buffer and then 500 of µl RPE Buffer. Afterwards, columns were washed with 500 µl of 80 % ethanol for 2 min at 10,000 rpm then transferred to fresh collecting tube and centrifuged for additional 5 min at 13,000 rpm in order to dry the membrane. After transferring the columns to fresh Eppendorf tubes, 33 µl of RNase-free water/column were added to elute RNA by centrifuging for 1 min at 13,000 rpm and stored at -20°C until usage.

II.2.1.3 Reverse Transcription

II.2.1.3.a cDNA Synthesis

500 ng to 1 µg of total RNA were reversely transcribed into cDNA in a 20-µl volume at 42°C for 1 h by 0.25 U/µl AMV reverse transcriptase (Promega) supplemented with 1x AMV Reverse Transcription Reaction Buffer in addition to 1 mM dNTPs, 20 ng/µl Oligo-$dT_{12\text{-}18}$. cDNA was then stored at 4°C for immediate usage or -20°C for longer storage.

When low RNA yield appeared, AffinityScript QPCR cDNA Synthesis Kit (Agilent Technologies) was used based on the manufacturer's instruction. Briefly, 100 to 250 ng RNA were reversely transcribed in a 20 µl volume by 1.0 µl of AffinityScript RT/ RNase Block enzyme mixture supplemented with 12.75 nM Oligo(dT) primer, 2.25 nM random primer and 1x First Strand Mastermix. Reaction started with primer annealing at 25°C for 5 min, then followed by two steps cDNA synthesis (5 min at 4°C, then 30 min at 55°C) and terminated at 95°C for 5 min. cDNA was then stored at 4°C for immediate usage or -20°C for longer storage.

II.2.1.3.b miRNA reverse transcription

50 ng total RNA in a 5 µl volume or 5 µl of purified serum RNA were used to reversely transcribe miRNA using TaqMan MicroRNA Reverse Transcription Kit (Life Technologies) in a 15 µl reaction volume. Reaction was performed by 50 U MultiScribe Reverse Transcriptase in 1x Reverse Transcription Buffer supplemented with 3.8 U RNase Inhibitor, 1 nM dNTPs and 3 µl of 5x miRNA-specific RT primer from TaqMan MicroRNA Assays (Life Technologies). Reaction started with primer annealing at 16°C for 30 min, then followed by reverse transcription at 42°C for 30 min and terminated at 85°C for 5 min. RT reaction solutions were then stored at 4°C for immediate usage or -20°C for longer storage.

II.2.1.4 Polymerase Chain Reaction (PCR)

50 ng cDNA, 50 ng gDNA or 10 ng plasmid DNA were used as template per PCR. DNA fragments were amplified by 0.02 U/µl AmpliTaq DNA Polymerase (Life Technologies) in a 25 µl reaction volume containing 1x PCR Buffer II supplemented with 0.4 µM primers, 0.2 mM dNTPs. The reaction began at 95°C for 5 min, then followed by 35 cycles containing a denaturation step (30 sec, 95°C), an annealing step (30 sec, 60°C) and an extension step (1kb/min, 72°C) and ended with an additional extension step (7 min, 72°C) on 9800 Fast Thermal Cycler (Life Technologies). PCR products were stored at 4°C for immediate usage or -20°C for longer storage.

To reduce the mismatch during amplification, GeneAmp High Fidelity PCR system (Life Technologies) was applied to amplify DNA fragments for downstream molecular cloning. Briefly, 50 ng cDNA, 50 ng gDNA or 10 ng plasmid DNA were used as template per reaction. DNA fragments were amplified by 0.05 U/µl GeneAmp High Fidelity PCR Enzyme Mix in a 25 µl reaction volume containing 1x GeneAmp High Fidelity PCR Buffer supplemented with 0.2 µM primers, 0.4 mM dNTPs. PCR was performed under standard amplifying program.

II.2.1.5 Real-time PCR

II.2.1.5.a Real-time PCR to detect gene expression level

Real-time PCR to detect gene expression level was performed in duplicates with TaqMan Gene Expression Assays in a 7500 Fast Real-time PCR System (all from Life Technologies). Each TaqMan Gene Expression Assay mix (20x) contains two unlabeled sequence specific primers and one 6-carboxyfluorescein (FAM) dye-labeled TaqMan minor groove binder

(MGB) probe or one 6-VIC (proprietary, no information provided by Life Technology) dye-labeled TaqMan MGB probe for TaqMan endogenous controls. The primer probe is constructed containing a reporter fluorescent dye (FAM or VIC) on the 5' end and a nonfluorescent quencher on the 3' end that quenches the reporter dye emission if the probe is intact. During amplification, the 5' nuclease activity of *Taq* DNA polymerase cleaves the probe and separates the reporter dye from the quencher to increase the reporter dye signal. Each PCR cycle brings additional reporter dye emission, which results in an increase in fluorescence signals in proportion to the amount of amplicon produced. 1 µl of cDNA were used in a 20 µl reaction volume containing 1x TaqMan Universal PCR Master Mix supplemented with 0.5 µl 20x TaqMan Gene Expression Assay mix. The mixture began reaction firstly for hot enzyme activation at 95°C for 10 min, then followed by 40 cycles containing a denaturation step (15 sec, 95°C), an annealing/extension step (1min, 60°C). Relative quantification was performed by calculating the difference in cross-threshold values (ΔCt) of the gene of interest and an endogenous control according to the formula $2^{-\Delta ct}$. To quantify the copy numbers of GARP mRNA serial dilutions of a vector encoding GARP cDNA (present in our lab) were analyzed along with the samples. The copy numbers were calculated based on the concentrations of the control curve.

II.2.1.5.b Real-time PCR to detect miRNA expression level

Real-time PCR to detect miRNA expression level was performed in duplicates with TaqMan MicroRNA Assays (Life Technologies). Each TaqMan MicroRNA Assay contains one tube of miRNA-specific RT primer for miRNA reverse transcription and one tube of 20X Probe mix including miRNA-specific forward PCR primer, specific reverse PCR primer and miRNA-specific TaqMan MGB probe for Real-time PCR detection. 5 µl of 1:11 diluted miRNA reverse transcription product were used in a 20 µl reaction volume containing 1X TaqMan Universal PCR Master Mix supplemented with 1 µl 20x Probe mix. Real-time PCR was performed under standard real-time PCR program. To quantify the copy numbers of miR-142-3p serial dilutions of the mimics of miR-142-3p were analyzed along with the samples. The copy numbers were calculated based on the concentrations of the control curve.

II.2.1.5.c Genotyping of SNPs

Genotypes of GARP 3'UTR were determined by TaqMan SNP Genotyping Assays based on the release of reporter fluorescent dye from the quencher using the *Taq* DNA polymerase's 5'-nuclease activity. Each pre-formulated SNP Genotyping Assay mix contains 2 unlabelled PCR primers (forward and reverse primers), 1 VIC dye – MGB labeled probe detects the

allele 1 sequence and 1 6-FAM dye – MGB labeled probe detects the allele 2 sequence. A fluorescent signal of a single dye (FAM or VIC) determines homozygosity for a respective allele and fluorescent signals of both dyes indicate heterozygosity. 10 ng DNA were reacted in a 10 µl reaction volume containing 1x TaqMan Universal PCR Master Mix supplemented with 0.25 µM SNP Genotyping Assay mix. The reaction began firstly for hot enzyme activation at 95°C for 10 min, then followed by 40 cycles containing a denaturation step (15 sec, 95°C), an annealing/extension step (1min, 60°C) on a 9800 Fast Thermal Cycler and was analyzed on 7500 Fast Real-time PCR System. Each sample was determined in duplicates and water was included into each PCR run as a no template control (NTC).

II.2.1.6 Agarose Gel electrophoresis

1 % Agarose gel containing 1x SYBR Safe DNA Gel Stain (Life Technologies) was used for gel electrophoresis of DNA fragments. 5 µl of DNA were diluted with 1 µl of 6x loading dye and loaded per well. To identify the size of the bands, 0.2 µg of GeneRuler DNA ladder (100bp and 1kb, Fermentas) were loaded as marker. Gel electrophoresis was performed at 100 V for 30 min in 1x TAE Buffer. DNA bands were visualized using UVT-28 MP transilluminator (Herolab, Wiesloch, Germany)

II.2.1.7 PCR products purification

PCR products were purified using QIAquick PCR Purification Kit (Qiagen) following the manufacturer's instructions. All centrifugation steps were performed at 13,000 rpm for 1min at room temperature. Briefly, one volume PCR sample was mixed with five volumes Buffer PBI and applied to QIAquick spin columns. Columns were then washed with 750 µl of Buffer PE. After discarding the flow-through from the washing step columns were centrifuged for additional 1 min and transferred to fresh Eppendorf tubes. 50 µl of distilled H_2O were added per column and centrifuged to elute purified DNA. The quality and quantity of DNA were controlled by analyzing the absorbance at 260 nm/280 nm (A_{260}/A_{280}) using an Eppendorf BioPhotometer. Purified DNA was then stored at 4°C for immediate usage or -20°C for longer storage.

II.2.1.8 Agarose Gel extraction

Desired DNA fragments were extracted using QIAquick Gel Extraction Kit (Qiagen) based on the manufacturer's instructions. All centrifugation steps were performed at 13,000 rpm for 1 min at room temperature. DNA bands were excised from 1.0% Agarose gel after gel electrophoreses and weighted. 3 volumes of QG Buffer were added per 1 volume gel (100mg

≈ 100µl) and mixtures were incubated at 50°C for 10 min by short vortexing every 2-3 min during incubation. After incubation, 1 volume of isopropanol was added. Mixtures were applied to the QIAquick columns and centrifuged for DNA binding. Columns were washed first with 500 µl of Buffer QG, then two times with 700 µl of Buffer PE. After discarding the last flow-through, columns were centrifuged for additional 1 min and transferred to fresh Eppendorf tube. 30 µl of distilled H_2O were added per column and centrifuged to elute extracted DNA. The quality and quantity of DNA were controlled by analyzing the absorbance at 260 nm/280 nm (A_{260}/A_{280}) using an Eppendorf BioPhotometer. Purified DNA was then stored at 4°C for immediate usage or -20°C for longer storage.

II.2.1.9 Cloning

II.2.1.9.a TOPO TA cloning

TOPO cloning reaction was performed using TOPO TA cloning kit (Life Technologies). 10 ng pCR2.1-TOPO vectors were mixed with 1 µl of fresh PCR product for 30 min at room temperature in a 6 µl volume supplemented with 1x salt solution (0.2 M NaCl and 0.01 M $MgCl_2$). The reaction mixtures were then placed on ice and used for transformation immediately.

II.2.1.9.b Ligation

50 ng vectors were ligated with a 3-fold molar excess of insert by 1 µl 400 U/µl Quick T4 DNA Ligase (New England Biolabs) for 5 min at room temperature in a 20 µl volume containing 1x Quick ligation reaction buffer. The reaction mixtures were then placed on ice and used for transformation immediately.

For the insertion of DNA oligonucleotides, 4 µM complementary s-oligonucleotides and as-oligonucleotides were annealed to each other in a 50-µl volume supplemented with 1x Oligo Annealing Buffer containing 10 mM Tris-HCl (pH 7.5), 100 mM NaCl and 1 mM EDTA at 95 °C for 5 min, then 37°C for 15 min. Annealed oligonucleotides were stored at 4°C for immediate usage or -20°C for longer storage. 50 ng vectors were ligated with 20-fold molar excess of oligonucleotides under standard ligation condition.

II.2.1.9.c Transformation

2 µl of TOPO cloning reaction or ligating reaction or 10 pg vectors (5 pg/µl) were transformed into OneShot TOP10 competent *E.coli* cells (Life Technologies) chemically according to manufacturer's instructions. DNA was gently mixed with 50 µl of carefully

thawed competent *E.coli* cells and incubated on ice for 30 min. Vials were then heat shocked for 30 sec at 42°C and incubated on ice for additional 2 min. After adding 250 µl of Super Optimal Broth (S.O.C) medium pre-equilibrated to room temperature, *E.coli* cultures were then shaken for 1 h at 300 rpm, 37°C. 100 µl of transformation were spread onto a pre-warmed selective LB Agar plate containing 50 µg/ml ampicillin or 50 µg/ml kanamycin and incubated at 37°C overnight. For TOPO cloning reaction, 40 µl of 40 mg/ml X-Gal (Life Technologies) dissolved in DMF (Sigma-Aldrich) were applied on to the plate at least 1 h in advance for blue-white selection. For site-directed mutagenesis, 10 µl of 100mM IPTG (Life Technologies) and 40 µl of 40 mg/ml X-Gal were applied on to the plate at least 1 h in advance for blue-white selection.

II.2.1.9.d Analysis of transformants

5 to 10 colonies (white or light blue colonies for TOPO cloning plates) were picked and cultured for 8-16 h at 225 rpm, 37°C in 3ml LB medium containing 50 µg/ml ampicillin or 50 µg/ml kanamycin. Plasmid DNA was isolated and digested by suitable restriction enzymes to confirm the presence and correct orientation of the insert. DNA sequencing was performed to control the sequence of the insert.

II.2.1.10 Plasmid DNA purification

Two scales of plasmid DNA purification kit were used based on the desired yield of plasmid DNA: QIAprep Spin Miniprep Kit (Qiagen) for desired DNA yield less than 20 µg, and QIAGEN Plasmid Maxi Kit (Qiagen) for desired DNA yield up to 500 µg.

II.2.1.10.a Plasmid DNA miniprep

1 to 3 ml *E.coli* overnight cultures were collected by centrifugation at 8,000 rpm for 3 min at room temperature. Pelleted bacterial cells were firstly resuspended in 250 µl of Buffer P1 containing 100 µg/ml RNase A, then mixed with 250 µl of Buffer P2 by inverting the tube gently and then mixed with 350 µl of Buffer N3. The mixtures were centrifuged for 10 min at 13,000 rpm and supernatants were applied to the QIAprep spin columns to allow the binding of plasmid DNA to the silica membrane. All centrifuge steps later on were performed at 13,000 rpm for 1 min at room temperature. After discarding the flow-through, columns were washed first with 500 µl of Buffer PB, then one time with 700 µl of Buffer PE. After discarding the last flow-through, columns were centrifuged for additional 1 min and transferred to fresh Eppendorf tubes. 50 µl of distilled H_2O/column were added and incubated for additional 1min before centrifugation to elute plasmid DNA. The quality and quantity of

DNA were controlled by analyzing the absorbance at 260 nm/280 nm (A_{260}/A_{280}) using an Eppendorf BioPhotometer. Purified plasmid DNA was then stored at 4°C for immediate usage or -20°C for longer storage.

II.2.1.10.b Plasmid DNA maxiprep

150ml *E.coli* overnight cultures were collected by centrifugation at 4,500 rpm for 20 min at room temperature. The pelleted bacterial cells were resuspended in 10 ml of Buffer P1 containing 100 µg/ml RNase A and thoroughly mixed with 10 ml of Buffer P2 by inverting 4 to 5 times and incubated for 5 min at room temperature. The mixtures were then vigorously mixed with 10 ml of pre-chilled Buffer P3, incubated on ice for 20min and centrifuged at 4,500 rpm for 20 min at 4°C. Meanwhile, the QIAGEN-tip 500 was equilibrated by applying 10 ml of Buffer QBT. All liquid applied to the columns later passed through only by gravity flow. The supernatants from centrifugation were carefully transferred into the columns without any disturbance of the pellet and allowed to flow through. The QIAGEN-tip 500 was then washed 2 times with 30 ml of Buffer QC and DNA was eluted by 15 ml of Buffer QC into a clean 50ml Falcon. To precipitate DNA, eluted DNA was mixed with 10.5 ml of isopropanol pre-equilibrated to room temperature and centrifuged at 4,500 rpm for 20 min. After discarding the supernatant, DNA pellets were first washed one time with 70% ethanol and then air-dry at room temperature for 5 to 10 min before being dissolved in 600 µl of distilled H_2O. The quality and quantity of DNA were controlled by analyzing the absorbance at 260 nm/280 nm (A_{260}/A_{280}) using an Eppendorf BioPhotometer. Purified plasmid DNA was then diluted to a concentration of 0.5 µg/ml and stored at 4°C for immediate usage or -20°C for longer storage.

II.2.1.11 Restriction enzyme (RE) digestion

1µg of DNA were digested in a 20 µl volume at 37°C for 2 h by 2.5 U/µl suitable restriction enzymes supplemented with respective 1x supplied reaction buffer as listed in Section II.1.5.1. If gel extraction was necessary, 8 µg of DNA were digested in a 160 µl volume.

II.2.1.12 DNA sequencing

DNA sequencing was performed using the service of Eurofins MWG Operon. 750 ng of plasmid DNA in a 15 µl total volume were used per sequencing. 2 µl of 10 µM sequencing primer were enclosed if necessary.

II.2.1.13 Vector construction

The sequences of all primers and oligonucleotides are listed in Section II.1.8. The sequences of all generated vectors were proven by DNA sequencing.

II.2.1.13.a Construction of pCR2.1-GARP 3'UTR

PCR products encoding a) the 5' fragment of human GARP 3'UTR (GARP-3'UTR-Up) corresponding to nucleotides 21676140-21673856 bp of NT_167190.1 (starts in the coding sequence and ends in the 3'UTR); and b) the 3' fragment of human GARP 3'UTR (GARP-3'UTR-Down) corresponding to nucleotides 21676571-21675120 of NT_167190.1 (starts in the 3'UTR and ends outside of the gene (507 bp downstream)) were amplified from genomic DNA using GeneAmp High Fidelity PCR system and cloned into pCR2.1-TOPO vector (Figure 2).

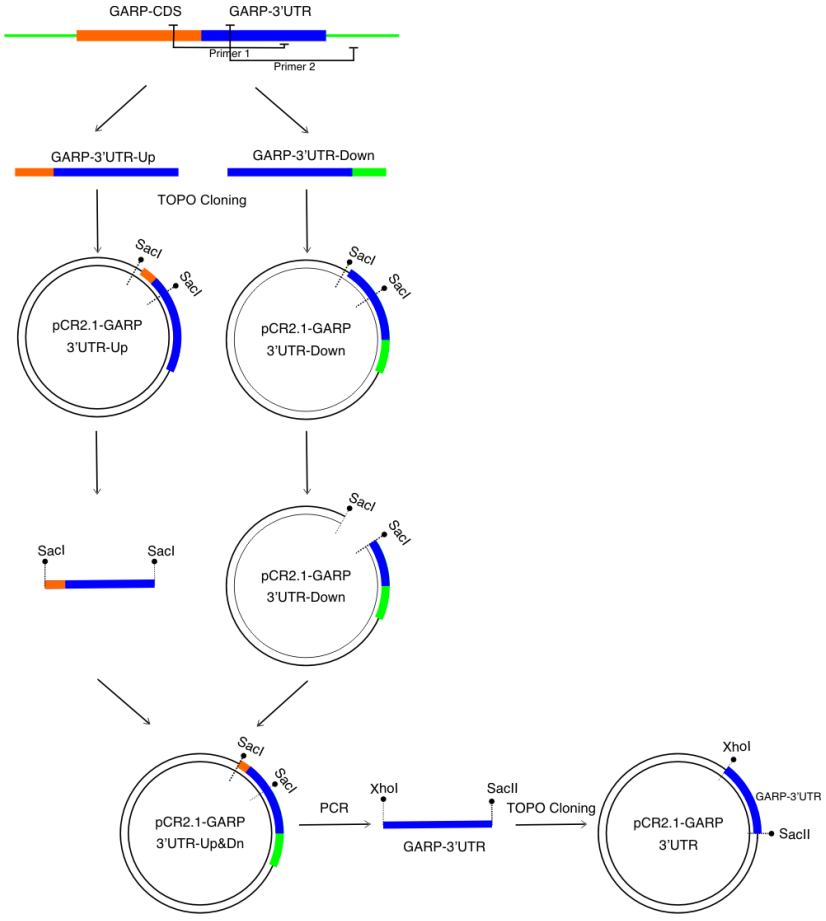

Figure 2. Schematic overview of generating pCR2.1-GARP 3'UTR vector.

After digestion by SacI the fragments released from pCR2.1-GARP-3'UTR-Up vector containing the 5' part of inserted 3'UTR fragment were purified by gel extraction and ligated into the backbone remained from pCR2.1-GARP-3'UTR-Down to generate a pCR2.1-GARP-3'UTR-Up&Down vector.

GARP 3'UTR (+2128-+4182bp, NM_001128922.1) was amplified using pCR2.1-GARP-3'UTR-Up&Down as template and cloned into the pCR2.1 vector. Restriction sites of XhoI and SacII were introduced in forward and reverse primer, respectively, for consecutive cloning steps.

II.2.1.13.b Construction of reporter vectors containing overlapping fragments of GARP 3'UTR

The pEGFP-C1* vector which was modified to contain stop codons and PmeI restriction site at the 3' end of GFP open reading frame was generated by inserting a Stop Codon-linker into a pEGFP-C1 vector (Clontech, Mountain View, USA) between XhoI and HindIII sites. Ten overlapping fragments of the GARP 3'UTR were amplified from pCR2.1-GARP-3'UTR and inserted into the pEGFP-C1* vector between PmeI and SalI sites.

To generate a vector containing the GARP coding sequence followed by the GARP 3'UTR (pcDNA3.1-GARPcds-3'UTR), the GARP 3'UTR fragment was released from the pCR2.1-GARP-3'UTR vector using XhoI and SacII restriction endonucleases and inserted into the pcDNA3.1-GARPcds vector (from our lab) between XhoI and SacII sites.

The distal part of GARP 3'UTR was amplified from pCR2.1-GARP-3'UTR and inserted into a pmirGlo vector (Promega) between PmeI and XbaI sites downstream of the luciferase sequence

II.2.1.13.c Construction of luciferase reporter vectors containing MREs

Perfect matching sequences of miRNAs (canonical miRNA recognition elements [MREs]), predicted MREs of miRNAs within the GARP 3'UTR (GARP MREs), or mutated GARP MREs and their complementary strands were synthesized as single-stranded unmodified DNA oligonucleotides by Eurofins MWG. For subsequent cloning, overhangs bearing a PmeI restriction site (forward oligonucleotide, 5'-AAAC, reverse oligonucleotide, 5'-TTTG) and an NheI restriction site (forward oligonucleotide, 5'-G, reverse oligonucleotide, 5'-CTAGC) were introduced at the 5' and 3' end of the synthesized oligonucleotides, respectively. Additionally, a NotI restriction site was introduced into the oligonucleotides for clone selection. Paired oligonucleotides were annealed and cloned into pmirGlo vectors downstream of the luciferase gene.

II.2.1.13.d Construction of mammalian expression vector encoding Radixin

PCR products encoding a) the Radixin-Frag1 corresponding to +311-+1151 bp of NM_001260492, b) the Radixin-Frag2 corresponding to +760-+1686 bp of NM_001260492

and c) the Radixin-Frag3 corresponding to +1535-+2125 bp of NM_001260492 were amplified from cDNA using GeneAmp High Fidelity PCR system and cloned into pCR2.1-TOPO vector. After digestion with HpaI and NheI, gel extraction and sequential ligation, a pCR2.1-Rdxcds vector was generated. Radixin cds (+311-+2125 bp, NM_001260492) was amplified using pCR2.1-Rdxcds as template and cloned into pcDNA3.1-V5-His between BamHI and XhoI sites.

II.2.1.14 Site-directed mutagenesis

Site-directed mutagenesis was performed in three steps using QuikChange Lightning Site-Directed Mutagenesis Kits (Agilent Technologies) based on the manufacturer's instructions. First, synthesis of the mutant strand was carried out. For this complementary forward and reverse oligonucleotides that carry the site of mutation were designed and synthesizeds as listed in Section II.1.8.3. 25 ng dsDNA templates were mixed with 0.5 µl of QuikChange Lightning Enzyme and 0.24 µM forward / reverse oligonucleotides in a 25 µl volume supplemented with 1x reaction buffer. The reaction began at 95°C for 2 min, then followed by 18 cycles containing a melting step (20 sec, 95°C), an annealing step (10 sec, 60°C) and an extension step (30 sec/kb, 68°C) and ended with an additional extension step (5 min, 68°C) on a 9800 Fast Thermal Cycler. In the next step, digestion of parental methylated DNA by DpnI was performed. 2 µl of the provided DpnI restriction enzyme were added directly to the tube and incubated at 37°C for 5min to digest the parental methylated DNA. At the last step, 45 µl gently thawed XL10-Gold ultracompetent cells were transfected by adding 2 µl of DpnI-treated DNA in addition to 2 µl of β-Mercaptoethanol mix. *E.coli* were incubated on ice for 30 min. Standard transformation was carried out and *E.coli* culture was spread onto pre-warmed selective LB Agar plates containing 10 µl of 100 mM IPTG and 40 µl of 40 mg/ml X-Gal for blue-white selection.

II.2.2 Cell Biological Methods

II.2.2.1 Cell purification

II.2.2.1.a Isolation of human $CD25^+$ CD4 T cells

Human $CD25^+$ and $CD25^-$ T cells were isolated from heparin-treated peripheral blood from healthy individuals and patients with RA. The whole procedure includes four sequential steps: isolation of peripheral blood mononuclear cells (PBMCs) from peripheral blood, resetting of $CD4^+$ and $CD8^+$ T cells, negative selection of $CD4^+$ T cells and positive selection of $CD25^+$ CD4 T cells. Briefly, 10 ml of Ficoll were carefully loaded under a mixture of 20 ml of blood and 20 ml of PBS, and centrifuged at 1,300 rpm for 20 min without forced stop at room temperature. PBMCs located above the Ficoll layer and beneath the plasma layer were harvested and washed once with PBS. PBMC were counted and incubated with sheep erythrocytes for the isolation of the rosette-positive cell fraction containing $CD4^+$ and $CD8^+$ T cells. As described before (Rosenberg and Lipsky 1979), CD58 homologue expressed on sheep erythrocytes binds to CD2 which is exclusively expressed on T cells and natural killer (NK) cells. Therefore, only T cells and NK cells, but not the other components of PBMC (termed as rosette negative cells, e.g. monocytes and B cells) are recruited in the heavier layer after centrifugation. Thus, PBMC were resuspended at 10 x 10^6 cells/ml and incubated with ½ volume FCS and ½ volume sheep erythrocytes (approximately 2 x 10^6 cells/ml) for 10 min at 37°C in a water bath with gentle shaking, followed by centrifugation at 1,040 rpm for 10 min and incubation for 40 min at 4°C to allow the formation of rosettes between sheep erythrocytes and CD2 positive cells. Afterwards, 10 ml of Ficoll were loaded under carefully resuspended PBMC/sheep erythrocytes mixture and centrifuged at 1,300 rpm for 20 min without forced stop at room temperature. The rosettes of T cells or NK cells bound to sheep erythrocytes were collected in the pellet beneath the Ficoll layer, while the rosette-negative cells were located above the Ficoll layer. The pellet of rosette-positive cells was resuspended in 10 ml/tube of 1x NH_4Cl solution to lyze the erythrocytes and then washed with PBS. For cell proliferation assay the rosette-negative cells were collected, incubated with 10 ml of 1x NH_4Cl solution to lyze contaminating sheep erythrocytes, washed twice with PBS and maintained in PBS at 4°C until usage.

$CD4^+$ T cells were then purified by negative selection from rosette-positive cells using human $CD4^+$ T cell isolation Kit II (Miltenyi Biotech) according to the manufacturer's instructions. Each 10 x 10^6 rosette-positive cells were resuspended in 40 µl of MACS buffer and incubated with 10 µl of biotin-antibody cocktail for 10 min at 4°C. The antibody cocktail contained

biotin-conjugated monoclonal antihuman antibodies against CD8, CD14, CD15, CD16, CD19, CD36, CD56, CD123, TCRγ/δ, and CD235a (Glycophorin A). The antibody-labeled cells were then resuspended in additional 30 µl of MACS buffer and incubated with 20 µl of MicroBeads conjugated to monoclonal antibiotin antibody and monoclonal anti-CD61 antibody for 15 min at 4°C. After washing cells with PBS, up to $2x10^9$ cells containing a maximum of 10^8 positive cells were resuspended in 1 ml of MACS buffer and applied on an LS MACS column placed in a magnetic field. Whereas magnetically labeled non-CD4 T cells stuck in the column, unlabeled $CD4^+$ T cells were collected in the flow through by washing the column three times with 3 ml of MACS buffer.

$CD25^+$ CD4 T cells were then purified by positive selection from $CD4^+$ T cells using human CD25 Microbeads II (Miltenyi Biotech) based on the manufacturer's instructions. Each 10 x 10^6 CD4 T cells were resuspended in 90 µl of MACS buffer and incubated with 10 µl of human CD25 Microbeads for 15 min at 4°C. After washing cells with PBS, up to $2x10^8$ cells containing a maximum of 10^7 positive cells were resuspended in 500 µl of MACS buffer and applied on an MS MACS column placed in the magnetic field. The magnetically labeled $CD25^+$ CD4 T cells stuck in the column, while unlabeled $CD25^-$ CD4 T cells were collected in the flow through by washing the column three times with 500 µl of MACS buffer. After removal of the column from the magnetic filed, $CD25^+$ CD4 T cells were eluted with 1 ml of MACS buffer by firmly pushing the plunger into the column. The $CD25^-$ CD4 T cell fraction was immediately transferred onto a LD column to remove the contaminating CD25+ T cells. The pure $CD25^-$ CD4 T cells were collected in collected in the flow through by washing the LD column three times with 3 ml MACS buffer. Purified cells were maintained at 4°C until usage. The purity of isolated cells was routinely controlled by flow cytometry.

II.2.2.1.b Isolation of mouse $CD25^+$ CD4 T cells

Spleen and lymph nodes were collected from C57BL/6 mouse. Splenocyte cell suspensions were obtained by passing cells through 70 µm Nylon Cell Strainer (BD Falcon, Bedford, USA). Afterwards, erythrocytes were lyzed with 1x NH_4Cl solution for 2 min at room temperature. $CD4^+$ T cells were then purified by negative selection from splenocytes cells using mouse $CD4^+$ T cell isolation Kit II (Miltenyi Biotech) in a similar procedure described in Section II.2.2.1.a. Afterwards $CD25^+$ CD4 T cells were purified by positive selection from $CD4^+$ T cells using mouse CD25 Microbead Kit (Miltenyi Biotech) based on the manufacturer's instructions. Each 10 x 10^6 $CD4^+$ T cells were resuspended in 100 µl of MACS buffer and incubated with 10 µl of CD25-PE-labeled antibody for 10 min at 4°C. Cells

were then washed with PBS and each 10 x 10^6 cells were resuspended in 90 µl of MACS buffer and incubated with 10 µl of magnetically labeled anti-PE microbeads for 15 min at 4°C. The $CD25^+$ CD4 T cells and $CD25^-$ CD4 T cells were collected and maintained at 4°C until usage. The purity of isolated cells was routinely controlled by flow cytometry.

II.2.2.2 Flow Cytometry

Fluorescence-activated cell sorting (FACS) was carried out to analyze the expression of cell surface molecules or intracellular proteins on a single cell level by a Cytomics FC500 flow cytometer (Beckman Coulter, Fullerton, USA). Fluorescence signals were determined using appropriate electronic compensation to exclude emission spectra overlap. All centrifugation steps were performed at 6,000 rpm for 2 min at room temperature.

II.2.2.2.a Flow Cytometry of surface molecules

For extracellular staining, 1 x 10^5 cells/sample were washed with 1 ml FACS PBS and resuspended in a 50 µl volume. To control the purity of isolated cells staining was performed in PBS with saturating amounts (2 µl) of suitable directly fluorochrome-conjugated antibodies for 15 min at 4°C in the dark. Afterwards cells were washed, resuspended in 300 µl of FACS PBS and analyzed. Typically, $CD4^+$ T cells after negative selection were ≥ 95% positve for CD3 and CD4, $CD25^+$ CD4 T cells after positive selection were ≥ 90% positive for CD25.

For surface staining of GARP, equal amount of cells were stained with 25 µl of anti-GARP hybridoma supernatant (Clone 7H2) or 0.25 µl of 0.5mg/ml rat IgG as isotype control for 15 min at 4°C in the dark. Then cells were washed and resuspended in a 50 µl volume and incubated with 0.25 µl of secondary antibody (PE-labeled anti-rat IgG) and 2 µl of FITC-labeled anti-CD4 antibody for 15 min at 4°C in the dark. Afterwards cells were washed, resuspended in 300 µl of FACS PBS and analyzed.

II.2.2.2.b Flow Cytometry of intracellular proteins

To perform the intracellular staining of total STAT1 and phosphorylated STAT1, 1-2 x 10^6 cells/staining were fixed with 4% PFA for 10 min at 37°C. Cells were then washed once with PBS and permeablized with FACS-PBS containing 0.1% (w/v) saponin (FACS-Saponin). Later on, cells were incubated with 4% rat and mouse serum for 10 min at 4°C to block unspecific binding sites. Cells were then washed once with FACS-Saponin and incubated with saturating amount of PE-labled anti-STAT1 (N-terminus, Clone 1/stat1) and Alexa Fluor 647-labeled anti-STAT1 (pS727, Clone K51-856) for 15 min at 4°C in the dark. Afterwards cells were washed, resuspended in 300 µl of FACS PBS and analyzed.

II.2.2.3 Cell culture

Cell cultures were carried out in medium supplemented with penicillin G (50 U/ml), streptomycin (50 µg/ml) and L-glutamine (2 mM) (All from Life Technologies) and 10% normal human serum (NHS) for human cells or 10% fetal calf serum (FCS) for cell lines and murine cells (termed as complete medium). Cell cultures were maintained at 37°C in a humidified atmosphere containing 5% CO_2 in Heracell 240 CO_2 incubators (Thermo Scientific).

II.2.2.3.a Cell culture of primary T cells

All T cell medium were supplemented with recombinant human IL-2 (Chiron). Human T cells were stimulated with anti-CD3/28-coated beads (Dynabeads Human T-Activator CD3/CD28, Life Technologies) in a 1:1 ratio and 100 RU/ml recombinant human IL-2 in RPMI 1640 complete medium for 1 to 4 d. For stable isotope labeling by amino acids in cell culture (SILAC), $CD25^+$ CD4 T cells were labeled by culturing them under stimulation condition for at least two weeks with RPMI media for SILAC (Thermo Scientific) supplemented with dialyzed FBS and natural Lysine (Lys0) and Arginine (Arg0) (termed as light medium) or heavy labeled L-$^{13}C_6$,$^{15}N_4$-Arginine (Arg10) and L-$^{13}C_6$,$^{15}N_2$-Lysine (Lys8) (termed as heavy medium) (All from Thermo Scientific).

II.2.2.3.b Maintenance of cell lines

Human embryonic kidney cells (HEK293) and a T cell leukemia line (Jurkat) were obtained from American Type Culture Collection (ATCC). HEK293 were split twice a week with Dulbecco's Modified Eagle Medium (DMEM) complete medium. Jurkat cells were maintained in Roswell Park Memorial Institute medium (RPMI 1640) complete medium and were split every 2 to 3 d.

II.2.2.4 Transfection

II.2.2.4.a Lipofectamine transfection

Lipofectamine transfection was performed to transfect HEK293 using Lipofectamine 2000 Transfection Reagent (Life Technologies). 5 x 10^4 HEK293 cells per well were seeded in 50 µl of DMEM medium supplemented with 10% FCS and 2 mM L-glutamine into 96 well flat-bottom plates and transfected on the next day. Each designed transfection condition was performed in triplicate. On the day of transfection, 155 ng of pmirGlo constructs and 0.2325 µl of 25nM miRNA mimics or 250nM antagomirs were diluted into a 62-µl volume by DMEM medium supplemented with 2 mM L-glutamine. 1.55 µl of Lipofectamine 2000 were

diluted at a 1:9 ratio using DMEM medium supplemented with 2 mM L-glutamine and incubated for 5 min at room temperature. Afterwards, the diluted reagent was applied to DNA mix and incubated for 20 min at room temperature to allow the formation of DNA-Lipofectamine 2000 complexes. 25 µl of DNA Lipofectamine 2000 complexes were then added to each well of the plates containing cells and mixed gently. 24h after transfection, luciferase activity was measured.

II.2.2.4.b Amaxa Transfection

Amaxa transfection was performed to transfect T cells (primary and Jurkat T cells) by using Amaxa Human T cell Nucleofector Kit or Jurkat cells using Amaxa Cell Line Nucelofector Kit V respectively (All from Lonza).

To analyze luciferase activity in T cells, $CD25^+$ CD4 T cells were stimulated with anti-CD3/28-coated beads for three days and transfected with desired luciferase reporter vectors. On the day of transfection, 6 x 10^5 $CD25^+$ CD4 T cells were collected, washed with PBS, carefully resuspended in 100 µl of nucleofector solution pre-equilibrated to room temperature. The cell suspension was then combined with 1 µg of luciferase constructs in the presence or absence of 1 µl of 250nM antagomirs and carefully transferred to a certified cuvette. Transfection was carried out using the nucleofector program, T-023 on a Nucleofector II device. After transfection, cells were carefully mixed with 500 µl of pre-equilibrated to 37^{o}C RPMI medium supplemented with 10% NHS and 2 mM L-glutamine, gently transferred into a 24-well plate to avoid repeated aspiration and maintained in culture for 3 h. Afterwards, cells were mixed with additional 100 µl of RPMI complete medium supplemented with recombinant human IL-2 to an end concentration of 10 RU/ml, split into three wells on a 96 well flat-bottom plate and cultured for additional 21 h. On the next day luciferase activity was measured.

To measure GFP expression in T cells, 6 x 10^5 freshly isolated $CD25^+$ CD4 T cells were transfected with 1 µg of pEGFP-C1* constructs using Amaxa Human T cell Nucleofector Kit. Transfection was carried out using the nucleofector program, U-014. After transfection, cells were cultured in RPMI 1640 complete medium in the presence of 10 RU/ml recombinant human IL-2. Expression of GFP was analyzed 24h after transfection by flow cytometry.

To perform ribonucleoprotein immunoprecipitation assay (RNP-IP, see Section), 60 x 10^6 Jurkat cells were transfected with 6 µg of pcDNA3.1-GARPcds-3'UTR vectors in the presence or absence of 5 µl of 250nM antagomirs using Amaxa Cell Line Nucleofector Kit V

(Lonza). Transfection was carried out using nucleofector program, X-005. After transfection, cells were incubated for 10 min at room temperature before adding pre-equilibrated to 37°C RPMI complete medium. The ribonucleoprotein immunoprecipitation was performed 24 h after transfection.

II.2.2.5 Creating stable cell lines

To successfully generate a stable cell line expressing human GARP and Radixin, Jurkat cells were transfected with either pcDNA3.1-GARPcds or pcDNA3.1-Radixin vector using Amaxa Cell Line Nucelofector Kit V. 24h after transfection, cells carrying the vectors were selected in RPMI complete medium with 250 µg/mL geneticin (Life Technologies) by replenishing the medium every three days for two weeks. The expression of GARP was confirmed by flow cytometry and the expression of Radixin in Jurkat cells was confirmed by western blot.

II.2.2.6 Measurement of T cell proliferation

II.2.2.6.a CFSE labeling

T cell proliferation assays were performed by assessing the proliferative capacity of CFSE-labeled T cells. Briefly, freshly isolated $CD25^+$ or $CD25^-$ CD4 T cells were resuspended in one volume of PBS at the concentration of 10 x 10^6/ml, labeled with 10 µM CFSE (Life Technologies) for 8 min at room temperature. Reaction was stopped by adding two volumes of NHS and cells were washed and resuspended in RPMI 1640 complete medium.

II.2.2.6.b Assessment of $CD25^+$ CD4 T cells proliferative capacity

6 x 10^5 CFSE-labeled cells were transfected with 1µl of 250 nM antagomirs or miRNA mimics and cultured in 96-well round-bottom plates under the stimulation of anti-CD3/CD28-coated beads in a 1:1 ratio and 100 RU/ml recombinant human IL-2 for 3 days. Proliferative capacity of Tregs was assessed by flow cytometry based on CFSE-dilution.

II.2.2.6.c Suppression assay of T cell proliferation

The potential inhibitory capacity of $CD25^+$ CD4 T cells treated with antagomirs or miRNA mimics was determined by co-culturing with CD25- CD4 responder T cells and measuring their proliferation in comparison to the proliferation of the $CD25^-$ CD4 cells co-cultured with non-transfected $CD25^+$ CD4 T cells. Briefly, freshly isolated Tregs were transfected with 1 µl 250 nM antagomirs or miRNA mimics. 1 x 10^5 transfected $CD25^+$ CD4 T cells were co-cultured with CFSE-labeled $CD25^-$ T cells at a ratio of 1:1 under the stimulation with 5 x 10^4 feeder cells and 1 µl of 1 mg/ml soluble anti-CD3 mAb in 96-well round-bottom plates for 5

days. Suppressive function of Tregs was assessed by flow cytometry based on CFSE-dilution.

II.2.3 Biochemical and Immunological Methods

II.2.3.1 Luciferase Assay

Luciferase activity was measured in triplicates using Dual-Glo Luciferase Assay System (Promega). Cells in 75 µl of culture medium were mixed with equal volume of Dual-Glo Reagent (applied in the kit) and incubated for 10 min at room temperature to allow cell lysis. Afterwards the firefly luminescence was measured on Centro LB 960 Microplate Luminometer (Berthold Technologies, Bad Wildbad, Germany). Dual-Glo Stop & Glo Reagent was freshly prepared by diluting Dual-Glo Stop & Glo Substrate 1:100 into Dual-Glo Stop & Glo Buffer. 75 µl of Dual-Glo Stop & Glo Reagent was added per well and incubated for 10 min at room temperature. Afterwards, the *Renilla* luminescence was assessed. The relative luciferase activity in each well was calculated as the ratio of luminescence of the firefly luciferase to luminescence of the *Renilla* luciferase. The mean value of triplicates was calculated to estimate the relative luciferase activity for each sample.

II.2.3.2 Measurement of protein concentration

Protein concentration in cell lysates was determined by Bio-Rad Protein Assay Kit (Bio-Rad) based on manufacturer's instructions. The assay is a dye-binding assay based on the method of Bradford (Bradford 1976). The Coomassie brilliant blue G-250 dye binds to primarily basic (especially arginine) and aromatic amino acid residues. By comparing the color change of a sample to a standard curve a relative measurement of protein concentration is provided. Briefly, 10 µl of cell lysates were incubated with 200 µl of 1x protein assay dye reagent (diluted fresh immediately before use from 5x protein assay dye reagent concentrate) for 5 min at room temperature. The quality and quantity of protein were controlled by analyzing the absorbance at 595 nm (A_{595}) using an Eppendorf BioPhotometer. Cell lysates were then kept on ice for immediate usage or snap-frozen using dry ice and then stored at -80°C for longer storage.

II.2.3.3 Ribonucleoprotein immunoprecipitation (RNP-IP) assay

RNP-IP assay was performed based on the protocol of Beitzinger and Meister (Beitzinger and Meister 2011) with minor adjustments. Briefly, 60 x 10^6 Jurkat cells transfected with pcDNA3.1-GARPcds-3'UTR vectors in the presence or absence of antagomirs were collected 24 h after transfection, resuspended in 1 ml of RNP-IP lysis buffer containing 0.5% NP-40,

150 mM KCl, 25 mM Tris-HCl (pH 7.5), 2 mM EDTA with 0.5 mM DTT and 1x complete protease inhibitor cocktail (Roche) added freshly immediately before use and incubated for 30 min on ice. All centrifugation steps were performed at 4°C. Cell lysates were then centrifuged at 13,000 rpm for 30 minutes and 100 µl of cell lysates were removed to present total input RNA. For immunoprecipitation, 80 µl per IP Protein-G Sepharose 4 fast flow beads (GE Healthcare) containing 50% slurry were washed with 1 ml of cold PBS by centrifuging at 3,000 rpm for 1 min and incubated for 3 h at 4°C with excess immunoprecipitating antibody, using either 1ml of anti-Ago1 (Clone 4B8) or anti-Ago2 (Clone 11A9) hybridoma supernatant (generous gifts from Dr. Meister) or 1 µg of rat IgG isotype control antibody (Sigma-Aldrich). The antibody-coated beads were washed with RNP-IP wash buffer containing 0.05% NP-40, 300 mM NaCl, 50 mM Tris-HCl (pH7.5) and 5 mM $MgCl_2$, resuspended in 500 µl of cold PBS and gently mixed with 300 µl of cell lysate. The tube was filled with RNP-IP lysis buffer to avoid larger volumes of air and incubated for 3 h at 4°C under rotation. After incubation, the beads were washed gently with RNP-IP wash buffer for six times, resuspended in 1 ml of cold PBS to remove residual detergent and transferred into a new tube to remove protein and/or RNA contamination that might bind to the walls of the tube. The beads were then pelleted, resuspended in 250 µl of 1x protease K reaction buffer containing 25 mM EDTA, 300 mM NaCl, 200 mM Tris-HCl (pH7.5) and 2 % SDS supplemented with 10 µl of proteinase K (20mg/ml) and incubated for 15 min at 65°C. RNA was isolated using QIAGEN's RNeasy Plus Mini Kit. GARP mRNA and miR-142-3p expression were assessed by TaqMan assays.

II.2.3.4 SILAC-Based peptide immunoprecipitation assay

To investigate the intracellular partners of GARP, SILAC-based peptide immunoprecipitation was performed as described previously (Schulze and Mann 2004). Snap centrifugation was performed if necessary to collect all liquid drops from the inside of the lid. 10 x 10^6 SILAC-labeled $CD25^+$ CD4 T cells cultivated in light medium (L-medium, Arg0 and Lys0-labeled) or heavy medium (H-medium, Arg10 and Lys8-labeled) for at least two weeks were collected, resuspended in 1 ml of M-PER buffer (Thermo Scientific) with 1x complete protease inhibitor cocktail and 1x phosphatase inhibitor cocktail 3 (Sigma-Aldrich) added freshly immediately

before use and incubated for 30 min on ice. Cell lysates were then centrifuged at 13,000 rpm for 15 minutes at 4°C and protein concentration was measured by Bio-Rad Protein Assay.

To perform peptide immunoprecipitation, biotinylated peptides that encoding the C-terminal sequence of GARP protein (WT) or scrambled (Scr) peptide were designed and synthesized as listed in Section II.1.2.4. The peptides were picked by a 'spatula' generated (~0.2 mg) from a cut blue pipette tip and dissolved in 1 ml lysis buffer (1:1 dilution of M-PER buffer with BupH modified Dulbecco's PBS) supplemented with 1 mM DTT added freshly immediately before use. 75 µl of dynabeads MyOne streptavidin C1 (Life Technologies) were washed 3 times with 600 µl of lysis buffer, resuspended in 500 µl of WT or Scr peptide solution, and rotated for 3 hours at 4°C. The peptide-coupled beads were washed three times with 1 ml of lysis buffer, gently mixed with 1 mg of cell lysate, filled with lysis buffer and incubated for 2 h at 4°C under rotation. After incubation, the beads were washed two times with 1 ml of lysis buffer. WT peptide-coupled beads incubated with L-Lysate (WT-L) were gently mixed with Scr peptide-coupled beads incubated with H-Lysate (Scr-H) for the forward experiment (WT L+ Scr H), while WT peptide-coupled beads incubated with H-Lysate (WT-H) were gently mixed with Scr peptide-coupled beads incubated with L-Lysate (Scr-L) for the reverse experiment (WT H+ Scr L). After combination, beads were washed one time with 1 ml BupH modified Dulbecco's PBS, resuspended in 300 µl of 20 nM biotin (Sigma-Aldrich) in PBS (pH 7.0) by vortexing vigorously and incubated for 30 min at 30°C while shaking at 1,100 rpm. The supernatant was transferred two times sequentially into fresh tubes to remove all the brownish beads traces and precipitated in 1.2 ml of pre-cooled (-20°C) acetone with 2 µl of GlycoBlue (Life Technologies) overnight at -20°C. The precipitated proteins were pelleted by gradually centrifuging the samples from 6,000 rpm to 13,000 rpm in 2 min intervals and maintaining centrifugation at 13,000 rpm for 10 min, washed with 1 ml of ethanol and dried for 5 min at room temperature.

Protein pellets were then resuspended in 20 µl of 2x SDS sample buffer, applied to NuPAGE 4-12% bis-tris gel (1.0 mm x 10 well) (Life Technologies) to perform polyacrylamide gel electrophoresis (PAGE) (See Section II.2.3.6). Afterwards, the gel was washed three times with distilled water, stained with GelCode blue stain reagent (Thermo Scientific) for 1 h at room temperature, and distained with distilled water overnight. The gel was subjected to a standard in-solution tryptic digestion and analyzed by a Liquid Chromatography-Mass Spectrometry (LC-MS). Data analysis was performed as described previously by Cox and Mann (Cox and Mann 2008). The ratio of Scr-H/WT-L (X axis) and WT-H/Scr-L (Y axis)

was visualized by scatter plot on a Cartesian coordinate system. True specific binding proteins of WT peptide were located at the II quadrant of the Cartesian coordinate system.

II.2.3.5 Immunoprecipitation

Immunoprecipitation was performed to confirm the specific binding of GARP and Radixin using Jurkat cells stable transfected with GARP and Radixin expressing vectors. Briefly, 40 x 10^6 cells were lyzed in 1 ml of NP-40 cell lysis/wash buffer containing 1% NP-40, 25mM NaCl, 50 mM Tris-HCl (pH 8.0), 2 mM EDTA with 1x complete protease inhibitor cocktail and 1x phosphatase inhibitor cocktail 3 added freshly immediately before use, incubated for 30 min on ice and centrifuged at 13,000 rpm for 30 minutes at 4°C. The cell lysates were incubated with 5 µg anti-GARP monoclonal antibody (Clone Plato-1, Enzo Life Sciences) or mouse IgG 2b, κ isotype control antibody (Biolegend) overnight at 4°C under rotation. To perform immunoprecipitation, 50 µl per IP rmp protein-A sepharose 4 fast flow beads (GE Healthcare) containing 50% slurry were washed with 1 ml of NP-40 cell lysis/wash buffer by centrifuging at 3,000 rpm for 1 min and incubated with cell lysates/antibodies mixture for 1 h at 4°C under rotation. Afterwards, the beads were washed four times with NP-40 cell lysis/wash buffer and resuspended in 20 µl of 2x SDS sample buffer.

II.2.3.6 SDS-Polyacrylamide gel electrophoresis (SDS-PAGE) and Western Blot

To perform SDS-PAGE, polyacrylamide gel was poured using Mini-PROTEAN Tetra Cell Casting Module (Bio-Rad). 3 ml of the resolving gel were poured per plate set (10 ml 8% resolving gel contained 3.5 ml 1 M Tris-HCl (pH 8.8), 2.7 ml 30% acrylamide/bis-acrylamide, 100 µl 10% SDS, 100 µl 10% APS, and 10 µl TEMED). After polymerization of the resolving gel, 1 ml of stacking gel was poured on top (5 ml 4% staking gel contained 0.633 ml 1 M Tris-HCl (pH 6.8), 0.683 ml 30% acrylamide/bis-acrylamide, 50 µl 10% SDS, 50 µl 10% APS, and 5 µl TEMED).

Samples for SDS-PAGE were boiled for 5 min at 95°C, centrifuged at 13,000 rpm for 5 min and loaded onto the gel. To estimate the size of the bands, biotinylated protein ladder (Cell signaling) and prestained protein marker (7-175 kDa, New England Biolabs) were included to each gel. The gel electrophoresis was carried out in SDS-running buffer containing 25 mM Tris-HCl, 192 mM Glycine and 0.1% SDS for 30 min at 100 V, followed by additional 1 h at 200 V.

For blotting, proteins were transferred onto a Protran nitrocellulose membrane (Whatman) in the blotting buffer containing 12.5 mM Tris-HCl, 86 mM Glycine, 0.05% SDS and 20%

methanol. The transfer was performed at 150 mA for 1.5 h using the EC140 Mini Blot Module (E-C Apparatus corporation, Holbrook, USA). Afterwards, the membrane was blocked with 5% nonfat milk powder in TBST buffer containing 20 mM Tris-HCl (pH 7.6), 140 mM NaCl and 0.1% Tween 20 for 1 h at room temperature. After washing three times with TBST buffer, the membrane was incubated with polyclonal anti-Radixin antibody (1:200 diluted in TBST buffer containing 5% BSA) for 2 hours at room temperature or overnight at 4°C. The membrane was then washed with TBST buffer three times and incubated with horseradish peroxidase (HRP)-conjugated anti-goat antibody (1:5000 diluted in TBST buffer containing 5% nonfat milk) for 1 hour at room temperature. After three times washing with TBST buffer, the membrane was incubated for 1 min with 2 ml of the ECL western blotting detection reagent (1:1 mixture of reagent 1 and reagent 2, all from GE Healthcare) and developed for 1-5 min using a FUJIFILM LAS-3000 (Fujifilm, Tokyo, Japan).

II.2.3.7 Enzyme-linked immunosorbent assay (ELISA)

Enzyme-linked immunosorbent assays (ELISAs) were performed to quantify cytokine levels in the serum and cell culture supernatants according to manufacture's instruction. Briefly, 100 µl samples were applied to each well to allow the binding of cytokine molecules to plate-bound specific primary antibody. After 3 hours incubation at room temperature, plate was washed carefully with wash buffer to remove any remaining samples. The cytokine conjugate were then applied to each well and incubate for 1 hour at room temperature to allow the binding of specific secondary antibody. The plate was washed thoroughly before the addition of substrate solution. After 30 min incubation in the dark, 50 µl stop solution was added and the absorption in each well was analyzed at 450 nm with a wavelength correction of 620 nm.

II.2.4 Statistical Analyse

Statistical analyses were performed to compare two different groups using a Student's t-test or to compare more than two groups using one-way analysis of variance (ANOVA) with a Tukey's correction for multiply comparison. For polymorphism analysis of GARP 3'UTR, the allele and genotype distributions were analyzed using Haplotype Analysis v1.0b and visualized in Haploview v4.2 software. *Chi*-squared (χ^2) test was performed to compare the haplotype in different sample size. Normal distribution was controlled by Kolmogorov–Smirnov. Spearman's rank correlation coefficient was calculated to determine statistical dependency between two variables. All statistical analyses were performed with the help of Prism 5 (GraphPad Software, La Jolla, USA) or InStat 3 (GraphPad Software). Statistical

significance was assigned when p-value was less than 0.05 and denoted as: * $p < 0.05$, ** $p < 0.01$, *** $p < 0.001$ and ns not significant.

Results

III.1 miRNA-mediated post-transcriptional regulation of GARP expression.

III.1.1 Analysis of molecular mechanism of miRNA-mediated GARP expression and its influence on Treg function.

III.1.1.1 The distal part of the GARP 3'UTR contains miRNA binding sequences capable of posttranscriptional regulation of gene expression.

Conserved elements in 3'UTR region are crucial for controlling post-transcriptional gene regulation and the stability of mRNAs via miRNA (Shabalina et al. 2003, Bartel 2009). The 3'UTR of GARP is ~2 kb long and possesses five highly conserved regions suggesting a possibility of miRNA involvement in the regulation of GARP expression (Figure 3 and Table 1).

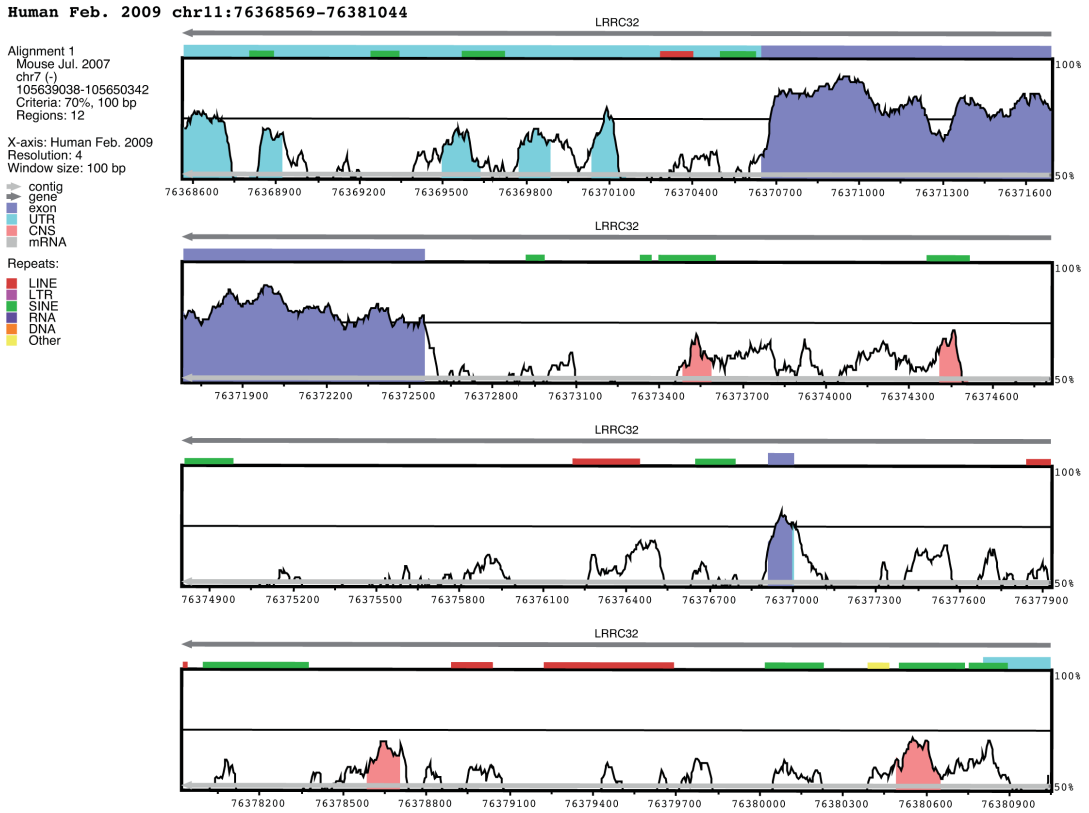

Figure 3. Schematic presentation of conserved non-coding sequences (CNS) in the GARP gene locus. Chromosome 11 (76368569-76381044) including the GARP gene is displayed. Exons are depicted in purple. The 3'UTR is shown in light blue. CNS regions were selected according to a conservation identity between mouse and human sequences by VISTA Genome Browser (Frazer et al. 2004).

In order to identify putative miRNA recognition sites that are capable of regulating GARP expression in the 3'UTR of GARP *in sillico* prediction was performed using miRbase Target (http://www.mirbase.org/) (Kozomara and Griffiths-Jones 2011), Diana Lab (http://diana.cslab.ece.ntua.gr/microT/) (Maragkakis et al. 2009), Pictar (http://pictar.mdc-berlin.de/) (Krek et al. 2005) and Target Scan (http://targetscan.org/) (Lewis et al. 2005).

Table 1. CNS regions of human GARP 3'UTR in the GARP gene locus[*¶]

	Start[§]	End[§]	Length	Homology
CNS5	76368571	76368756	187bp	76.2% UTR
CNS4	76368807	76368920	119bp	71.4% UTR
CNS3	76369497	76369633	137bp	66.4% UTR
CNS2	76369776	76369886	113bp	72.6% UTR
CNS1	76370038	76370154	118bp	77.1% UTR
exon	76370650	76372552	1903bp	81.1% exon

[*]CNS regions were selected according to a conservation identity between mouse and human by the VISTA genome Browser.
[§]Genomic position of the start and end point for each CNS region.

Total of 21 miRNAs were predicted as shown in Figure 4A: eleven miRNAs were predicted by miRbase Target (purple), five miRNAs by Diana Lab (blue), five miRNAs by Pictar (red) and one miRNA by Target Scan (green). miR-181a, miR-181b and miR-181c were predicted to recognize the same miRNA recognition elements (MREs) within the GARP 3'UTR.

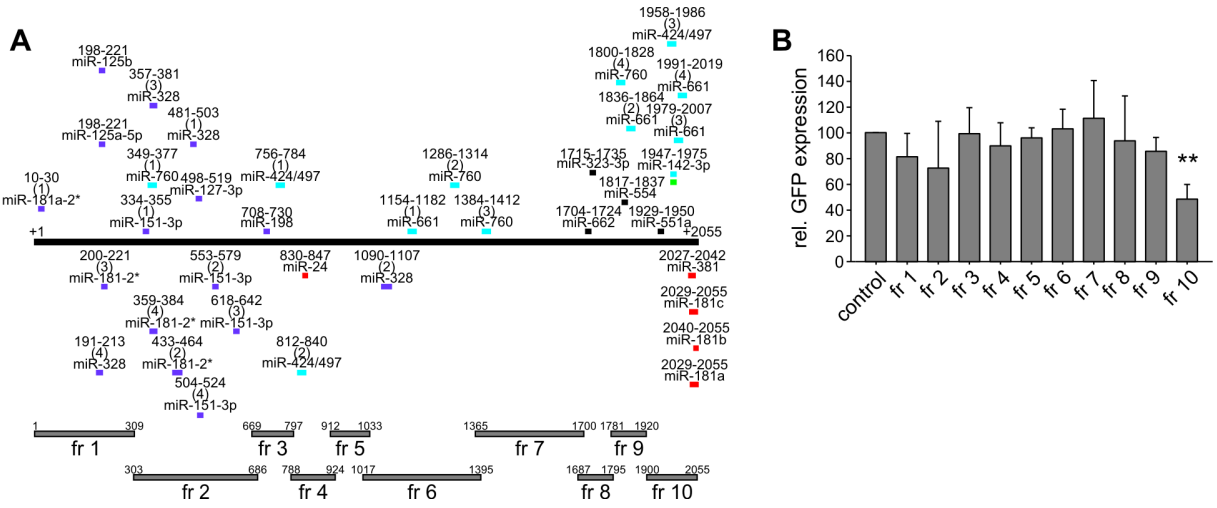

Figure 4. **The GARP 3'UTR contains sequences capable of down regulation of protein expression.**
(A) Schematic presentation of the GARP 3'UTR. *In silico* predicted miRNA binding sites in the 3'UTR of GARP mRNA are shown as dashes. Positions are indicated by nucleotide numbers above. Numbers in parentheses indicate the running number of MREs, if more than one was predicted. Based on the distribution of MREs, the full-length GARP3'UTR was subdivided into ten overlapping fragments, fragment 1 to 10. **(B)** Fragments 1 to 10 were cloned into pEGFP-C1* vector downstream of the GFP gene and transfected into freshly isolated $CD25^+$ CD4 T cells. Mean fluorescence intensity of GFP was analyzed 24h after transfection by flow cytometry. Results within one experiment were normalized to the value obtained from cells transfected with a control vector without any insert. Mean ± SD of five independent experiments is shown. Statistical analyses were performed by a Student's t-test. ** $p < 0.01$.

Based on the distribution of predicted MREs within the GARP 3'UTR, full length GARP 3'UTR was subdivided into ten overlapping fragments and cloned separately into the pEGFP-C1* reporter vector (Figure 4A) downstream of the GFP gene. Vectors were transfected into freshly isolated $CD25^+$ CD4 T cells. Mean fluorescent intensity (MFI) of GFP expression was analyzed to determine the effect of the inserted sequences on GFP expression in $CD25^+$ CD4 T cell. As shown in Figure 4B, only the vector containing the distal part of the GARP3'UTR (fragment 10) showed significantly reduction of GFP expression, indicating that this part of the GARP 3'UTR contains sequences capable of posttranscriptional regulation of protein expression.

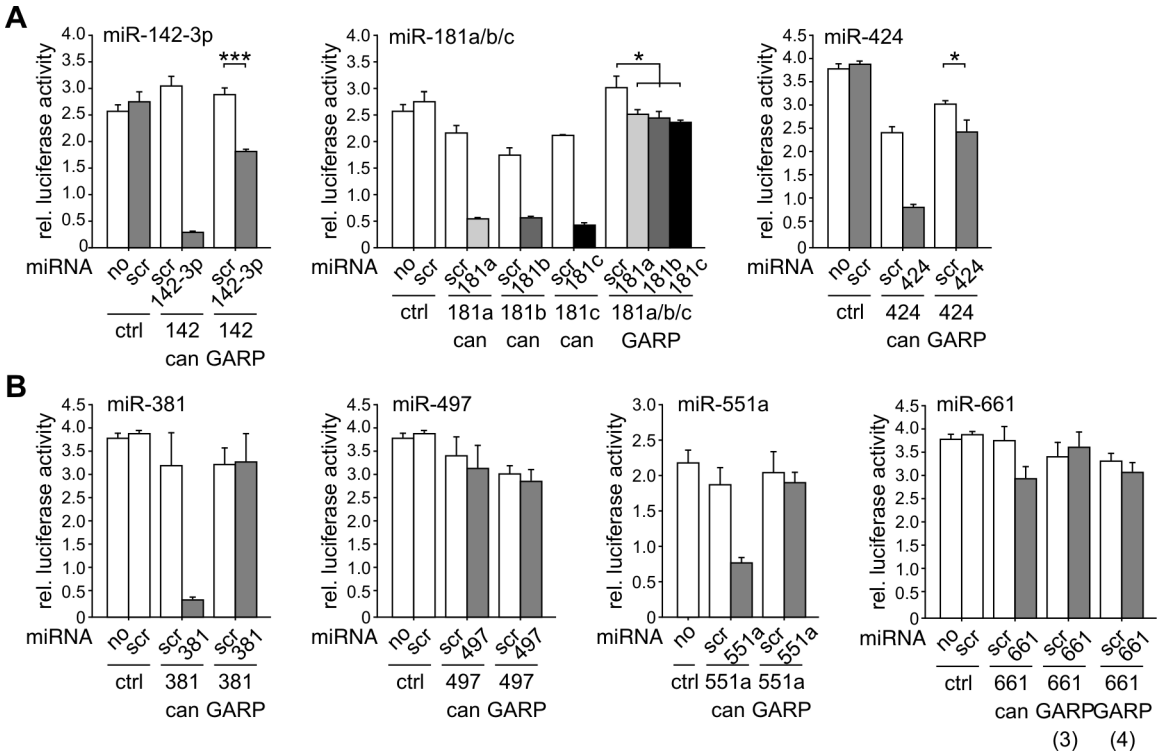

Figure 5. **miR-142-3p, miR-181a/b/c and miR-424 recognize their respective MREs.**
(A) MREs for miR-142-3p, miR-181a, miR-181b, miR-181c and miR-424 and **(B)** MREs for miR-381, miR-497, miR-551 and miR-661 predicted in the distal part of the GARP 3'UTR were cloned into the pmirGlo luciferase reporter vector downstream of the firefly luciferase gene and cotransfected with 25nM respective miRNA or scrambled miRNA (scr) into HEK293 cells. Luciferase activity was analyzed 24h after transfection. Vectors containing canonical sequences of MREs (can) and the pmirGlo vector without an insert (ctrl) were used as positive and negative controls, respectively. Mean ± SD of five independent experiments is shown. Statistical analyses were performed by a Student's t-test. * $p < 0.05$, *** $p < 0.001$.

To investigate whether and which miRNA can recognize fragment 10 of the GARP 3'UTR and thus contribute to the post-transcriptional regulation of protein expression, nine miRNAs (miR-142-3p, miR-181a, miR-181b, miR-181c, miR-381, miR-424, miR-497, miR-551, and miR-661) which were predicted to recognize this region were further analyzed. MREs of these miRNAs were cloned separately into the pmirGlo luciferase reporter vector downstream of the luciferase gene. Reporter vectors containing canonical miRNA recognition sites were

generated as positive control. Luciferase activity was measured 24h after cotransfection of miRNA mimics and the respective vectors into HEK293 cells. As indicated in Figure 5A, luciferase activity was significantly reduced in the cells cotransfected with miRNA mimics of miR-142-3p, miR-181a, miR-181b, miR-181c or miR424 and their respective vectors, indicating that these miRNAs indeed recognize their predicted MREs in the GARP 3'UTR. However, cotransfection of miR-381, miR-497, miR-551 and miR-661 mimics with their respective vectors had no effect on interfering reporter gene expression (Figure 5B). Therefore, miR-142-3p, miR-181a, miR-181b, miR-181c and miR424 are the miRNAs that recognize their MREs within GARP 3'UTR.

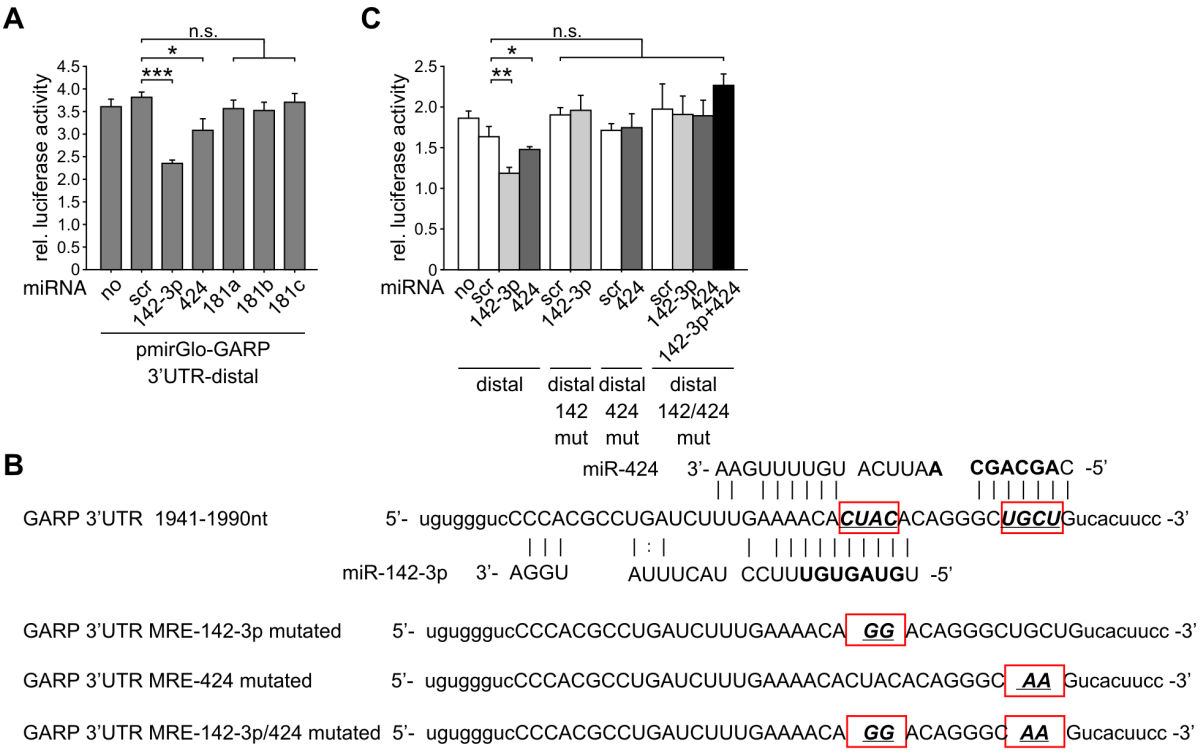

Figure 6 miR-142-3p and miR-424 recognize their MREs in the context of GARP 3'UTR
(A) The pmirGlo luciferase reporter vector containing distal the 400bp fragment of GARP 3'UTR downstream of the firefly luciferase gene was cotransfected with 25nM miR-142-3p, miR-181a, miR-181b, miR-181c or miR-424 miRNA or with scrambled miRNA into HEK293 cells. Luciferase activity was analyzed 24h after transfection. **(B)** Mutations in the region complementary to the miRNA seed sequence (shown in bold) of miR-142-3p and/or miR-424 were generated by site-directed mutagenesis as indicated. **(C)** pmirGlo luciferase reporter vectors containing distal 400bp fragment of GARP 3'UTR with mutated binding sites as shown in C were cotransfected with miRNA mimics into HEK293 cells. Luciferase activity was analyzed 24h after transfection. Mean ± SD of at least three experiments is shown. Statistical analyses were performed by ANOVA. * $p < 0.05$, ** $p < 0.01$, *** $p < 0.001$, n.s. non-significant.

To further confirm the binding of miRNAs to the GARP 3'UTR, we then examined the putative miRNA binding in the context of the GARP 3'UTR by using a luciferase vector which contains an approximately 400bp DNA fragment covering the distal part of the GARP 3'UTR. Diminished luciferase activity was observed in HEK293 cells cotransfected by this vector with miRNA mimics of either miR-142-3p or miR-424, whereas reporter gene

expression was not interfered in cells cotransfected with the vector and miRNA mimics of miR-181a, miR-181b, or miR-181c (Figure 6A). To verify the specificity of miRNA-MRE binding, the MREs for miR-142-3p and miR-424 were mutated by site-directed mutagenesis as shown in Figure 6B. After cotransfection of these mutated vectors with respective miRNA mimics, the inhibitory effect of the mimics was abrogated (Figure 6C). Hence miR-142-3p and miR-424 recognize their MREs in the context of GARP 3'UTR.

III.1.1.2 miR-142-3p but not miR-424 is relevant for recognition of the GARP 3'UTR in CD25+ CD4 T cells.

To further confirm the function of miR-142-3p and miR-424 in regulating GARP expression in human $CD25^+$ and $CD25^-$ CD4 T cells, we firstly analyzed the expression pattern of these two miRNAs in both cell type. As shown in Figure 7A, both $CD25^+$ and $CD25^-$ CD4 T cells expressed abundant amount of miR-142-3p. However, the endogenous expression levels of miR-424 were fairly low in both cell types.

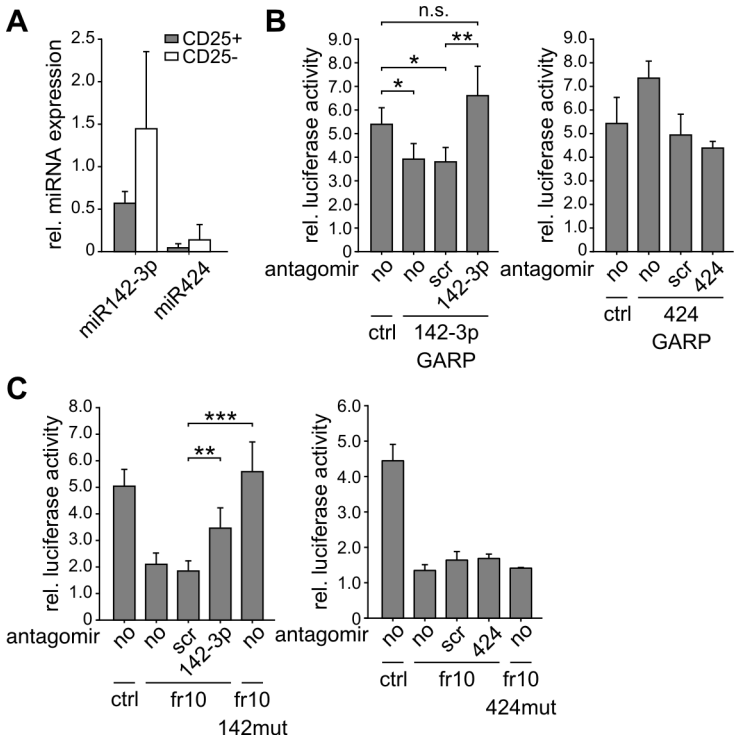

Figure 7. Endogenous miR-142-3p interacts with its MRE in GARP 3'UTR in $CD25^+$ CD4 T cells.
(**A**) Expression of miR-142-3p and miR-424 was determined in $CD25^+$ and $CD25^-$ CD4 T cells by real-time PCR using TaqMan miRNA assays. Relative expression to RNU6B is demonstrated. Mean ± SD of 3 independent experiments is shown. (**B** and **C**) $CD25^+$ CD4 T cells activated for 3 days with anti-CD3/CD28 dynabeads were transfected with pmirGlo vectors containing miR-142-3p or miR-424 MREs predicted in the GARP 3'UTR (B) or the distal fragment of the GARP 3'UTR (fragment 10), wild type or mutated as shown in Figure 6B (C), and cotransfected with respective specific or scrambled (scr) antagomirs as control. Luciferase activity was analyzed 24h after transfection. Results are demonstrated as mean ± SEM of four experiments (right panel) or as one representative of two independent experiments with similar outcome (left panel). Statistical analyses were performed by a Student's t-test. * $p < 0.05$, ** $p < 0.01$, *** $p < 0.001$, n.s. non-significant.

The effect of both miRNAs on the reporter gene activity was then analyzed based on their endogenously expression levels. To address this, microRNA hairpin inhibitors (antagomirs), which prevent endogenous miRNAs binding to their targets were cotransfected with respective luciferase reporter vectors into $CD25^+$ CD4 T cells. For control, pmirGlo vector with no insert was used. Reduced luciferase activity was observed in $CD25^+$ CD4 T cells transfected only with a vector containing the predicted GARP miR-142-3p MRE (without any cotransfection) as compared with the control vector (Figure 7B). On the other hand, luciferase activity in $CD25^+$ CD4 T cells transfected only with a vector containing the predicted GARP miR-424 MRE was similar to that of the control vector (Figure 7B). These findings indicate that endogenous expression of miR-142-3p is in a sufficient extent to down-modulate expression of the reporter gene, whereas endogenous expression of miR-424 is conceivably too low. To further confirm this, antagomirs were cotransfected into $CD25^+$ CD4 T cells to inhibit the endogenous miRNA biological activity. Cotransfection of the GARP miR-142-3p MRE reporter vector with an antagomir to miR-142-3p restored the luciferase activity, while cotransfection of the GARP miR-424 MRE reporter vector with a respective antagomir had no effect on the reporter gene activity (Figure 7B).

In the context of GARP 3'UTR, transfection of $CD25^+$ CD4 T cells with a vector containing the distal part of the GARP 3'UTR lead to reduced activity of the reporter gene as compared to control (Figure 7C). Inhibition of miR-142-3p biological activity by cotransfection of this reporter vector with a respective antagomir restored the luciferase activity in the cells. Similar finding was noticed in cells transfected with a reporter vector containing the mutation of putative miR-142-3p MRE (Figure 7C). In contrast, luciferase activity was not restored in cells either cotransfected by the GARP 3'UTR reporter vector with an antagomir to miR-424 or transfected with a vector containing mutation of miR-424 binding site (Figure 7C). Thus, miR-142-3p is identified as the miRNA involved in post-transcriptional regulation of GARP expression in $CD25^+$ CD4 T cells.

III.1.1.3 miR-142-3p launches Ago2-mediated GARP mRNA degradation.

MiRNA mediated repression of target gene expression requires binding of miRNA to the argonaute (Ago) protein within the RNA-induced silencing complex (RISC). The degree of base paring in miRNA/mRNA duplex influence the types of Ago proteins that miRNAs is loaded into. When fully complementary base paring occurs between miRNA seed sequence and target mRNA, the miRNA/mRNA duplex are preferentially loaded into Ago2 resulting in mRNA degradation. In case of unpaired bulges between miRNA seed sequence and target

mRNA, the duplex are loaded into Ago1 leading to translational repression (Meister et al. 2004, Czech et al. 2008).

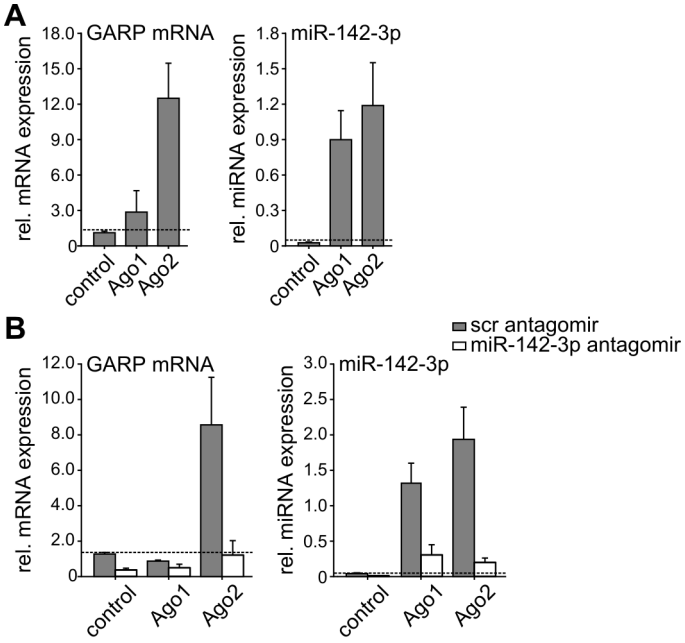

Figure 8. Down-regulation of GARP expression is mediated via the Ago2-associated pathway.
The GARP coding sequence and the GARP 3'UTR were sequentially cloned into the pcDNA3.1 vector and transfected into Jurkat cells. (**A**) Endogenous ribonucleoproteins were immunoprecipitated with anti-Ago1 or anti-Ago2 antibodies 24h after transfection. Isotype IgG was used as a control. (**B**) To evaluate the involvement of miR-142-3p, cells were cotransfected with an antagomir to miR-142-3p or with a scrambled antagomir. RNA was isolated, reversely transcribed and analyzed by real-time PCR for GARP mRNA or miR-142-3p. Relative expression normalized to input is demonstrated. Means ± SEM of five (A) and four (B) independent experiments are shown. Dashed lines indicate the background of the assay determined as means ± SD from immunoprecipitations with isotype control.

The *in sillico* predicted miR-142-3p MRE in the GARP 3'UTR is perfectly matched to the seed region of miR-142-3p (GUAGUGU) (Figure 6B) indicating that Ago2-mediated mRNA cleavage may contribute to the inhibition of GARP expression via miR-142-3p. To address this, we performed ribonucleoprotein (RNP) immunoprecipitation (IP) using antibodies against Ago1 and Ago2 in Jurkat cells transfected with a vector containing the GARP cds followed by the GARP 3'UTR. miR-142-3p was detected in both Ago1- and Ago2-associated RNP complexes as expected, whereas GARP mRNA was present only in IPs of Ago2 (Figure 8A).

To further analyze the simultaneous occurrence of miR-142-3p and GARP mRNA in the Ago2-associated RNP complex, Jurkat cells were cotransfected with an antagomir to miR-142-3p to inhibit the biological activity of miR-142-3p. The antagomir blocked miR-142-3p loading into both Ago1- and Ago2-associated RNPs, whereas it prevented GARP mRNA loading into the Ago2-associated RNP complex (Figure 8B). This confirmed the hypothesis

that miR-142-3p functions as the conductor to recruit GARP mRNA into Ago2-associated RISC. Thus, post-transcriptional regulation of GARP expression involves miR-142-3p-mediated Ago2-associated GARP mRNA degradation.

III.1.1.4 Endogenous expression of miR-142-3p regulates GARP expression in CD25+ CD4 T cells.

We next addressed expression pattern of GARP and miR-142-3p in $CD25^+$ CD4 T cells in respective activation. Expression levels of both GARP mRNA and protein were up-regulated in $CD25^+$ CD4 T cells within 24 hours in response to activation and disappeared in three days (Figure 9A and B). Expression of miR-142-3p also rose significantly in response to T cell activation. However, the up-regulation was observed firstly at day two after activation, and diminished on the following day (Figure 9C). The up-regulation of miR-142-3p in response to T cell activation correlated negatively with the down-modulation of GARP mRNA and protein expression in $CD25^+$ CD4 T cells. This finding is consistent with the launched GARP mRNA cleavage by miR-142-3p via the Ago2-associated RISC complex (Figure 8A).

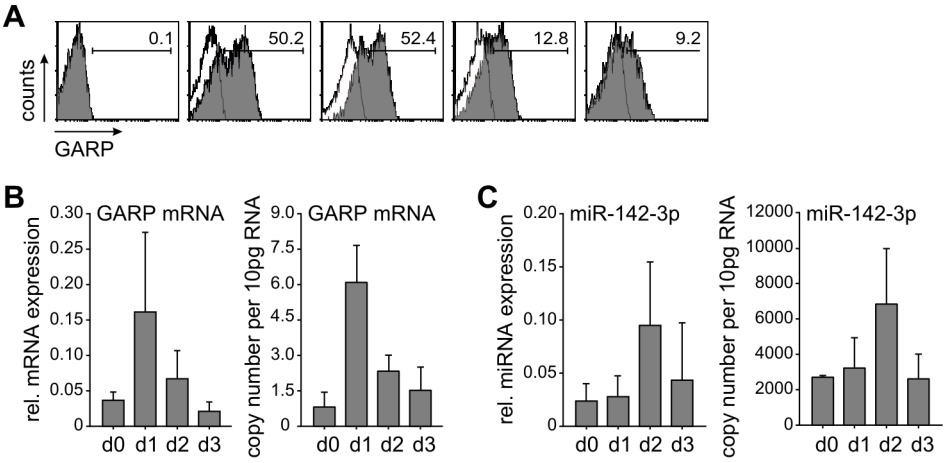

Figure 9. Expression of GARP and miR-142-3p in $CD25^+$ CD4 T cells in response to activation.
$CD25^+$ CD4 T cells were isolated and stimulated with anti-CD3/CD28 dynabeads for a total of four days. (**A**) Expression of GARP was assessed by flow cytometry using a monoclonal anti-GARP anti-body (grey). Isotype control is indicated as thin line histograms. (**B** and **C**) GARP mRNA and miR-142-3p expression were analyzed by real-time PCR. Relative expression normalized to cyclophilin (B) or RNU-6B (C), respectively, is demonstrated. For protein expression, one representative of six independent experiments with similar outcome is shown. For mRNA and miRNA expression, means ± SD of three experiments are shown.

To estimate whether the up-regulated expression level of miR-142-3p upon activation causes down-modulation of GARP expression, we assessed GARP expression in $CD25^+$ CD4 T cells transfected with an antagomir to miR-142-3p. Transfection was performed at day one after stimulation, just before expression of miR-142-3p peaks. As shown in Figure 10, a ~2-fold reduction in the miRNA level was observed in response to the transfection with an antagomir. The blockage of miR-142-3p affected obviously both GARP surface protein level and mRNA

expression level.

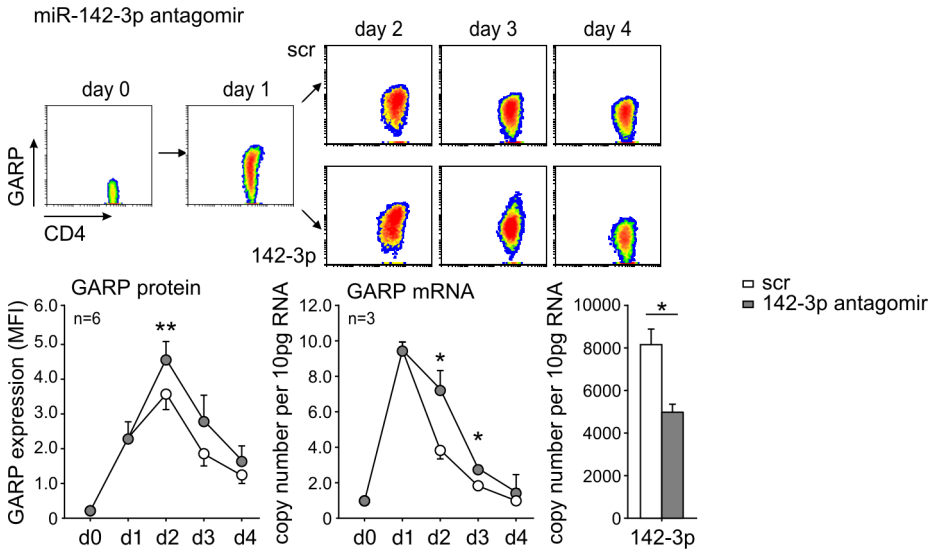

Figure 10. Blockage of miR-142-3p delayed the down-modulation of GARP expression in CD25$^+$ CD4 T cells.
CD25$^+$ CD4 T cells were isolated and stimulated with anti-CD3/CD28 dynabeads for a total of four days. Cells were transfected with 250nM antagomir of miR-142-3p or scrambled antagomir at day one. Surface expression of GARP was assessed by flow cytometry using a monoclonal anti-GARP antibody. GARP mRNA expression was analyzed daily by real-time PCR. miR-142-3p expression was assessed one day after transfection. One representative of four independent experiments with similar outcome is shown for surface GARP staining. Means ± SEM of at least three independent experiments are shown. Statistical analyses were performed by a Student's t-test. * $p < 0.05$, ** $p < 0.01$.

In contrast, when cells were treated with a mimic of miR-142-3p before activation, the up-regulation of GARP expression was markedly diminished as observed for both surface protein and mRNA expression (Figure 11) resulting in a ~4-fold increase in the miRNA level in response to the transfection with a mimic.

The miR-142-3p MRE covers 1947-1975 bp of GARP 3'UTR and locates in a 187-bp long conserved region that has 76.2% homology with the mouse GARP 3'UTR (CNS 5, Table 1). To investigate the effect of miR-142-3p on GARP expression in mouse CD25$^+$ CD4 T cells, we interfered the biological activity of murine miR-142-3p by transfecting cells with either an antagomir or a mimic of miR-142-3p. As shown in Figure 12, inhibition of biological activity of this miRNA resulted in higher GARP expression on the cell surface, whereas the transfection of miRNA mimic led to a lower GARP expression. These data correspond with the observation in human T cells, indicating the important role of miR-142-3p in regulating of GARP expression in CD25$^+$ CD4 cells.

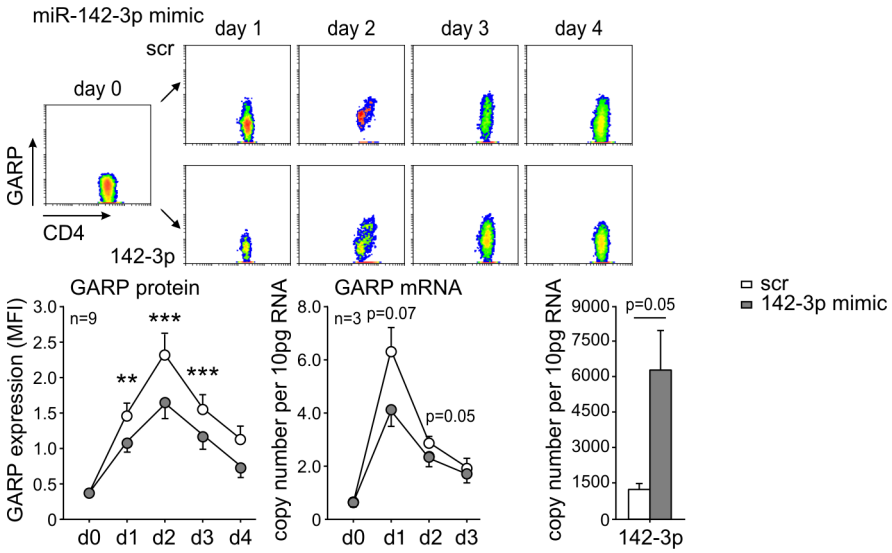

Figure 11. miR-142-3p mimics accelerated the down-modulation of GARP expression in CD25$^+$ CD4 T cells.
CD25$^+$ CD4 T cells were isolated and stimulated with anti-CD3/CD28 dynabeads for a total of four days. Cells were transfected with 250nM miRNA mimics of miR-142-3p or scrambled miRNA at day 0. Surface expression of GARP was assessed by flow cytometry using a monoclonal anti-GARP antibody. GARP mRNA expression was analyzed daily by real-time PCR. miR-142-3p expression was assessed one day after transfection. One representative of the nine independent experiments with similar outcome is depicted. Means ± SEM of at least three experiments are shown. Statistical analyses were performed by a Student's t-test. ** $p < 0.01$, *** $p < 0.001$.

Taken together, our data suggest that the magnitude and duration of GARP expression on the surface of CD25$^+$ CD4 T cells correlates with up-regulation of miR-142-3p in response to activation and thereby demonstrate that miR-142-3p is involved in the post-transcriptional regulation of endogenous GARP expression in CD25$^+$ CD4 T cells.

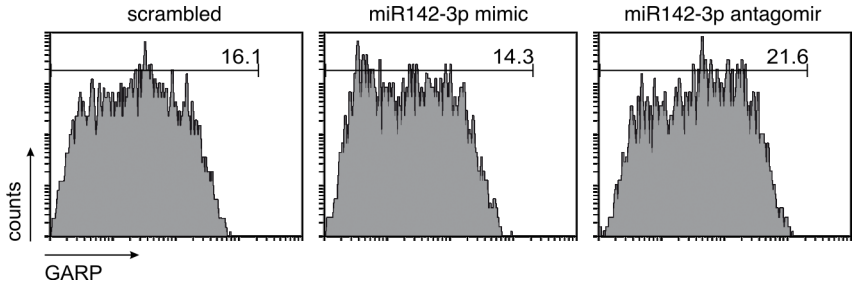

Figure 12. Interference with miR-142-3p biological activity in mouse T cells.
CD25$^+$ CD4 T cells were isolated from spleen and lymph nodes of C57B/6 mouse, transfected either with an antagomir or with mimics of miR-142-3p and stimulated for 24h with anti-CD3/CD28 beads. GARP expression was assessed by flow cytometry. Numbers indicate mean fluorescence intensity of labeled cell. One representative experiment out of three independent experiments is shown.

III.1.1.5 miR-142-3p intervenes CD25$^+$ CD4 T cells proliferation and function.

To explore the biological function of miR-142-3p in CD25$^+$ CD4 T cells, we firstly followed the proliferative capacity of cells treated with an antagomir of miR-142-3p. Inhibition of biological activity of miR-142-3p by the antagomir before activation led to an immediate reduction in the endogenous miR-142-3p expression level in CD25$^+$ CD4 T cells and

subsequently an obviously higher expression level of GARP mRNA and protein (Figure 13B). The proliferation of $CD25^+$ CD4 T cells treated with the antagomir was significantly increased upon stimulation (Figure 13A).

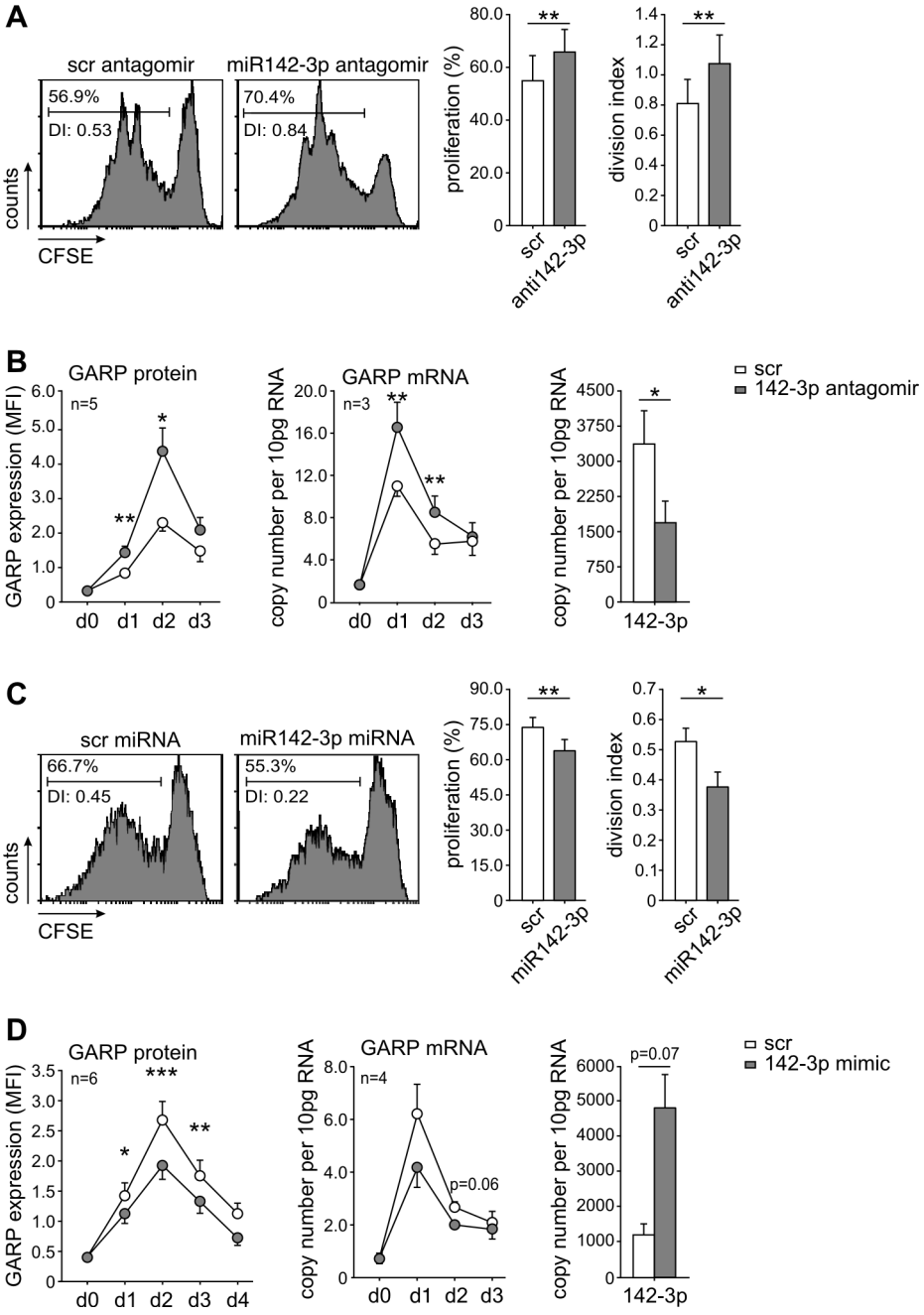

Figure 13. Involvement of miR-142-3p in proliferation of $CD25^+$ CD4 T cells.
$CD25^+$ CD4 T cells were isolated. Cells were split into two fractions and one fraction of the cells were labeled with CFSE. (**A** and **B**) cells were transfected with an antagomir to miR-142-3p. (**C** and **D**) cells were transfected with mimic of miR-142-3p. Cells were then stimulated for four days with anti-CD3/CD28 beads. Proliferation was assessed by flow cytometry in CFSE-labeled cultures. Numbers indicate the frequency of proliferating cells and the division index (DI). Nonlabeled cells were followed daily for GARP expression. Surface expression of GARP was assessed by flow cytometry using a monoclonal anti-GARP antibody. GARP mRNA expression was analyzed by real-time PCR. miR-142-3p expression was assessed one day after transfection. Means ± SEM of at least three experiments are shown. Statistical analyses were performed by a Student's t-test. * $p< 0.05$, ** $p < 0.01$, *** $p < 0.001$.

On the other hand, when $CD25^+$ CD4 T cells were transfected with a mimic of miR-142-3p, a ~4-fold increase was detected in miR-142-3p level and as a consequence, a diminution of GARP mRNA and protein expression was observed (Figure 13D). This was accompanied by a significant reduction of cell proliferation (Figure 13C). Taken together, these observations suggest that miR-142-3p intervenes into the proliferation of $CD25^+$ CD4 T cells.

We next evaluated the influence of miR-142-3p on the regulatory capacity of $CD25^+$ CD4 T cells. $CD25^+$ CD4 T cells were transfected with a mimic of miR-142-3p and cocultured with CFSE-labeled $CD25^-$ CD4 T cells to examine the suppressive capacity. miR-142-3p mimic-treated $CD25^+$ CD4 T cells, which possessed lowered GARP expression on the cell surface (Figure 13D), showed a consistent reduction of their suppressive capacity (Figure 14). These data suggested that miR-142-3p is involved in modulation of $CD25^+$ CD4 T cell proliferation and function.

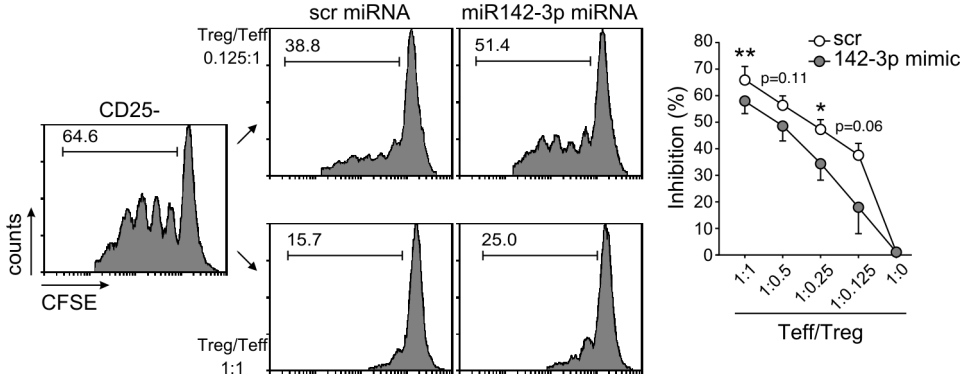

Figure 14. Involvement of miR-142-3p in suppression of $CD25^+$ CD4 T cells.
$CD25^+$ and $CD25^-$ CD4 T cells were isolated. $CD25^-$ CD4 T cells were labeled with CFSE. $CD25^+$ CD4 T cells were transfected with a mimic of miR-142-3p. CFSE-labeled $CD25^-$ CD4 T cells were cultured with non-labeled $CD25^+$ CD4 T cells in 1:0, 1:0.125, 1:0.25, 1:0.5 and 1:1 ratios in the presence of anti-CD3 for four days. Proliferation was assessed by flow cytometry based on CFSE-dilution. One representative experiment is depicted. Means ± SEM of at least three experiments are shown. Statistical analyses were performed by a Student's t-test. * $p< 0.05$, ** $p < 0.01$, *** $p < 0.001$.

III.1.1.6 miR-142-3p mediated modulation of GARP expression correlates with T cells proliferation.

To explore the role of GARP and miR-142-3p in T cells proliferation in more detail, $CD25^-$ CD4 T cells that do not naturally express GARP and do express miR-142-3p in a level comparable to that of $CD25^+$ CD4 T cells (Figure 7A) were transfected with vectors containing GARP sequence and followed for their proliferative capacity (Figure 15). For this, a series of vectors containing the GARP coding sequence followed by the wild-type or mutated GARP miR-142-3p MRE were generated. Vectors without any insertion were used as control. As shown in Figure 15A, $CD25^-$ CD4 T cells transfected with a vector encoding only

the GARP coding sequence expressed GARP ectopically on the cell surface. This ectopic GARP expression was markedly diminished when the cells were transfected with vectors carrying GARP miR-142-3p MRE downstream of the GARP coding sequence. Instead, when mutated MRE was inserted downstream of the GARP coding sequence, the expression of GARP on the cells was fully restored (Figure 15A).

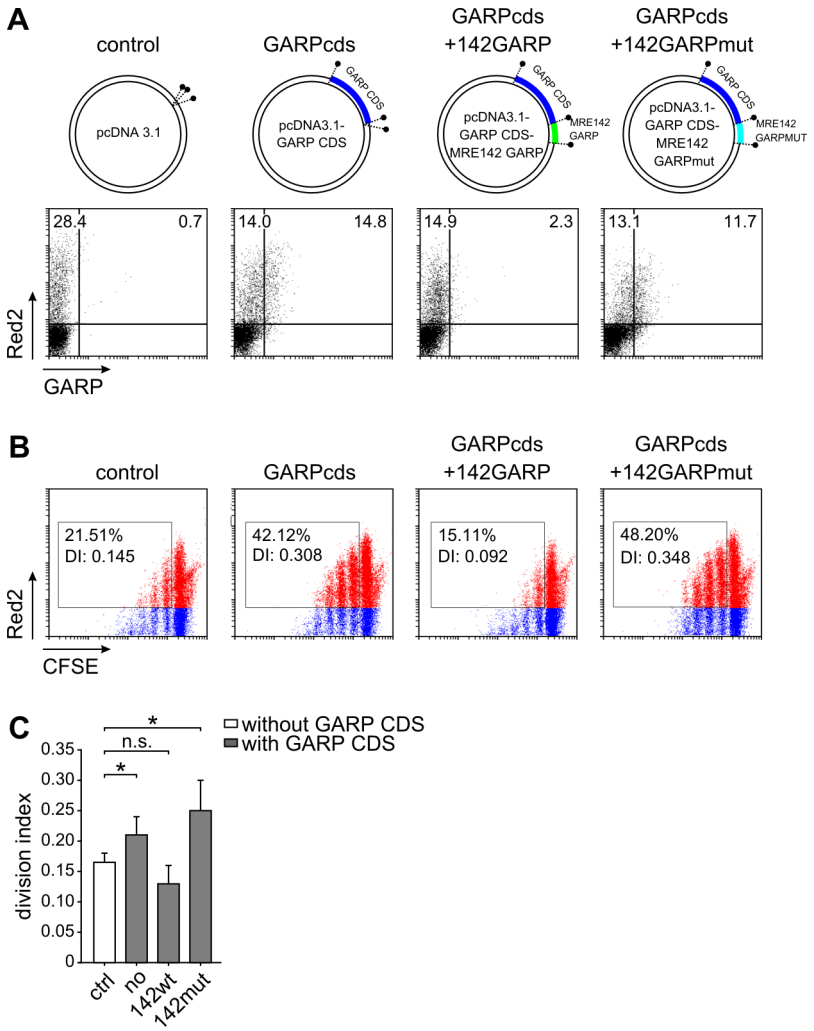

Figure 15. Regulation of T cell proliferation by miR-142-3p via GARP.
CD25- CD4 T cells were purified and labeled with CFSE to follow the proliferation or left unlabeled to control surface protein expression. Cells were transfected with vectors encoding the GARP coding sequence (GARPcds) alone or accompanied by the downstream wild-type or mutated sequence of miR-142-3p MRE from the GARP 3'UTR (142GARP and 142GARPmut, respectively). The vector without an insert was used as a control. To track the proliferation of transfected cells, T cells were cotransfected with pDsRed2-N1. CFSE dilution was followed in Red2-expressing cells at days 3, 4, and 5. (**A**) GARP surface expression one day after transfection is demonstrated. (**B** and **C**) CFSE dilution in proliferating cells at day 4 of cell culture is shown. Numbers indicate the frequency of proliferating cells and division index (DI) within the Red2-expressing population. Representative results (B) or means ± SEM of five independent experiments (C) are shown. Statistical analyses were performed by a Student's t-test. * $p < 0.05$

To analyze the proliferative capacity of the $CD25^-$ CD4 cells with enforced GARP expression, T cells was cotransfected with pDsRed2-N1 and labeled with CFSE. Cells transfected with a vector encoding only the GARP coding sequence showed increased

proliferation capacity as compared to cells transfected with control vector (Figure 15B and C). This promoted proliferation was apparently abrogated when the cells were transfected with vector containing GARP miR-142-3p MRE downstream of the coding sequence. Mutation of the GARP miR-142-3p MRE fully restored cell proliferation. These data suggested that the miR-142-3p might modulate proliferation of $CD25^+$ CD4 T cells by regulating the expression of GARP.

To further verify the important role of GARP in cell proliferation, Hela cells were transfected with GARP expressing vector and a clone that stably expresses high amount of GARP on the cell surface was selected (from our lab). Effect of GARP on cell proliferation was followed after transfecting GARP high-expressing clone with a vector encoding GARP siRNA. As shown in Figure 16, GARP expression was remarkably reduced in GARP high-expressing clone transfected with the siRNA. Besides, cell proliferation of the GARP siRNA transfected clone was highly attenuated compared to clones transfected with scramble siRNA. Therefore, our data indicate that GARP modulate cell proliferation suggesting the important role of this protein in T cell homeostasis.

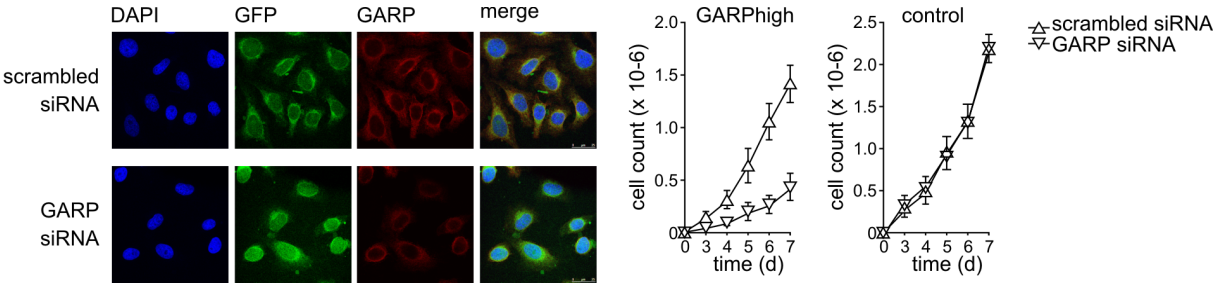

Figure 16. GARP is involved in the modulation of cell proliferation.
HeLa clones that stably transfected with a GARP cDNA-encoding vector to express high GARP on the cell surface or a control vector were transfected with pcDNA6.2 vectors encoding *in silico* designed siRNA targeting GARP or an irrelevant scrambled sequence and GFP for siRNA expression tracking. GFP^+ cells were analyzed for GFP and GARP expression by immunofluorescence microscopy (original magnification X40). The proliferative capacity of clones transfected with scrambled siRNA or GARP siRNA was determined by cell counting. Data are shown as means ± SD or as one representative of at least three independent experiments.

III.1.1.7 Analysis of intracellular proteins interacting with GARP.

To study the molecular mechanism of GARP in modulating cell proliferation, the possible intracellular connection of GARP to other proteins was further investigated. Stable isotope labeling by amino acids in cell culture (SILAC)-based quantitative proteomics was performed in $CD25^+$ CD4 T cells expanded in light medium (L-medium, Arg0 and Lys0-labeled) or heavy medium (H-medium, Arg10 and Lys8-labeled) using peptide encoding the C-terminal intracellular part of GARP. The binding affinity of proteins immunoprecipitated by GARP wild type (WT) peptide from cells cultivated in heavy medium was compared to that of

proteins immunoprecipitated by a scrambled (Scr) peptide from cells cultivated in light medium (termed as the ratio of WT-H/Scr-L, Y-axis). To reduce unspecific background binding, a reverse experiment was included to compare the binding affinity of proteins immunoprecipitated by Scr peptide from cells cultivated in heavy medium to that proteins immunoprecipitated by a WT peptide from cells cultivated in light medium (termed as the ratio of Scr-H/WT-L, X-axis). The results are shown in Figure 17B. Each spot represented one protein immunoprecipitated by the peptide and proteins that were truly bound to WT peptide were located at the II quadrant of the Cartesian coordinate system.

A total of five proteins (eRF1, Radixin, Spin1, Tomm70a and Uba6) were identified based on the data from three independent experiments (Figure 17C). Analysis of their expression levels in $CD25^+$ and $CD25^-$ cells indicated that Radixin and eRF1 were highly expressed in CD4 T cells in response to stimulation, whereas expression of Spin1, Tomm70a and Uba6 maintained in a low extent. Together with the consideration of the location and reported function of these two proteins (Hoeflich and Ikura 2004, Wong et al. 2012, Kryuchkova et al.), Radixin was selected as a candidate for further analysis.

A

peptide, synthesized (aa638-662):
wild-type Desthiobiotin-SGSAILLTTLAACCCVRRQKFNQQYKA-OH
scrambled Desthiobiotin-SGRACQCTAQRIKLQSFLACNVTAYKL-OH

B

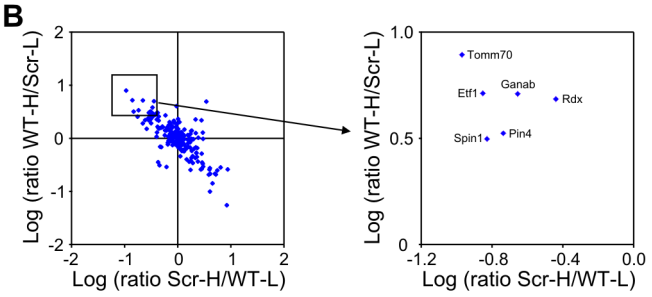

C

	Exp1	Exp2	Exp3
eRF1		yes	
Radixin		yes	yes
Spin1	yes	yes	
Tomm70a	yes	yes	
Uba6	yes		

Figure 17. SILAC-based peptide immunoprecipitation.
$CD25^+$ CD4 T cells were isolated, expanded in light medium (L-medium, Arg0 and Lys0-labeled) or heavy medium for at least 14 days and lyzed in M-PER buffer. Immunoprecipitation was performed using desthiobiotin-labeled peptide. Protein pellet were resolved by gel electrophoresis, subjected to a standard tryptic in-solution digest and analyzed by LC-MS. (**A**) Amino acid sequence of desthiobiotinylated synthesized GARP peptides. (**B**) The interaction of the GARP WT peptide compared with a scrambled peptide. Each spot represents one protein co-IPed with peptide. Data are shown as one representative of three independent experiments. (**C**) Possible candidates that bind to the GARP WT peptide from three independent experiments.

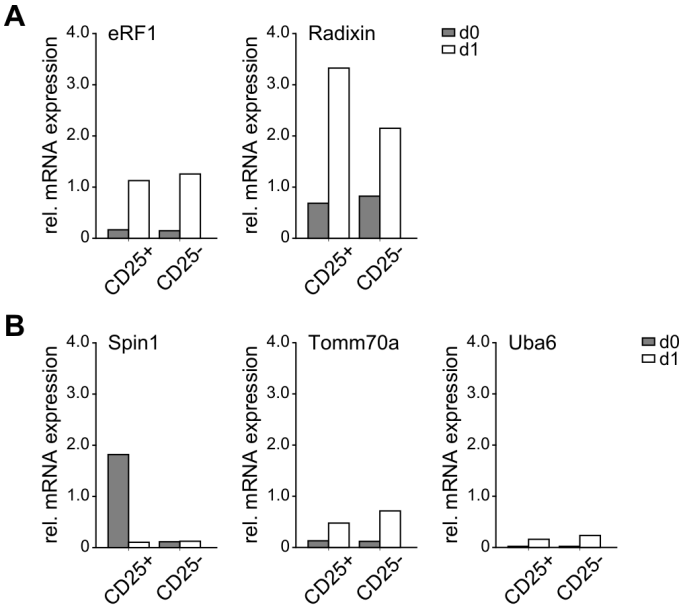

Figure 18. Expression of eRF1, Radixin, Spin1, Tomm70a and Uba6 in CD25$^+$ CD4 T cells.
CD25$^+$ CD4 T cells were isolated from spleen and lymph nodes of C57B/6 mouse and stimulated for 24h with anti-CD3/CD28 beads. Expression of eRF1, Radixin(A), Spin1, Tomm70 and Uba6 (B) was determined by real-time PCR using Taqman gene expression assays. Relative expression compared to cyclophilin was demonstrated. Results are shown as one representative of two independent experiments.

To further prove the binding of GARP and Radixin in a greater detail, co-IP studies were performed in human cell line. Jurkat cells stably transfected with a Radixin cDNA-encoding vector were transiently transfected with pcDNA3.1-GARPcds vector to generate cells overexpressing both proteins (Figure 19A). Radixin was not found in the immunoprecipitates obtained by anti-GARP antibody as well as in that with control IgG (Figure 19B), indicating the disprove of co-IP of Radixin with GARP. These results do not correspond with the findings using SILAC-based peptide immunoprecipitation, suggesting necessity of further investigation.

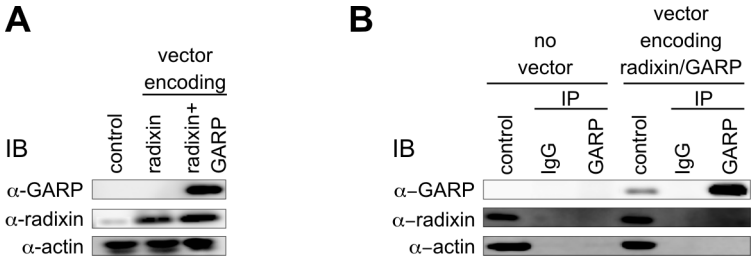

Figure 19. Co-immunoprecipitation of Radixin with GARP. Jurkat cell line stably transfected with a Radixin cDNA-encoding vector or a control vector were transfected with pcDNA3.1-GARPcds vector. (**A**) Expression of GARP and Radixin were confirmed by western blot. (**B**) Co-immunoprecipitation (Co-IP) of Radixin with GARP. Jurkat cells expressing Radixin and GARP were subjected to immunoprecipitation with anti-GARP or control IgG followed by immunoblotting with anti-GARP, anti-radixin and anti-actin. Cell lysates were used as control. Data are shown as one representative of two independent experiments.

III.2 Analysis of GARP and miR-142-3p expression in patients with rheumatoid arthritis

III.2.1 Characteristics of study population

GARP and miR-142-3p expression was analyzed in 25 patients with RA and 27 age- and gender- matched healthy individuals. All Patients fulfilled with the 2010 EULAR/ACR or the ACR 1987 classification criteria for RA (Arnett et al. 1988, Aletaha et al. 2010). Demographic and clinical parameters were documented at the Division of Rheumatology, University of Munich and summarized in Table 2.

Table 2. Characteristics of the study population[*]

	RA Patients	Healthy controls
Sample number	25	27
Age, years	60.8±12.1	51.0±7.5
Female/Male, no.	20/5	22/5
Disease duration, years	3.8±4.7	n.a.[§]
RF positive, %	88.0	n.d.[¶]
Anti-CCP positive, %	72.0	n.d.
DAS28	3.6±1.8	n.a.
TJC28, no.	4.5±6.3	n.a.
SJC28, no.	3.4±4.9	n.a.
CRP, mg/dl	1.0±1.9	n.d.
ESR, mm/hour	21.7±16.2	n.d.
Erosions, %	54.0	n.a.

[*]Data are shown as mean ± SD or absolute numbers.
[§]n.a., not applicable.
[¶]n.d., not determined.
Abbreviations: RA, rheumatoid arthritis; RF, rheumatoid factor; Anti-CCP, anti-cyclic citrullinated peptide; DAS28, disease activity score in 28 joints; TJC28, tender joint count on 28 joints; SJC28, swollen joint count on 28 joints; CRP, C-reactive protein; ESR, erythrocyte sedimentation rate.

III.2.2 Diminished expression level of GARP and elevated expression level of miR-142-3p in CD25$^+$ CD4 T cells from patients with RA.

To investigate the expression of GARP in patients with RA surface staining and real-time PCR was performed to address protein and mRNA level of GARP. As shown in Figure 20A, expression levels of both GARP protein and mRNA were up-regulated in CD25$^+$ CD4 T cells within 24 hours in both patients with RA and healthy individuals in response to activation. These data are in line with our previous results (Figure 9). The comparison of GARP expression between healthy individuals and RA patients revealed no difference in freshly isolated cells. In response to activation, the expression of GARP on protein and mRNA levels in CD25$^+$ CD4 T cells were significantly lower in patients with RA compared to healthy

individuals. On the other hand, as shown in Figure 20B, expression levels of miR-142-3p were up-regulated in $CD25^+$ CD4 T cells for two days in both patients with RA and healthy individuals in response to activation, which are in line with our previous results (Figure 9). The expression of miR-142-3p was significantly higher in patients with RA as compared to healthy individuals in both freshly isolated and activated $CD25^+$ CD4 T cells. These data negatively correlated well with the GARP mRNA expression (Figure 20A).

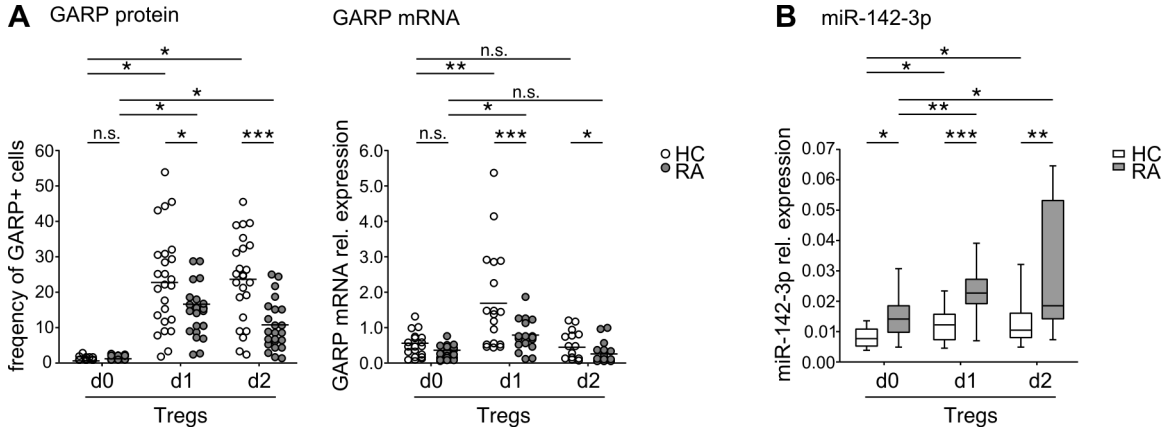

Figure 20. Expression of GARP and miR-142-3p in $CD25^+$ CD4 T cells in patients with RA.
$CD25^+$ CD4 T cells were isolated and stimulated with anti-CD3/CD28 dynabeads for a total of two days. (**A**) Left panel: Expression of GARP was assessed in $CD25^+$ CD4 T cells by flow cytometry using a monoclonal anti-GARP antibody. Frequency of $GARP^+$ cells among the total $CD25^+$ CD4 T cells from 25 healthy individuals (HC) and 23 patients with RA is shown. Right panel: Expression of GARP mRNA was analyzed by real-time PCR using TaqMan Gene Expression Assays. Relative expression normalized to cyclophilin is demonstrated. GARP mRNA level from 20 healthy individuals (HC) and 17 patients with RA is shown. (**B**) Expression level of miR-142-3p from 24 healthy individuals (HC) and 19 patients with RA is shown. miRNA expression in relation to expression levels of RNU48 is demonstrated. Data are presented as box plots demonstrating minimum, maximum, median and 25th and 75th percentiles. Statistical analyses were performed by a Student's t-test. * $p<0.05$, ** $p<0.01$, *** $p<0.001$.

III.2.3 Expression level of GARP and miR-142-3p in $CD25^+$ CD4 T cells differs in treated and non-treated patients.

Analyzed RA patients were then subdivided into two groups: non-treated (therapy naive) and treated patients. Interestingly, although there was no difference in the protein level of GARP between the treated and non-treated patient groups (Figure 21A, left panel), there was a significant difference in the expression level of GARP mRNA between these two groups (Figure 21A, right panel). For GARP protein expression, both non-treated patients and treated patients showed significantly lower protein levels as compared to healthy individuals (Figure 21A). For GARP mRNA expression, whereas treated patients did not show any difference in their mRNA level of GARP expression from healthy individuals, non-treated patients possessed significantly lower levels of GARP mRNA in response to activation as compared to that of treated patients and healthy individuals (Figure 21A, right panel). These data suggest a

trend of treatment-specific down-modulation of GARP expression in $CD25^+$ CD4 T cells from patients with RA.

On the other hand, we observed an elevated expression of miR-142-3p in freshly isolated $CD25^+$ CD4 T cells from both non-treated and treated patients as compared to the healthy individuals (Figure 21B). In response to TCR stimulation, a more pronounced up-regulation of miR-142-3p expression was observed in Tregs from non-treated patients as compared to that of healthy individuals and treated patients. Together with the expression of GARP mRNA in those two RA groups as described previously (Figure 21, right panel), our data indicate a trend of treatment-specific down-modulation of GARP expression via miR-142-3p in $CD25^+$ T cells from patients with RA.

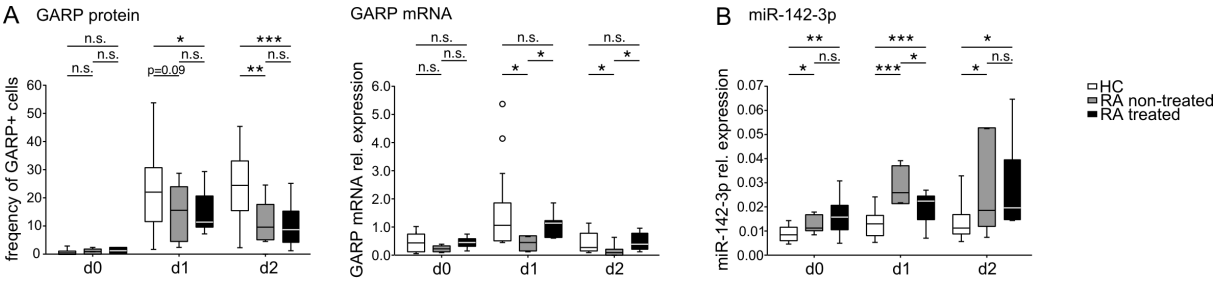

Figure 21. Expression of GARP and miR-142-3p in $CD25^+$ CD4 T cells in patients with RA stratified based on treatment.
$CD25^+$ CD4 T cells were isolated and stimulated with anti-CD3/CD28 dynabeads for a total of two days. (**A**) Left panel: Expression of GARP was assessed by flow cytometry using a monoclonal anti-GARP antibody. Frequency of $GARP^+$ cells among the total $CD25^+$ CD4 T cells from 25 healthy individuals (HC) and patients with non-treated RA (n=9) and treated RA (n=14) is shown. Right panel: Expression of GARP mRNA was analyzed by real-time PCR using TaqMan Gene Expression Assays. Relative expression normalized to cyclophilin is demonstrated. GARP mRNA level from 20 healthy individuals (HC) and patients with non-treated RA (n=8) and treated RA (n=9) is shown. Data are presented as box plots demonstrating minimum, maximum, median and 25th and 75th percentiles. (**B**) miRNA expression in relation to expression levels of RNU48 is demonstrated. Expression level of miR-142-3p from 24 healthy individuals (HC) and patients with non-treated RA (n=9) and treated RA (n=10) is shown. Data are shown as box plots demonstrating minimum, maximum, median and 25th and 75th percentiles. Statistical analyses were performed by a Student's t-test. * $p<0.05$, ** $p<0.01$, *** $p<0.001$.

III.2.4 Expression level of GARP and miR-142-3p in $CD25^+$ CD4 T cells differs in RA groups stratified according to disease activity.

Next, we subdivided analyzed RA patients into two groups stratified according to disease activity: patients with active disease (DAS28>3.2) and patients with low disease activity (DAS28≤3.2). Here we observed similar expression pattern in both protein and mRNA of GARP (Figure 22). A diminished expression of GARP protein and mRNA in response to TCR stimulation was observed in Tregs from patients with active disease (DAS28>3.2) compared to that of healthy individuals and RA patients with low disease activity

(DAS28≤3.2). These findings concede a correlation of down-modulated GARP expression to disease activity in $CD25^+$ T cells from patients with RA.

On the other hand, a pronounced up-regulation of miR-142-3p in response to TCR stimulation was observed in Tregs from patients with active disease (DAS28>3.2) compared to that of healthy individuals and RA patients with low disease activity (DAS28≤3.2) (Figure 22B). Together with the expression of GARP mRNA in those two RA groups as described previously (Figure 22A), our data indicate that miR-142-3p-mediated GARP expression in Tregs from patients with RA correlates with disease activity.

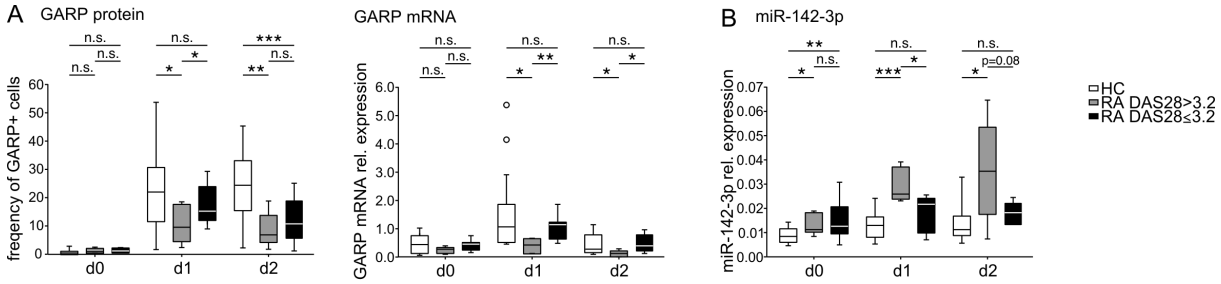

Figure 22. Expression of GARP and miR-142-3p in $CD25^+$ CD4 T cells in patients with RA stratified according to disease activity.

$CD25^+$ CD4 T cells were isolated and stimulated with anti-CD3/CD28 dynabeads for a total of two days. (**A**) Left panel: Expression of GARP was assessed by flow cytometry using a monoclonal anti-GARP antibody. Frequency of $GARP^+$ cells among the total $CD25^+$ CD4 T cells from 25 healthy individuals (HC) and patients with active disease (DAS28>3.2) (n=10) and low disease activity (DAS28≤3.2) (n=13) is shown. Right panel: Expression of GARP mRNA was analyzed by real-time PCR using TaqMan Gene Expression Assays. Relative expression normalized to cyclophilin is demonstrated. GARP mRNA level from 20 healthy individuals (HC) and patients with active disease (DAS28>3.2) (n=9) and low disease activity (DAS28≤3.2) (n=8) is shown. Data are presented as box plots demonstrating minimum, maximum, median and 25th and 75th percentiles. **(B)** miRNA expression in relation to expression levels of RNU48 is demonstrated. Expression level of miR-142-3p from 24 healthy individuals (HC) and patients with active disease (DAS28>3.2) (n=8) and low disease activity (DAS28≤3.2) (n=11) is shown. Data are shown as box plots demonstrating minimum, maximum, median and 25th and 75th percentiles. Statistical analyses were performed by a Student's t-test. * $p<0.05$, ** $p<0.01$, *** $p<0.001$.

III.2.5 SNPs on the 3'UTR of GARP might be associated with RA susceptibility

Next we examined the possible contribution of GARP 3'UTR polymorphisms to RA susceptibility. Genomic DNA of 269 RA patients and 238 HCs were genotyped for 8 SNP alleles located on the 3'UTR of GARP (Table 3 and Table 4). The majority of analyzed SNPs showed high incidence in both RA and HC groups, except for SNP 6 that demonstrated by the very rare appearance of minor allele homozygosity (~1%) in both investigated groups. There were no significant differences in the genotype and allele frequencies of SNP 6 and 7 ($p\geq0.1$) between RA patients and HC. However SNP 1, 4, 5 and 8 showed a trend of difference ($0.05\leq p<0.1$) and SNP 2 and 3 demonstrated significant differences ($p<0.5$) in the genotype and allele frequencies between analyzed cohorts. Thus, SNP 1, 4, 5 and 8, especially SNP 6 and 7 might be associated with RA susceptibility.

Table 3 Allele counts in analyzed GARP 3'UTR SNPs in RA patients and HCs

Name	SNP ID	location (mRNA)	Allele (major/minor)	Allele count (major/minor)		P*
				RA (n=269)	HC (n=238)	
SNP1	rs1320644	2588	G/A	363/175	297/179	0.0990
SNP2	rs1320645	2687	A/C	252/286	255/221	**0.0378**
SNP3	rs1320646	2728	C/T	388/150	371/105	**0.0355**
SNP4	rs3781699	2990	T/G	362/176	295/181	0.0867
SNP5	rs3781700	3066	C/A	362/176	295/181	0.0867
SNP6	rs1803627	3431	A/C	483/55	428/48	1.0000
SNP7	rs3197153	3703	T/C	359/179	295/181	0.1153
SNP8	rs7685	4136	A/C	359/179	292/184	0.0767

*P-values were calculated based on the individual numbers, using Fisher's exact test.

Table 4 Frequency of genotypes (%) in analyzed GARP 3'UTR SNPs in RA patients and HCs

Name	Allele (major/minor)	Genotype frequency (AA/AB/BB§, shown as %)		χ^{2*}	P *
		RA (n=269)	HC (n=238)		
SNP1	G/A	48.7/37.5/13.8	40.3/44.1/15.5	2.59	0.1075
SNP2	A/C	25.7/42.4/32.0	26.9/53.4/19.7	4.363	**0.0367**
SNP3	C/T	51.7/40.9/7.4	60.1/35.7/4.2	4.649	**0.0311**
SNP4	T/G	48.3/37.9/13.8	40.3/43.3/16.4	2.804	0.094
SNP5	C/A	48.3/37.9/13.8	40.3/43.3/16.4	2.804	0.094
SNP6	A/C	79.9/19.7/0.4	81.1/17.6/1.3	0.006	0.9409
SNP7	T/C	47.6/38.3/14.1	40.3/43.3/16.4	2.24	0.1345
SNP8	A/C	47.2/39.0/13.8	39.9/43.7/16.4	2.465	0.1164

*χ^2 and P-values were calculated based on the individual numbers, using Chi-square test.
§AA: major allele homozygote; AB: heterozygote; BB: minor allele homozygote.

III.2.6 Haplotype distribution of the 3'UTR of GARP might be associated with RA susceptibility

Analysis of haplotypes revealed two distinct blocks of haplotypes in the 3'UTR of GARP, termed as block1 and block 2 (Figure 23 and Table 5). Block 1 encompassed SNP 1 to SNP 3 and suggested a significant association with RA as demonstrated by the global p-value of association p=0.0439). Block 2 covered SNP 4 to SNP 8 and revealed a trend of association with RA (p=0.0564). Within block 1, four common haplotypes were observed and two of them were significantly associated with RA. Haplotype AAC were decreased in RA patients and might function as a protective haplotype (p=0.035), while haplotype GCT were over-presented in RA patients and might function as a susceptible haplotype (p=0.0246). Within block 2, three common haplotypes were observed including haplotype TCATA as susceptible haplotype (p=0.0138) and haplotype GAACC as protective haplotype (p=0.0358). Therefore,

our results suggested that haplotype distribution of GARP 3'UTR might associate with RA susceptibility. However, the detailed molecular mechanisms need to be further investigated.

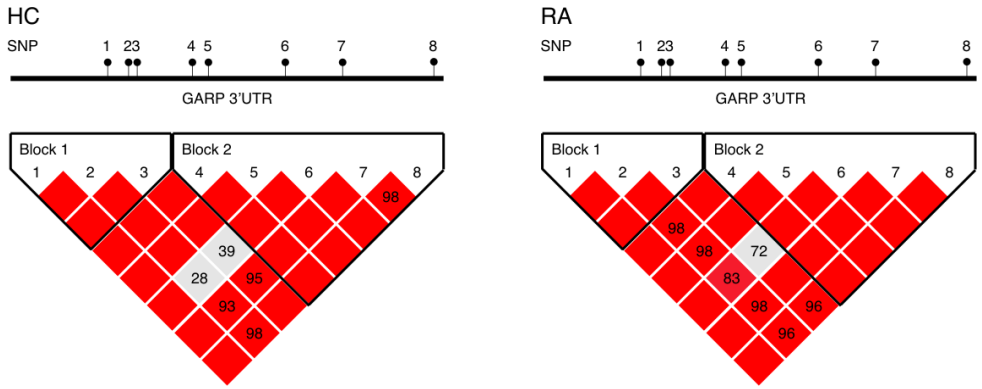

Figure 23 Haplotype of SNPs in the 3'UTR of GARP. Haplotype block structure was predicted on the basis of the strength of pairwise LD, which is presented as a 2×2 matrix; red represents very high LD (D'), white indicates absence of correlation between SNPs. The schematic overview of the location of SNPs on the GARP 3'UTR are indicated in the upper panel.

Table 5 Haplotype distribution in the 3'UTR of GARP

Haplotype Block 1

Haplotype	Count (RA/HC)	Frequency (RA/HC)	Global P*	P§
AAC	173:365/179:297	0.321/0.376	**0.0439**	**0.0350**
GCC	136:402/109:367	0.252/0.229		0.4255
GCT	150:388/103:373	0.279/0.216		**0.0246**
GAC	73:465/76:380	0.136/0.156		0.3734

Haplotype Block 2

Haplotype	Count (RA/HC)	Frequency (RA/HC)	Global P	P
TCATA	312:226/239:237	0.579/0.502	0.0564	**0.0138**
GAACC	176:362/186:290	0.327/0.391		**0.0358**
TCCTA	50:488/49:427	0.092/0.103		0.5980

*Global p-values were calculated based on the individual numbers, using Chi-square test.
§P-values were calculated based on the individual numbers, using Fisher's exact test.

III.3 Expression of other miRNAs in patients with rheumatoid arthritis

III.3.1 Characteristics of study population

Heparin-treated peripheral blood and serum samples were collected from 61 patients with RA and 49 age- and gender- matched healthy individuals. All Patients fulfilled with the 2010 EULAR/ACR or the ACR 1987 classification criteria for RA (Arnett et al. 1988, Aletaha et al. 2010). Demographic and clinical parameters were documented at the Division of Rheumatology, University of Munich and summarized in Table 6. At the study entree 23/61 of patients were untreated, 17/61 were on steroids either alone or in combination with disease modifying anti-rheumatic drugs (DMARDs) and/or biologics, 35/61 were treated with DMARDs (methotrexate or leflunomide) either alone or in combination with prednisolone and/or biologics, and 19/61 were receiving biologics alone or in combination (TNF inhibitors, tocilizumab, rituximab, or abatacept). $CD25^+$ and $CD25^-$ CD4 T cells were purified and the purity of isolated cells was controlled by flow cytometry. Typically, ≥95% of isolated cell populations were CD3/CD4 positive. $CD25^+$ CD4 T cells were ≥90% CD25 positive and ~80% CD127 negative. $CD25^-$ CD4 T cells were ≥98% negative for CD25 and ≥98% positive for CD127. The purity and number of the isolated cell populations were comparable between RA patients and healthy controls (Figure 24).

Table 6. Characteristics of the study population[*]

	RA Patients	Healthy controls
Sample number	61	49
Age, years	56.7±13.1	50.1±8.3
Female/Male, no.	48/13	36/13
Disease duration, years	6.7±9.0	n.a.[§]
RF positive, %	80.3%	n.d.[¶]
Anti-CCP positive, %	80.3%	n.d.
DAS28	3.8±1.5	n.a.
TJC28, no.	4.6±5.3	n.a.
SJC28, no.	4.5±5.1	n.a.
CRP, mg/dl	1.0±2.0	n.d.
ESR, mm/hour	13.9±12.4	n.d.

[*]Data are shown as mean ± SD or absolute numbers.
[§]n.a., not applicable.
[¶]n.d., not determined.
Abbreviations: RA, rheumatoid arthritis; RF, rheumatoid factor; Anti-CCP, anti-cyclic citrullinated peptide; DAS28, disease activity score in 28 joints; TJC28, tender joint count on 28 joints; SJC28, swollen joint count on 28 joints; CRP, C-reactive protein; ESR, erythrocyte sedimentation rate.

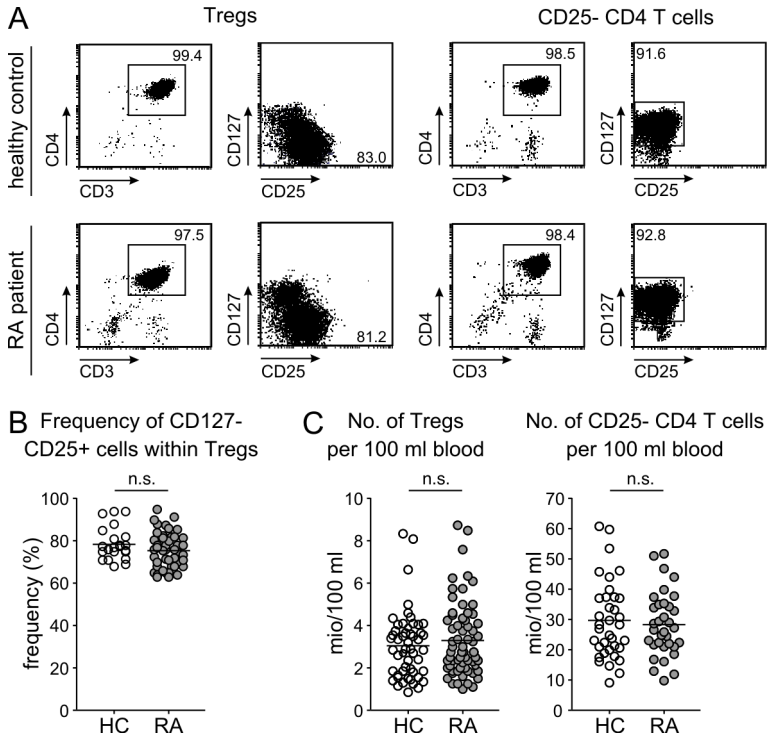

Figure 24. Purity and numbers of isolated Tregs and CD25$^-$ CD4 T cells.
CD25$^+$ CD4 T cells from 49 healthy individuals (HC) and 72 patients with RA; and CD25$^-$ CD4 T cells from 36 HC and 34 patients with RA were isolated and stained using monoclonal Ab against CD3, CD4, CD25 and CD127. **(A)** Representative stain of isolated cells is demonstrated. **(B)** Numbers of CD25$^+$ and CD25$^-$ CD4 T cells purified from 100 ml peripheral blood are show. Statistical analyses were performed by Student's t-test. n.s. non-significant.

III.3.2 Reduced expression level of miR-146a and miR-155 in CD25$^+$ CD4 T cells from patients with RA.

To investigate the expression of miR-146a and miR-155 in patients with RA, real-time PCR using TaqMan MicroRNA Assays was performed. As shown in Figure 25A and Table 7, miR-146a was expressed in a comparable level between patients with RA and healthy individuals in both freshly isolated CD25$^+$ and CD25$^-$ CD4 T cells. Upon stimulation, the expression of miR-146a decreased mildly in CD25$^+$ CD4 T cells after two days activation in both patients with RA and healthy individuals, while its expression in CD25$^-$ CD4 T cells was severely down-regulated. Interestingly, CD25$^+$ CD4 T cells from patients with RA expressed notably lower level of miR-146a as compared to healthy individuals, whereas no difference in the expression level of miR-146a in CD25$^-$ CD4 T cells was observed between patients with RA and healthy individuals. These data suggest that the expression pattern of miR-146a is characteristic for CD25$^+$ CD4 T cells in RA.

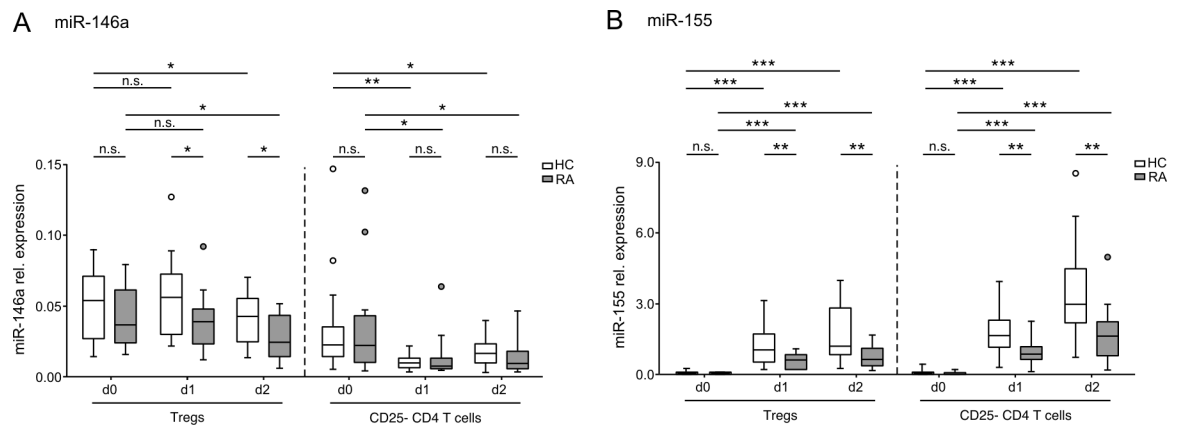

Figure 25. Expression of miR-146a and miR-155 in CD25$^+$ and CD25$^-$ CD4 T cells in patients with RA. CD25$^+$ and CD25$^-$ CD4 T cells were isolated and stimulated with anti-CD3/CD28 dynabeads for a total of two days. miRNA expression was assessed in freshly isolated cells (d0), at 24h (d1) and 48h (d2) by real-time PCR using TaqMan miRNA assays. miRNA expression in relation to expression levels of RNU48 is demonstrated. Expression level of miR-146a (**A**) and miR-155 (**B**) from 24 healthy individuals (HC) and 19 patients with RA is shown. Data are presented as box plots demonstrating minimum, maximum, median and 25th and 75th percentiles. Statistical analyses were performed by a Student's t-test. * $p<0.05$, ** $p<0.01$, *** $p<0.001$.

Table 7. Mean±SD and fold-change of miR-146a and miR-155 expression levels in CD25$^+$ and CD25$^-$ CD4 T cells.

miR-146a		Mean±SD		fold-change
		HC	RA	RA-HC
CD25$^+$	d0	0,04761±0,02555	0,04014±0,02129	0.843
	d1	0,05479±0,02684	0,03610±0,02175	0.659
	d2	0,04047±0,01684	0,02698±0,01559	0.667
CD25$^-$	d0	0,03313±0,03133	0,0335±0,03215	1.011
	d1	0,01045±0,004908	0,01329±0,01442	1.272
	d2	0,01726±0,01004	0,01358±0,01093	0.787
miR-155		Mean±SD		fold-change
		HC	RA	RA-HC
CD25$^+$	d0	0,05543±0,05309	0,04707±0,02517	0,849
	d1	1,130 ±0,7787	0,5509±0,3157	0,488
	d2	1,721 ±1,113	0,7678±0,4823	0,446
CD25$^-$	d0	0,07704±0,1010	0,03795±0,04138	0,503
	d1	1,733±0,9322	0,8468±0,5226	0,489
	d2	3,509±1,914	1,724±1,202	0,491

On the other hand, the expression of miR-155 revealed a similar pattern between $CD25^+$ and $CD25^-$ CD4 T cells (Figure 25B and Table 7). In response to stimulation, the expression of this miRNA was significantly up-regulated in both RA patients and healthy individuals. Similar to the findings about miR-146a, level of miR-155 expression was comparable between patients with RA and healthy individuals in freshly isolated cells of both cell types. After one and two days stimulation, the expression levels of miR-155 in both cell population were markedly increased. Different to the expression pattern of miR-146a, the expression of miR-155 were reduced in both $CD25^+$ and $CD25^-$ CD4 T cells from patients of RA as compared to those from healthy individuals suggesting that the diminished expression of miR-155 in RA is rather in a CD4 T cell context.

III.3.3 Expression level of miR-146a but not of miR-155 in $CD25^+$ CD4 T cells differs in treated and non-treated patients.

We then subdivided analyzed RA patients into two groups: non-treated (therapy naive) and treated patients. As shown in Figure 26 and Table 8, in $CD25^+$ CD4 T cells, the expression level of miR-146a in patients with non-treated RA was 2-fold lower as compared to patients with treated RA or healthy individuals, whereas patients with treated RA expressed comparable level of miR-146a to that of healthy individuals. After TCR stimulation, levels of miR-146a were significantly lower in patients with non-treated RA as compared to patients with treated RA or healthy individuals. On the other hand, in $CD25^-$ CD4 T cells, the expression level of miR-146a maintained in similar levels among different study groups (right panel, Figure 26A), suggesting a Treg-specific regulation of the expression pattern of this miRNA.

For the expression of miR-155, both non-treated patients and treated-patients up-regulated the expression of this miRNA in a similar level in response to activation (Figure 26B and Table 8). However, the expression levels of miR-155 in both RA groups were dramatically deceased as compared to that of healthy individuals. A similar finding was observed in $CD25^-$ CD4 T cells (right panel, Figure 26B), further confirmed that the expression pattern of miR-155 in RA is rather in a CD4 T cell context.

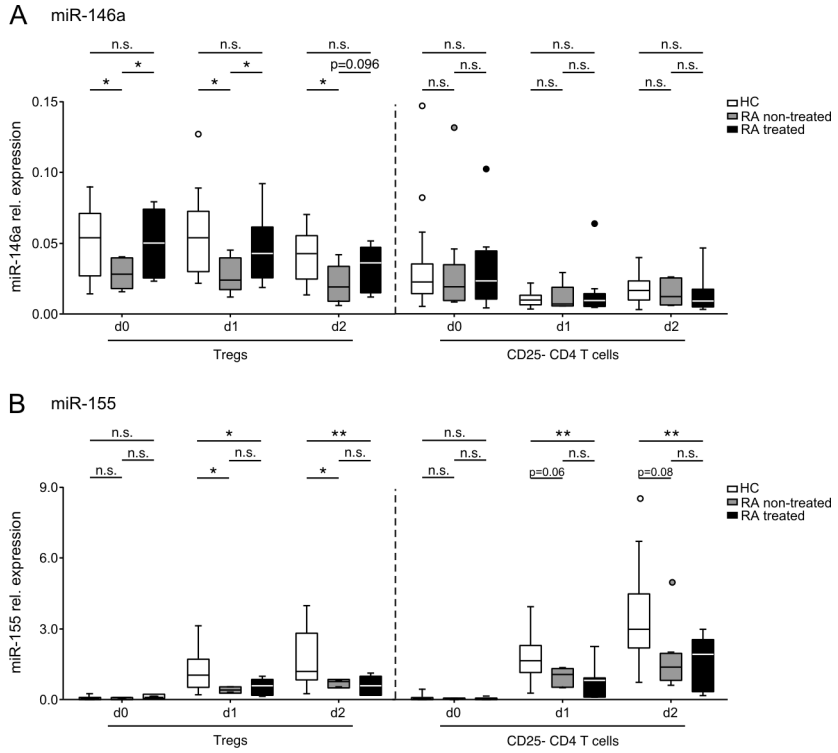

Figure 26. Expression of miR-146a and miR-155 in CD25$^+$ CD4 T cells in patients with RA stratified based on treatment.

CD25$^+$ and CD25$^-$ CD4 T cells were isolated and stimulated with anti-CD3/CD28 dynabeads for a total of two days. miRNA expression was assessed in freshly isolated cells (d0), at 24h (d1) and 48h (d2) by real-time PCR using TaqMan miRNA assays. miRNA expression in relation to expression levels of RNU48 is demonstrated. Expression level of miR-146a (**A**) and miR-155 (**B**) from 24 healthy individuals (HC) and patients with non-treated RA (n=9) and treated RA (n=10) is shown. Data are presented as box plots demonstrating minimum, maximum, median and 25th and 75th percentiles. Statistical analyses were performed by a Student's t-test. * $p<0.05$, ** $p<0.01$, *** $p<0.001$.

Table 8. Mean±SD and fold-change of miR-146a and miR-155 expression levels in patient groups stratified according to treatment.

miR-146a		Mean±SD			fold-change		
		HC	RA non-treated	RA treated	RA non-treated /HC	RA treated /HC	RA non-treated /RA treated
$CD25^+$	d0	0,04761±0,02555	0,03161±0,01370	0,04635±0,02417	0,664	0,974	0,682
	d1	0,05479±0,02684	0,02435±0,01361	0,04250±0,02315	0,444	0,776	0,573
	d2	0,04047±0,01684	0,02033±0,01287	0,03061±0,01629	0,502	0,756	0,664
$CD25^-$	d0	0,03313±0,03133	0,03472±0,03893	0,0325±0,02737	1,048	0,981	1,068
	d1	0,01045±0,004908	0,0105±0,009247	0,01481±0,01681	1,005	1,417	0,709
	d2	0,01726±0,01004	0,01453±0,008770	0,01306±0,01232	0,842	0,757	1,113
miR-155		Mean±SD			fold-change		
		HC	RA non-treated	RA treated	RA non-treated /HC	RA treated /HC	RA non-treated /RA treated
$CD25^+$	d0	0,05543±0,05309	0,04178±0,02390	0,04727±0,02491	0,754	0,853	0,884
	d1	1,130 ±0,7787	0,4326±0,1228	0,4891±0,3107	0,383	0,433	0,884
	d2	1,721 ±1,113	0,6968±0,1303	0,5866±0,3319	0,405	0,341	1,188
$CD25^-$	d0	0,07704±0,1010	0,03433±0,01845	0,04091±0,05440	0,446	0,531	0,839
	d1	1,733±0,9322	0,9617±0,3518	0,7841±0,6023	0,555	0,452	1,227
	d2	3,509±1,914	1,986±1,554	1,581±1,020	0,566	0,451	1,256

III.3.4 Expression level of miR-146a but not of miR-155 in $CD25^+$ CD4 T cells differs in RA groups stratified according to treatment efficacy.

To further investigate the association of miR-146a and miR-155 expression to treatment efficacy, patients with RA received treatment on the day of sample collection were further subdivided into two groups: patients with active RA (DAS≥2.6) and patients with remitted RA (DAS<2.6) (Figure 27). In freshly isolated $CD25^+$ CD4 T cells, the expression level of miR-146a was higher in patients with remitted RA as compared to non-treated patients and patients with active RA, but in a comparable level to healthy individuals. After TCR stimulation, there was a trend that higher levels of miR-146a were expressed in $CD25^+$ CD4 T cells from patients with remitted RA as compared to non-treated patients and patients with active RA. The expression level of miR-146a in patients with remitted RA after TCR stimulation was comparable to that of healthy individuals (Figure 27A). In contrast, expression levels of miR-155 were comparable among all three RA groups, but all significantly lower as compared to healthy individuals (Figure 27B).

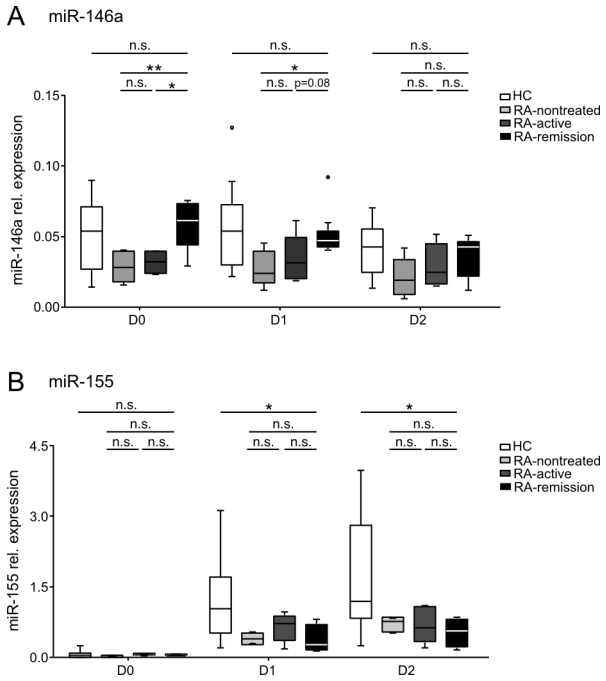

Figure 27. Expression of miR-146a and miR-155 in CD25$^+$ CD4 T cells in patients with RA stratified based on treatment efficacy.

CD25$^+$ and CD25$^-$ CD4 T cells were isolated and stimulated with anti-CD3/CD28 dynabeads for a total of two days. miRNA expression was assessed in freshly isolated cells (d0), at 24h (d1) and 48h (d2) by real-time PCR using TaqMan miRNA assays. miRNA expression in relation to expression levels of RNU48 is demonstrated. Expression level of miR-146a (**A**) and miR-155 (**B**) from 24 healthy individuals (HC), 9 non-treated RA, 5 active RA (DAS≥2.6) and 5 patients with remitted RA (DAS<2.6) is shown. Data are presented as box plots demonstrating minimum, maximum, median and 25th and 75th percentiles. Statistical analyses were performed by a Student's t-test. * $p<0.05$, ** $p<0.01$, *** $p<0.001$.)

III.3.5 Expression level of miR-146a but not of miR-155 in CD25$^+$ CD4 T cells differs in RA groups stratified according to disease activity.

Next, the analyzed RA patients were subdivided into two groups stratified according to disease activity: patients with active disease (DAS28>3.2) and patients with low disease activity (DAS28≤3.2). A dramatic difference of expression levels of miR-146a was observed between different patients groups in CD25$^+$ CD4 T cells (Figure 28A and Table 9). Whereas a similar expression level of miR-146a was observed between patients with low disease activity and healthy individuals, patients with active disease expressed significantly lower level of miR-146a. CD25$^+$ CD4 T cells from patients with active RA expressed around 1.5 to 2-fold lower levels of miR-146a as compared to healthy controls or patients with low disease activity. In CD25$^-$ CD4 T cells, no difference was observed among both RA patients groups and healthy individuals (right panel, Figure 28A). Taken together, our data imply a possible correlation of disease activity to the expression level of miR-146a.

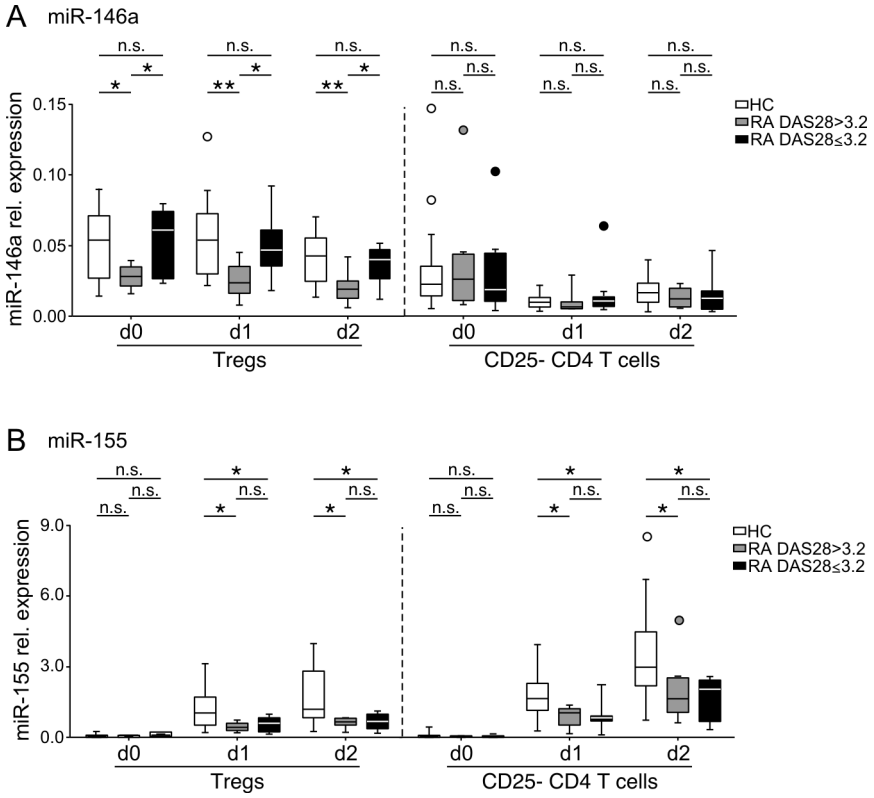

Figure 28. Expression of miR-146a and miR-155 in CD25$^+$ CD4 T cells in patients with RA stratified according to disease activity.
CD25$^+$ CD4 T cells were isolated and stimulated with anti-CD3/CD28 dynabeads for a total of two days. miRNA expression was assessed in freshly isolated cells (d0), at 24h (d1) and 48h (d2) by real-time PCR using TaqMan miRNA assays. miRNA expression in relation to expression levels of RNU48 is demonstrated. Expression level of miR-146a (**A**) and miR-155 (**B**) from 24 healthy individuals (HC), 4 patients with high disease activity (DAS28>5.1), 4 patients with moderate disease activity (3.2<DAS28≤5.1) and 11 patients with low disease activity (DAS28≤3.2) is shown. Data are shown as box plots demonstrating minimum, maximum, median and 25th and 75th percentiles. Statistical analyses were performed by a Student's t-test. * $p<0.05$, ** $p<0.01$, *** $p<0.001$.

Table 9. Mean±SD and fold-change of miR-146a and miR-155 expression levels in patient groups stratified according to disease activity.

miR-146a		Mean±SD			fold-change		
		HC	RA DAS28>3.2	RA DAS28≤3.2	RA DAS28 >3.2 /HC	RA DAS28 ≤3.2 /HC	RA DAS28>3.2 /RA DAS28≤3.2
$CD25^+$	d0	0,04761±0,02555	0,02821±0,008180	0,05334±0,008180	0,568	1,073	0,529
	d1	0,05479±0,02684	0,02560±0,01247	0,04976±0,02224	0,453	0,880	0,514
	d2	0,04047±0,01684	0,02018±0,01122	0,03646±0,01446	0,487	0,880	0,553
$CD25^-$	d0	0,03313±0,03133	0,03737±0,03597	0,03323±0,03193	1,128	1,003	1,125
	d1	0,01045±0,004908	0,01006±0,008058	0,01743±0,01926	0,963	1,668	0,577
	d2	0,01726±0,01004	0,01294±0,008012	0,01526±0,01397	0,750	0,884	0,848
miR-155		Mean±SD			fold-change		
		HC	RA DAS28>3.2	RA DAS28≤3.2	RA DAS28 >3.2 /HC	RA DAS28 ≤3.2 /HC	RA DAS28>3.2 /RA DAS28≤3.2
$CD25^+$	d0	0,05543±0,05309	0,03712±0,01953	0,05245±0,02460	0,670	0,946	0,708
	d1	1,130±0,7787	0,4378±0,1785	0,5395±0,3129	0,387	0,477	0,811
	d2	1,721±1,113	0,6273±0,2045	0,6632±0,3443	0,364	0,385	0,946
$CD25^-$	d0	0,07704±0,1010	0,03564±0,01881	0,04444±0,06381	0,463	0,577	0,802
	d1	1,733±0,9322	0,8805±0,4246	0,9037±0,6033	0,508	0,521	0,974
	d2	3,509±1,914	1,998±1,407	1,642±0,9423	0,569	0,468	1,217

For the expression of miR-155, both RA patients groups up-regulated the expression of this miRNA to a similar level in response to TCR stimulation in $CD25^+$ CD4 T cells (Figure 28B and Table 9). However, the up-regulation is less obvious as compared to healthy individuals (left panel, Figure 28B). These findings were also observed in $CD25^-$ CD4 T cells (right panel, Figure 28B).

III.3.6 Expression level of miR-146a in RA correlates with clinical parameters.

The expression of miR-146a in patients with RA was in a Treg-specific manner (Figure 25A) and a possible correlation of disease activity was implied to the expression level of miR-146a (Figure 28A). Hence, we performed correlation analysis of the expression of miR-146a in $CD25^+$ CD4 T cells to clinical parameters in a greater detail (Figure 29).

Disease activity score DAS 28 was negatively correlated with the expression levels of miR146a (Figure 29A). For the parameters indicating local inflammation, swollen joint count (SJC28, SJC66) and tender joint count (TJC28, TJC68) were inversely correlated with the

expression of miR-146a (Figure 29B, C). On the other hand, for the parameters indicating systemic inflammation, no obvious correlations were observed between CRP, ESR and miR-146a expression (Figure 29D, F). Therefore, our data reveal that the expression of miR-146a in $CD25^+$ CD4 T cells from patients with RA correlates with clinical parameters, especially with the ones suggesting the local joint inflammation.

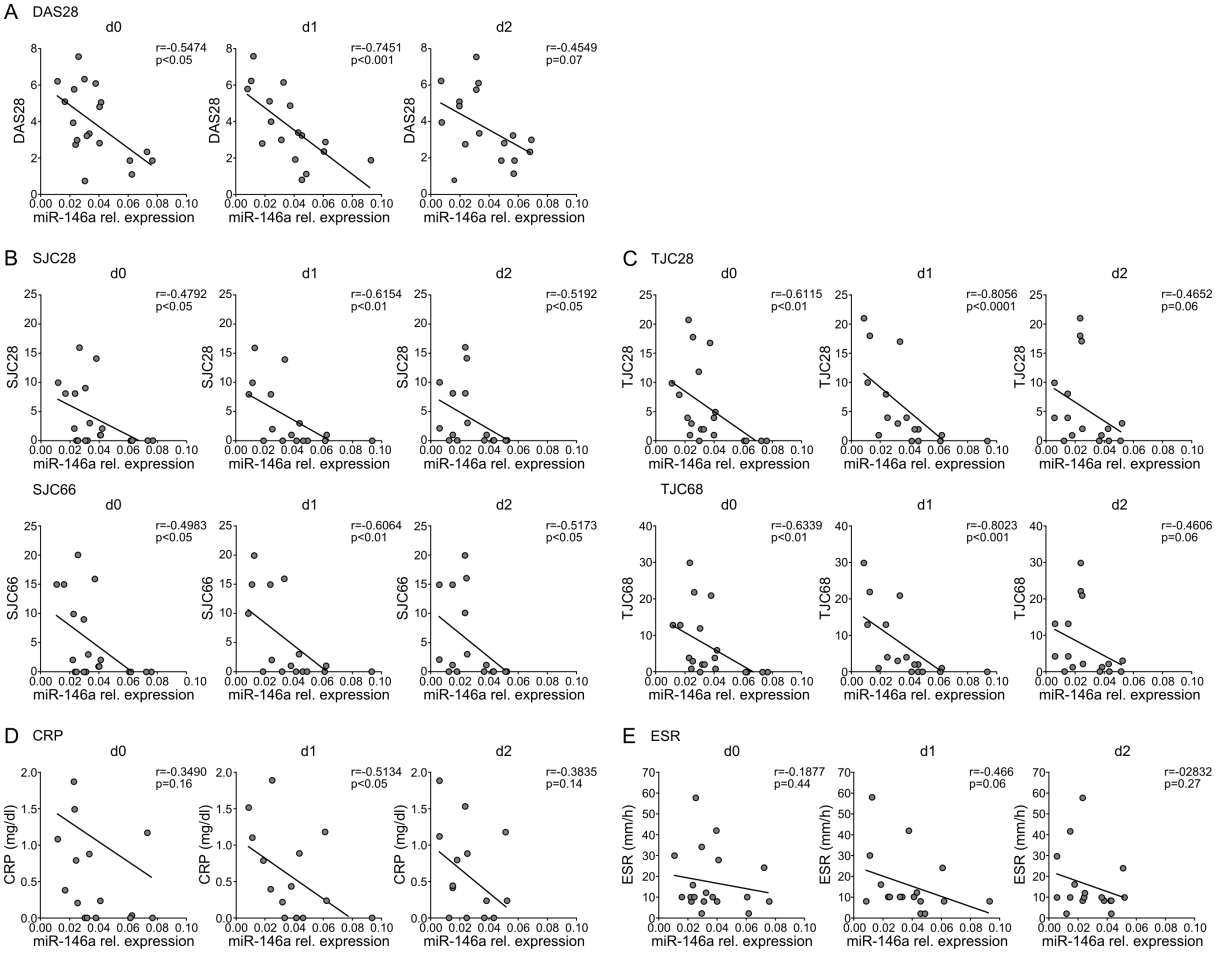

Figure 29. Correlation of clinical scores to the expression levels of miR-146a in $CD25^+$ CD4 T cells.
$CD25^+$ CD4 T cells were isolated from 19 patients with RA and stimulated with anti-CD3/CD28 beads for a total of two days. miRNA expression was assessed in freshly isolated cells (d0), at 24h (d1) and 48h (d2) by real-time PCR using TaqMan miRNA assays. miRNA expression in relation to the expression levels of RNU48 is demonstrated. Disease activity score in 28 joints (DAS28; with erythrocyte sedimentation rate [ESR]) (**A**), 28-swollen joint count (SJC28) and 66-swollen joint count (SJC66) (**B**), 28-tender joint count (TJC28) and 68-tender joint count (TJC68) (**C**), serum C-reactive protein (CRP) (**D**) and ESR (**E**) in patients with RA were plotted against miR-146a expression level from each time point (do, d1 and d2). Correlations were determined by Spearman's rank correlation coefficient.

III.3.7 Expression levels of miR-146a and miR-155 in RA do not associate with NF-κB signaling pathway.

Both miR-146a and miR-155 have been reported to contribute to a negative feedback loop of the NF-κB signaling pathway. The expression of these two miRNAs are positively regulated downstream of the NF-κB signaling and on the other hand they function as negative

regulators of the signaling pathway by targeting the genes within the pathway and promoting the inhibition of target gene expression (Ma et al.). To gain insight into the biological function of altered expression of miR-146a and miR-155 in patients with RA, we then assessed expression levels of their target genes involved in the NF-κB signaling in $CD25^+$ CD4 T cells from patients with RA and healthy individuals.

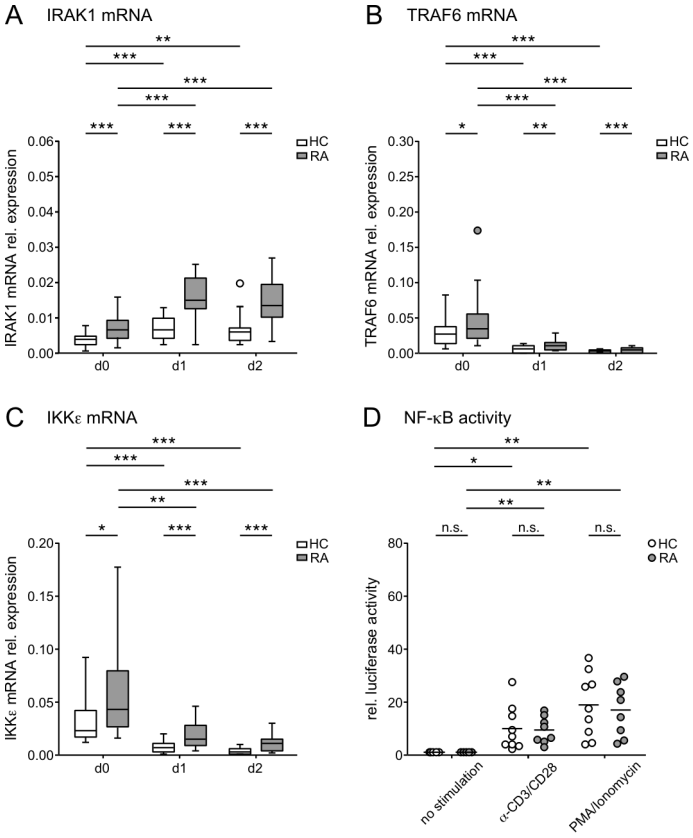

Figure 30. Expression of miRNA target genes involved in NF-κB pathway.
$CD25^+$ CD4 T cells were isolated and stimulated with anti-CD3/CD28 dynabeads for a total of two days. mRNA expression was assessed in freshly isolated cells (d0), at 24h (d1) and 48h (d2) by real-time PCR using TaqMan gene expression assays. mRNA expression in relation to expression levels of β-actin mRNA is demonstrated. Expression level of IRAK1 (**A**), TRAF6 (**B**) and IKKε (**C**) from 24 healthy individuals (HC) and 19 patients with RA is shown. Data are shown as box plots demonstrating minimum, maximum, median and 25th and 75th percentiles. (**D**) $CD25^+$ CD4 T cells were isolated and transfected with a NF-κB reporter vector (pGL4.32) and stimulated with either anti-CD3/CD28 beads or with PMA and ionomycin. Luciferase activity was analyzed 17 hours later. Relative luciferase activity from 9 HC and 8 RA patients is shown. Statistical analyses were performed by a Student's t-test. * $p<0.05$, ** $p<0.01$, *** $p<0.001$.

miR-146a regulates the expression of interleukin-1 receptor-associated kinase 1 (IRAK1) and TNF receptor associated factor 6 (TRAF6) (Iyer et al. 2012, Schulte et al. 2013), whereas miR-155 targets on I-kappa B kinase epsilon IKKε (Tili et al. 2007, Liang et al.). In response to TCR stimulation, expression of the IRAK1 mRNA was up-regulated in both patients with RA and healthy individuals (Figure 30A). On the other hand, expression of TRAF6 and IKKε was rather down-regulated (Figure 30B). Interestingly, expression levels of all three genes differed significantly between HC and patients with RA in both freshly isolated and

stimulated CD25$^+$ CD4 T cells. However, detection of NF-κB activity by transfecting cells with a NF-κB luciferase reporter vector revealed comparable luciferase activity between patients with RA and healthy individuals (Figure 30D). In addition, no correlation was observed between the expression levels of miR-146a or miR-155 and the NF-κB signalling pathway (Figure 31). Hence, the correlation between the expression levels of miR-146a or miR-155 to the NF-κB signaling pathway was not clear in CD25$^+$ CD4 T cells from patients with RA.

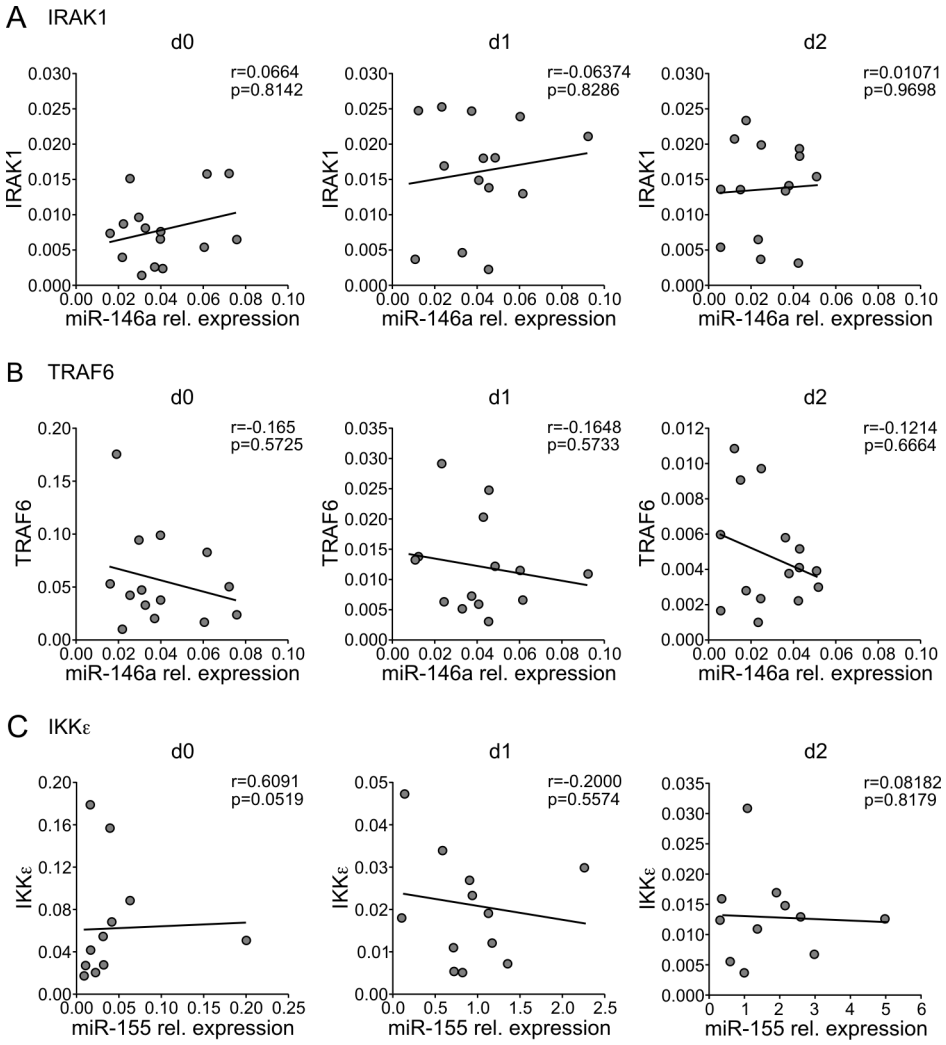

Figure 31. Correlation between expression levels of miR-146a and its targets IRAK1, TRAF6 and of miR-155 and its target IKKε in CD25$^+$ CD4 T cells in RA.
CD25$^+$ CD4 T cells from RA patients (n=11-14) were isolated and stimulated with anti-CD3/CD28 beads for a total of two days. miRNA expression and mRNA expression were assessed in freshly isolated cells (d0), at 24h (d1) and 48h (d2) after stimulation by real-time PCR using TaqMan miRNA assays and TaqMan gene expression assays. miRNA expression in relation to the expression levels of RNU48 and relative mRNA expression in relation to the expression levels of ß-actin mRNA are demonstrated. Expression levels of IRAK1 **(A)**, TRAF6 **(B)** mRNAs were plotted against the miR-146a expression levels at d0, d1 and d2. Expression levels of IKKε **(C)** were plotted against the miR-155 expression levels. Correlations were determined by Spearman's rank correlation coefficient.

III.3.8 Expression levels of miR-146a and miR-155 in RA correlate with expression of STAT1 and SOCS1.

We next analyzed two other genes, signal transducer and activator of transcription 1 (STAT1) and suppressor of cytokine signaling 1 (SOCS1) which have been reported to be the targets of miR-146a and miR-155 respectively in $CD25^+$ CD4 T cells from patients with RA (Kohlhaas et al. 2009, Lu et al. 2010, Lu et al. 2010). Again, the analyzed patient groups were stratified based on disease activity into two groups: patients with active disease (DAS28>3.2) and patients with low disease activity (DAS28≤3.2).

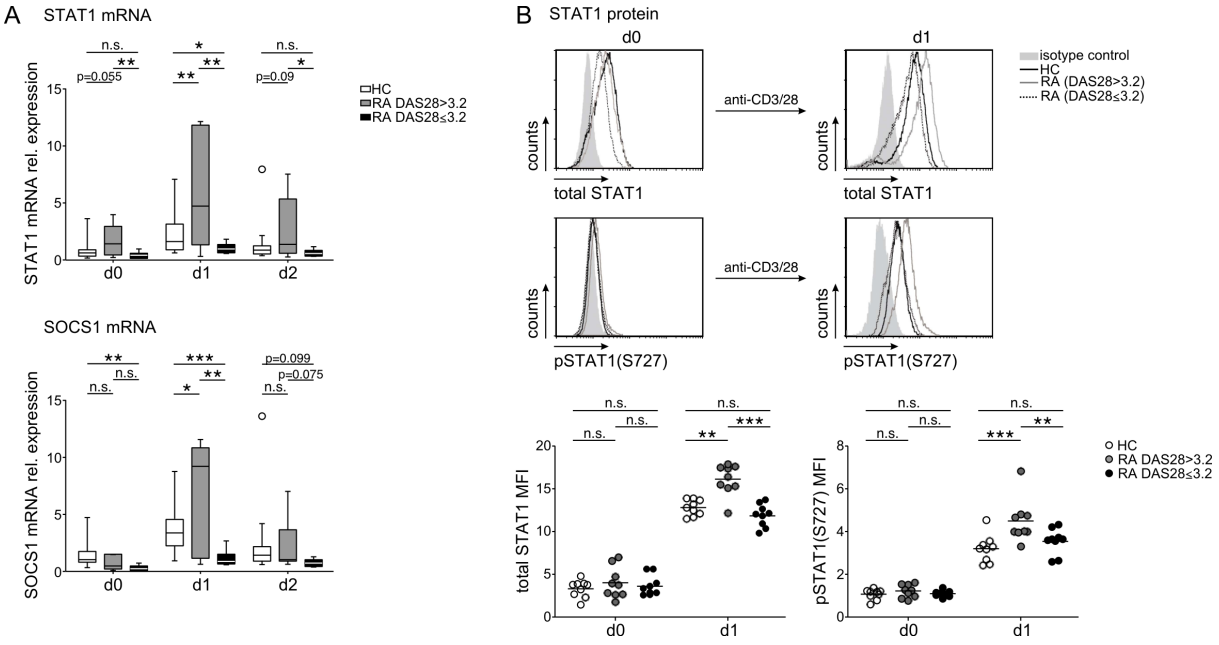

Figure 32 Expression of STAT1 and SOCS1 in patients with RA stratified according to disease activity. $CD25^+$ CD4 T cells were isolated and stimulated with anti-CD3/CD28 dynabeads for a total of two days. mRNA expression was assessed in freshly isolated cells (d0), at 24h (d1) and 48h (d2) by real-time PCR using TaqMan gene expression assays. mRNA expression in relation to expression levels of β-actin mRNA is demonstrated. Protein expression was assessed in freshly isolated (d0) and/or in 24h-stimulated (d1) cells by intracellular staining (STAT1). (**A**) Expression levels of STAT1 and SOCS1 from 22 healthy individuals (HC) and 19 RA patients are shown. Data are shown as box plots demonstrating minimum, maximum, median and 25th and 75th percentiles. (**B**) Expression of total STAT1 protein and of phosphorylated STAT1 (pSTAT1) was assessed as mean fluorescence intensity (MFI). Representative stainings are demonstrated in the upper panel. In the lower panel results from 9 HC and 18 RA patients are summarized. Patients were stratified according to disease activity: active RA - DAS28>3.2 and low disease activity - DAS28≤3.2. * $p < 0.05$, ** $p < 0.01$, *** $p < 0.001$ by Student's t-test.

Expression levels of STAT1 and SOCS1 were highly up-regulated in response to stimulation in healthy individuals (Figure 32). Strikingly, patients with active disease expressed significant higher level of STAT1 as compared to patients with low disease activity and healthy individuals, which correlated well with the diminished expression level of miR-146a in $CD25^+$ CD4 T cells from patients with active disease but not with low disease activity (Figure 32A and Figure 33A). Moreover, higher STAT1 protein expression and

phosphorylation in response to stimulation in patients with active disease was observed (Figure 32B). In contrast, expression of SOCS1 in $CD25^+$ CD4 T cells did not completely correlate with the expression pattern of miR-155 as shown in Figure 33B. While patients with active disease indeed expressed an increased level of SOCS1 corresponding to a down-regulated level of miR-155, patients with low disease activity showed diminished level of both miR-155 and SOCS1 (Figure 33B), suggesting that there is an additional mechanism controlling SOCS1 expression in $CD25^+$ CD4 T cells from patients with RA.

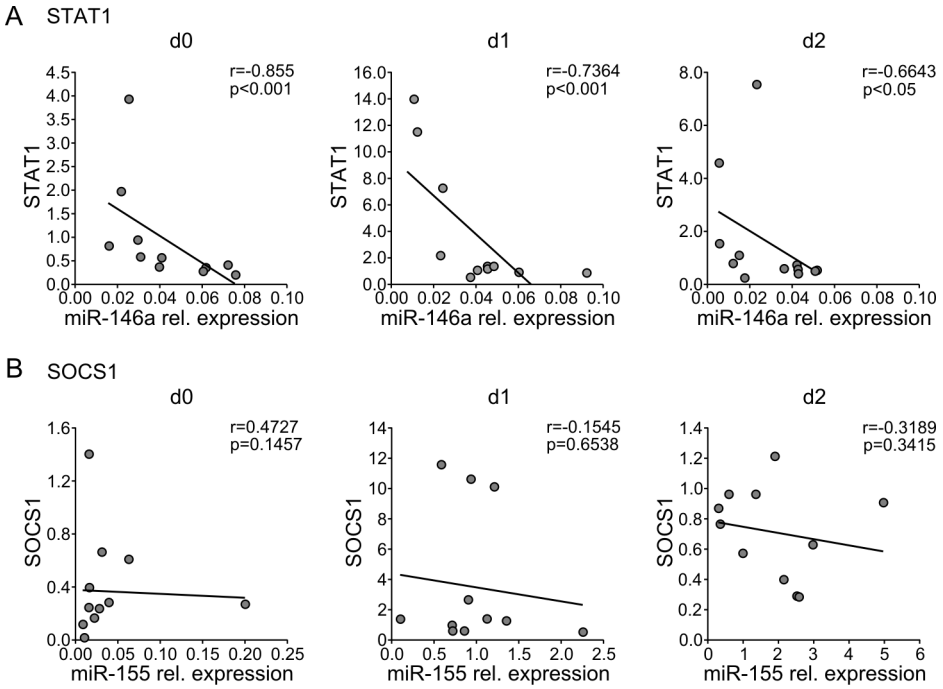

Figure 33. Correlation between expression levels of miR-146a and its target STAT1 and of miR-155 and its target SOCS1 in $CD25^+$ CD4 T cells in RA.
$CD25^+$ CD4 T cells from RA patients (n=11-14) were isolated and stimulated with anti-CD3/CD28 beads for a total of two days. miRNA expression and mRNA expression were assessed in freshly isolated cells (d0), at 24h (d1) and 48h (d2) after stimulation by real-time PCR using TaqMan miRNA assays and TaqMan gene expression assays. miRNA expression in relation to the expression levels of RNU48 and relative mRNA expression in relation to the expression levels of ß-actin mRNA are demonstrated. Expression levels of STAT1 **(A)** mRNA were plotted against the miR-146a expression levels at d0, d1 and d2. Expression levels of SOCS1 **(B)** were plotted against the miR-155 expression levels. Correlations were determined by Spearman's rank correlation coefficient.

III.3.9 Altered cytokine secretion pattern in $CD25^+$ CD4 T cells from patients with active RA.

The alteration of STAT1 and SOCS1 as a consequence of altered expression of miR-146a or miR-155 has been reported to modify CD4 T cells cytokine secretion profiles (Rodriguez et al. 2007, Thai et al. 2007, Lu et al. 2010). Therefore, expression of the pro-inflammatory cytokines, IL-2, TNF, IL-17 and IFNγ, was analyzed in $CD25^+$ CD4 T cell from patients with RA. As described above, two groups of RA patients were stratified based on disease activity:

patients with active disease (DAS28>3.2) and patients with low disease activity (DAS28≤3.2) **(**Figure 34).

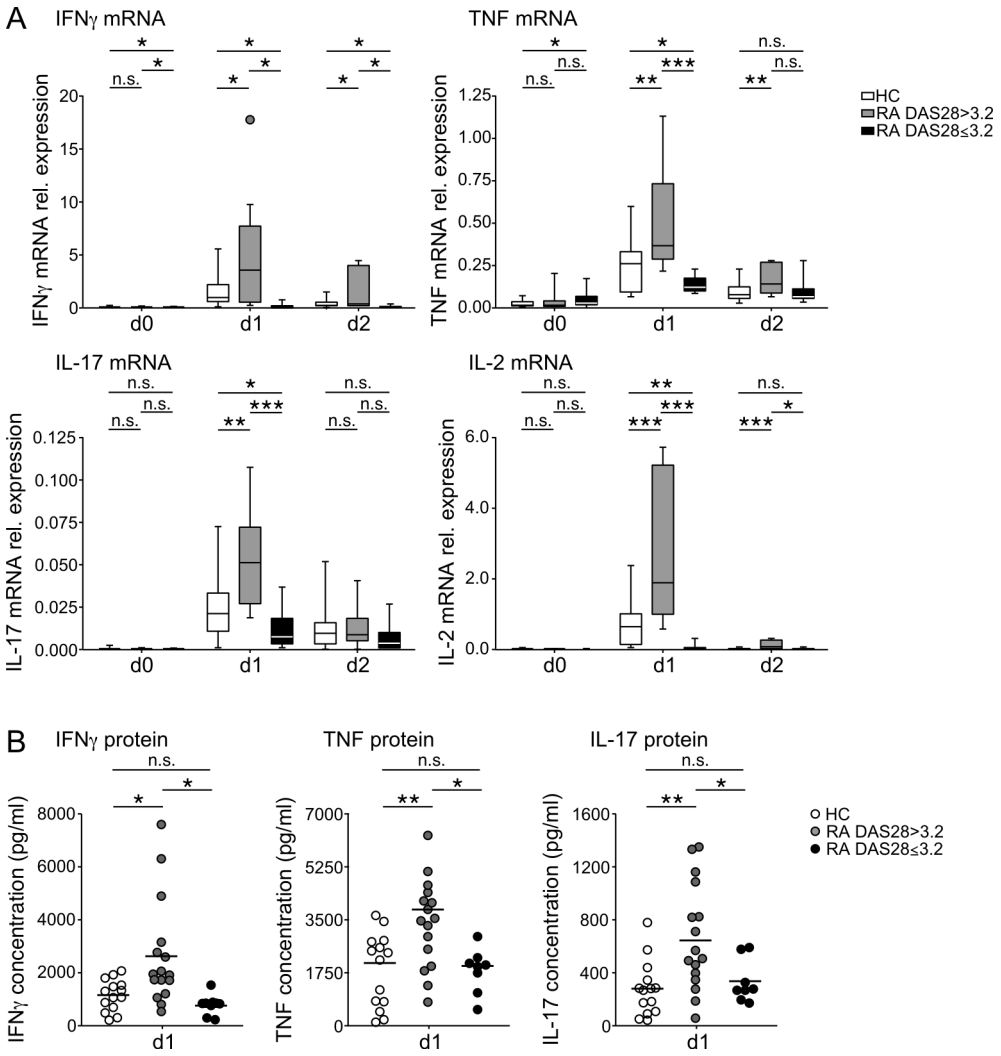

Figure 34 Analysis of cytokine expression in CD25$^+$ CD4 T cells from patients with RA stratified according to disease activity.

CD25$^+$ CD4 T cells were isolated and stimulated with anti-CD3/CD28 dynabeads for a total of two days. mRNA expression was assessed in freshly isolated cells (d0), at 24h (d1) and 48h (d2) by real-time PCR using TaqMan gene expression assays. mRNA expression in relation to expression levels of β-actin mRNA is demonstrated. (**A**) mRNA expression levels of IL-2, TNF, IL-17 and IFNγ from 22 healthy individuals (HC) and 19 RA patients are shown as box plots demonstrating minimum, maximum, median and 25th and 75th percentiles. (**B**) TNF, IL-17 and IFNγ at protein level were assessed in cell culture supernatants from 14 HC and 24 RA patients 24h after stimulation by ELISA. Patients were stratified according to disease activity: active RA - DAS28>3.2 and low disease activity - DAS28≤3.2. Statistical analyses were performed by a Student's t-test. * $p<0.05$, ** $p<0.01$, *** $p<0.001$.

Remarkably, cytokine productions by CD25$^+$ CD4 T cells were up-regulated in response to TCR stimulation within 24h and down-regulated after 48h in both patients with RA and healthy individuals. Patients with active disease expressed strikingly increased levels of all analyzed cytokines as compared to patients with low disease activity or healthy individuals. In contrast, patients with low disease activity expressed even diminished levels of pro-inflammatory cytokines as compared to healthy individuals. The changes in cytokine mRNA

after 24 of stimulation in Tregs of patients with active disease were reflected by cytokine concentrations in cell culture supernatants (Figure 34B). Taken together, our data suggest that altered expression of miR-146a and miR-155 levels in $CD25^+$ CD4 T cells might indeed result in an altered Treg phenotype of these cells.

III.3.10 Cytokine secretion pattern but not the suppressive capacity of Tregs correlates with miR-146 and miR-155 expression.

To verify the hypothesis that changes in miR-146a and miR-155 expression might result in an impaired Treg phenotype in RA, we analyzed cytokine expression in $CD25^+$ CD4 T cells treated with either mimics or antagomirs of miR-146a and miR-155 (Figure 35A). Treatment with mimics of miR-146a reduced the pro-inflammatory cytokine secretion whereas mimics of miR-155 increased the cytokine production. Neutralization of endogenous miRNAs by the treatment of antagomirs resulted in opposite consequences. Interestingly, when both miRNAs were mimicked or neutralized simultaneously the cytokine secretion profile was rather similar to that observed by altering miR-146a biological activity, suggesting a predominant role of miR-146a over miR-155 in $CD25^+$ CD4 T cells (Figure 35A). The interference of miR-146a also resulted in significant alterations in STAT1 expression and phosphorylation (Figure 35B). Whereas cells treated with miR-146a mimics showed diminished STAT1 expression and phosphorylation, neutralization of the miRNA by antagomirs increased both. Remarkably, despite the pronounced effect on cytokine expression profile intervention with the expression of these two miRNAs did not affect the *in vitro* suppressive capacity of Tregs (Figure 35C).

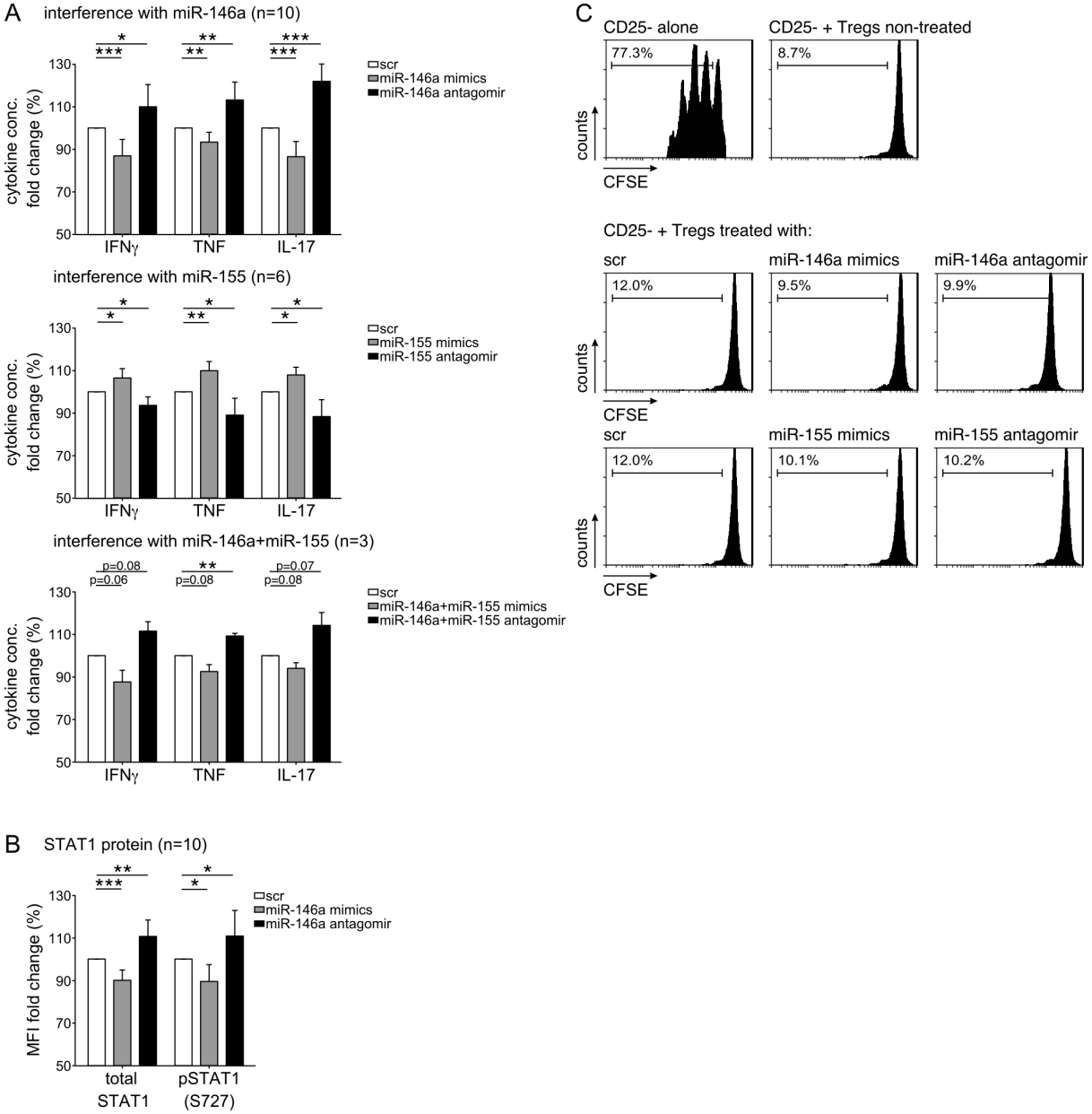

Figure 35. Effect of miR-146a and miR-155 on Treg cytokine production and suppressive capacity.
$CD25^+$ CD4 T cells were isolated, transfected with mimics or antagomirs of miR-146a or miR-155 and (**A, B**) stimulated with anti-CD3/28. 24h after stimulation IFNγ, TNF and IL-17 were assessed in cell culture supernatants by ELISA (A) or expression and phosphorylation status of STAT1 (total STAT1 and pSTAT1, respectively) were assessed intracellularly based on MFI (B). Data are shown as fold changes normalized to cells transfected with scrambled (scr) oligos. Mean ± SD of 3 to 10 experiments are shown. (**C**) To verify the effect of intervention with miRNA activity on the suppressive capacity of Tregs CD25- CD4 T cells were isolated in addition and labeled with CFSE. Transfected Tregs were cultured with CFSE-labeled CD25- CD4 T cells in a 1:1 ratio in the presence of anti-CD3 and feeder cells for four days. Proliferation of CD25- CD4 T cells was assessed by flow cytometry based on CFSE dilution. One representative experiment of three experiments is depicted. * $p<0.05$, ** $p<0.01$, *** $p<0.001$ by Student's t-test.

III.3.11 Serum levels of miRNA-146a and miR-155 as potential biomarkers in RA.

Recent publication has highlighted the possibility to use circulating miRNAs as biomarkers to diagnose and prognose human diseases (Grasedieck et al. 2013). We therefore analyzed the expression level of miR-146a and miR-155 in serum from patients with RA. The expression level of circulating miR-146a was dramatically lower in patients with RA as compared to healthy individuals. In contrast, the expression of miR-155 was in a comparable level between patients with RA to healthy individuals (Figure 36A). We further stratified the analyzed RA patients according to disease activity into two groups: patients with active disease (DAS28>3.2) and patients with low disease activity (DAS28≤3.2). Whereas patients with low disease activity expressed comparable level of circulating miR-146a and circulating miR-155 as compared to healthy individuals, a strikingly lower level of circulating miR-146a and circulating miR-155 was observed in patients with active disease as compared to patients with low disease activity and healthy individuals. These data together suggested expression levels of circulating miR-146a and miR-155 in serum might be used as biomarkers for prediction of active phases of the disease in RA.

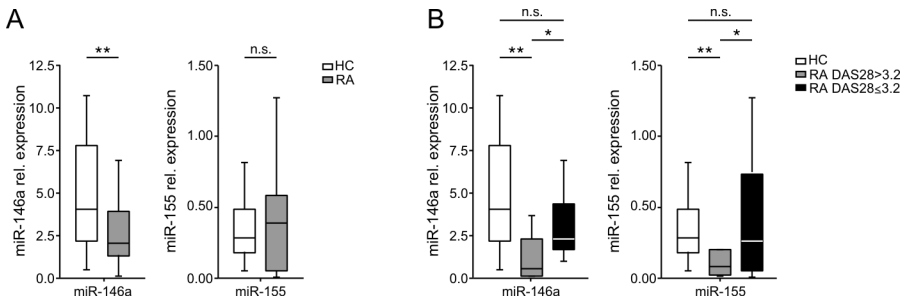

Figure 36 Expression level of circulating miR-146a and miR-155 in patients with RA.
miRNA was excessed in RNA isolated by real-time PCR using TaqMan miRNA expression assays. miRNA expression in relation to expression levels of RNU48 is demonstrated. Expression level of miR-146a and miR-155 from (**A**) 24 healthy individuals (HC) and 19 RA patients or (**B**) 24 healthy individuals (HC), 8 patients with active disease (DAS28>3.2) and 11 patients with low disease activity (DAS28≤3.2) is shown. Data are shown as box plots demonstrating minimum, maximum, median and 25th and 75th percentiles. Statistical analyses were performed by a Student's t-test. * $p<0.05$, ** $p<0.01$, *** $p<0.001$.

4 Discussion

Tregs, including nTregs and iTregs, are important for tightly controlling destructive immune response to pathogens and sustaining immunological self-tolerance and homeostasis (Ohkura et al.). A failure in the expansion and the function of Tregs and as a consequence an uncontrolled effector T cells expansion and pro-inflammatory cytokine production will result in autoimmune diseases, including RA (Frey et al. 2010, Pesce et al. 2013). miRNAs have been shown to be involved in the process by mediating post-transcriptional regulation of target genes of the immunological processes. (Iliopoulos et al. 2009, Kawai and Akira 2010). Thereby, it is of great interest to understand the detailed function of miRNAs in their regulation of Tregs and their contribution to the pathogenesis of autoimmune disease, especially RA.

4.1 miR-142-3p mediated GARP expression in Tregs

In the first part of the study, miRNA-mediated regulation of GARP expression was dissected in human regulatory $CD25^+$ CD4 T cells. One specific miRNA, miR-142-3p, was identified to target the distal part of GARP 3'UTR and to perform post-transcriptional regulation.

miR-142-3p was predicted by Diana Lab (Maragkakis et al. 2009) and Target Scan (Lewis et al. 2005) to recognize its MRE located in CNS5 region of GARP 3'UTR, which is the distal 187-bp long conserved region that is 76.2% homologous to the mouse GARP 3'UTR. Besides miR-142-3p, several other miRNAs were also predicted in this region which might be capable of recognizing GARP mRNA. However, only miR-142-3p and miR-424 were able to recognize their MREs in the context of GARP 3'UTR using artificial luciferase reporter system. In addition, site-directed mutation of MREs abolished their modulatory effects on the activity of GARP 3'UTR. Thus, these observations demonstrated that MREs of miR-142-3p, as well as miR-424 in the GARP 3'UTR are responsible for respective miRNA binding.

Yet, analysis of miR-142-3p and miR-424 expression in $CD25^+$ CD4 T cells revealed constant expression of miR-142-3p as described previously (Liston et al. 2008), but reported very low level of miR-424 expression. Indeed both the neutralization of endogenous miR-142-3p and mutation of its binding sites in $CD25^+$ CD4 T cells restored the reporter gene activity. In contrast, neither the inhibition of the biological activity of endogenous miR-424 nor the mutation of its MRE in the GARP 3'UTR showed any effects in the $CD25^+$ CD4 T cells.

Hence, our data indicated that only miR-142-3p is involved in the post-transcriptional regulation of GARP in $CD25^+$ CD4 T cells, whereas the expression level of miR-424 in the Tregs is not sufficient to have any effect. Moreover, we observed a cooperation of this miRNA with GARP mRNA in Ago2-associated RISC. A recent study using next-generation sequencing of co-precipitated RNAs (RIP-Seq) demonstrates miRNA-specific accessibilities and Ago2-RISC loading efficiencies and suggests that miRNAs function can only be achieved when they are incorporated into RISC complexes (Meier et al. 2013). Therefore, our findings of the co-occurrence of miR-142-3p and GARP mRNA in the Ago2-associated RISC further strengthened our hypothesis that miR-142-3p is involved in the regulation of GARP expression by initiating mRNA degradation.

The complementarity between the target mRNA and the seed region comprising 2-8 nucleotides of miRNA largely contributes to the activity of miRNA, resulting either mRNA degradation by perfect complementarity or on the other hand inhibition of translation. (Williams 2008, Eulalio et al. 2009). When fully complementary base pairing occurs between miRNA seed sequence and target mRNA, the miRNA/mRNA duplex preferentially loads into Ago2-associated RISC and results in mRNA degradation; whereas if unpaired bulges exist between miRNA seed sequence and target mRNA, the duplex loads into Ago1-RISC and leads to translational repression (Meister et al. 2004, Czech et al. 2008, Pratt and MacRae 2009). The recognition of miR-142-3p to its MRE in the GARP 3'UTR is a 8mer motif with a perfect complementarity. Our RNP-IP data positively confirmed that the cause of sequential diminished expression of GARP mRNA by miR-142-3p is associated with Ago-2 mediated mRNA degradation pathway.

The relationship between miR-142-3p and GARP expression pattern in the $CD25^+$ CD4 T cells is well matched to our above indication that miR-142-3p functions as a post-transcriptional inhibitor of GARP. Whereas expression of miR-142-3p arose at 48h and 72h after TCR stimulation, the initial transcription of GARP mRNA was already detectable 4h after stimulation (observations from our lab), reached peak value at 24h, diminished at 48h, and completely disappeared at 72h after TCR-triggering. The inverse correlation in the sequential expression of both counterparts is consistent with function of miR-142-3p as a post-transcriptional repressor of GARP. This finding provided an experimental support of the theory that there is a mutual exclusive interplay between miRNA and its target, which was firstly identified in *Drosophilla* (Stark et al. 2005). Interestingly, an abundant expression of miR-142-3p was detected in freshly isolated $CD25^+$ CD4 T cells, observed by us and other

groups independently (Huang et al. 2009). These findings are understandable by considering the fact that it is evolutionarily necessary to have a more strict control of transcriptional activity in order to diminish the noise of gene expression during cell fate decision (Cohen et al. 2006). Indeed, the inhibition of miR-142-3p biological activity by transfecting $CD25^+$ CD4 T cells with an antagomir directly after activation resulted in higher levels of GARP expression.

Human cells express thousands of miRNAs, targeting more than half of the genes (Bentwich et al. 2005, Lewis et al. 2005, Friedman et al. 2009). The post-transcriptional regulation of the target genes expression by miRNAs is adapted depending on cell types and is identical within same cell type. Instead of functioning as an on-off switch, miRNAs modulate the expression of their target genes by impacting the gene expression from 1.2- to 4- fold (O'Neill et al. 2011, O'Connell et al. 2012). Indeed, inhibition of endogenous miR-142-3p level by an antagomir led to an immediate reduction in the endogenous miR-142-3p expression level in $CD25^+$ CD4 T cells and subsequently a ~1.5-fold increase in the GARP expression, whereas when $CD25^+$ CD4 T cells were transfected with a mimic of miR-142-3p, an accession was detected in miR-142-3p level and as a consequence, a ~2-fold diminution of GARP mRNA and protein expression was observed. To ask whether these small differences in the gene expression level especially the protein concentration can have meaningful physiological effects, studies have been performed using heterozygous mice lacking a single copy of gene which causes the loss of about half of the protein. PU.1 heterozygous mice display overproduction of granulocytes over macrophage during hematopoietic development (Dahl et al. 2003). Moreover, insufficient expression of SOCS1 level in the heterozygous mice results in hypersensitivity to endotoxemia (Kinjyo et al. 2002). These findings suggest that miRNA-mediated few-fold change on gene expression is physiologically important in controlling a dosage-sensitive phenotype.

The expression of miR-142-3p has been detected in B cells and T-cell subsets and has been suggested to mediate lineage differentiation of T lymphocytes (Chen et al. 2004, Sun et al. 2011). In the present study, we showed that miR-142-3p interfered the proliferation of $CD25^+$ CD4 T cells. In addition to an obviously higher expression level of GARP, inhibition of biological activity of miR-142-3p by the antagomir led to increased proliferation. Furthermore, cells with overexpressed miR-142-3p displayed a diminished expression of GARP, which was accompanied by deducted proliferation capacity of the cells. However, as it is well accepted, one miRNA can target on multiple genes from the same signaling pathway

(Friedman et al. 2009). *In silico* prediction of putative miR-142-3p target resulted in a list consisting of hundreds of genes. Indeed, 18 genes from the list have been further identified by gene ontology analysis to involve in the cell cycle processes. Therefore, it is of great importance to bring expedient evidence to rebut such concerns. Ectopic expression of GARP in $CD25^-$ CD4 T cells with a vector encoding only the GARP coding sequence showed increased proliferation capacity as compared to cells transfected with control vector. Furthermore, in the presence of miR-142-3p MRE downstream of GARP coding sequence, miR-142-3p was able to disturb the ectopical GARP expression and sequentially abrogated cell proliferation. However, when the mutated MRE was introduced, miR-142-3p failed to suppress GARP expression and the proliferation of cell was restored as a result of recovered GARP expression. These data strongly supported the direct effect of miR-142-3p, by targeting GARP, in the modulation of CD4 T cell proliferation.

We then explored the function of GARP in $CD25^+$ CD4 T cells by RNAi including the usage of miRNA and siRNA. After transfecting cells with a mimic of miR-142-3p, which diminished GARP expression on the cell surface, $CD25^+$ CD4 T cells showed a consistent reduction of their suppressive capacity. These findings are in line with description using *in vitro* expanded $GARP^+$ $CD25^+$ clones (Wang et al. 2009). Moreover, as described above, GARP was important in the modulation of T cell homeostasis through miR-142-3p mediated post-transcriptional regulation. siRNA knock-down of ectopically expressed GARP in Hela cells further confirmed these findings, although the molecular mechanisms behind is not understood. Cells with lower GARP expression on the cell surface presented a slower cell cycle progression, as well as elevated expression of proteins function as inhibitors of cell cycle, such as p53, p21/Cip1 and p27/Kip (observations from our lab). Therefore, we attempted to investigate the possible intracellular connection of GARP to these molecules using SILAC-associated immunoprecipitation. Indeed, 5 candidates were suggested, however, none of them were further confirmed by later experiments. Hence, further deep investigations are desirable in order to explore the molecular mechanism of GARP in modulating cell proliferation.

Taken together, we identify miRNA-142-3p as the miRNA regulating GARP expression on regulatory $CD25^+$ CD4 T cells. GARP mRNA is up-regulated in $CD25^+$ CD4 T cells in response to TCR stimulation. The expression of GARP promotes cell proliferation and contributes to Treg suppressive function. Sequentially, expression of miR-142-3p is up-regulated and initiates Ago2-mediated degradation of GARP mRNA by perfect

complementarity of the seed region to its target sequence within the GARP 3'UTR. Therefore, GARP expression is damped and the expansion of $CD25^+$ CD4 T cells is controlled.

4.2 Elevated expression of miR-142-3p and reduced GARP expression in Tregs from patients with RA

Given the observation that miR-142-3p-mediated regulation of GARP expression contributes to the proliferation and function of human regulatory $CD25^+$ CD4 T cells, we therefore in the second party of the study followed their expression in patients with RA. We demonstrated a delineation of miR-142-3p expression and the linked GARP expression in RA. Moreover, we showed difference in the SNP alleles, genotype and haplotype frequency in GARP 3'UTR region between RA and healthy individuals (HC), which provided an important hint to understand the mechanism driving reduced GARP expression in RA.

We observed a diminished expression of GARP in $CD25^+$ CD4 T cells from patients with RA. GARP was identified as a specific marker on human $CD25^+$ CD4 T cells after TCR stimulation by microarray analysis (Wang et al. 2008, Probst-Kepper et al. 2009). The induction of GARP expression in $CD25^+$ CD4 T cells is Foxp3-dependent (Wang et al. 2008, Probst-Kepper et al. 2010). IL-2 and IL-4, but not TGF-β or retinoic acid can induce the expression *in vitro* (Edwards et al. 2013, Haupt et al. under preparation). GARP has been reported as a potential receptor of latent TGF-β (Stockis et al. 2009, Chan et al. 2011). Wang and colleagues show that GARP captures latent TGF-β by forming disulfide bonds on Cys-192 and Cys-331 and presents it on the cell surface (Wang et al. 2012). Expression of GARP on cell surface co-occurs with the surface expression of latent TGF-β (Edwards et al. 2013) Ectopic expression of GARP in effector T cells leads to Treg-like phenotype with suppressive capacity (Wang et al. 2008, Probst-Kepper et al. 2010). Down-modulation of GARP expression by specific siRNA in Tregs results in impaired Treg suppressive function (Probst-Kepper et al. 2010). In addition, our previous results also suggest an alternative fuction of GARP by contributing to the proliferation of human $CD25^+$ CD4 T cells. Moreover, mice lacking GARP in CD4 T cells or in Foxp3-expressing Tregs show lower $CD25^+$ regulatory T cell numbers in inflamed tissues (observations from our lab). Thereby, the diminished expression of GARP in Tregs from RA patients may contribute to RA pathogenesis by affecting the function and the frequency of Tregs in the patients, which is in line with pervious findings (Bayry et al. 2007, Han et al. 2008, Kawashiri et al. 2011, Matsuki et al.).

Our previous results have shown that miR-142-3p involved in the post-transcriptional regulation of GARP expression in $CD25^+$ CD4 T cells. Inversely correlated to the expression of GARP in $CD25^+$ CD4 T cells from RA, the expression of miR-142-3p in these cells was unsurprisingly higher than in the healthy individuals. miR-142-3p has been reported to be abundantly expressed in hematopoietic cells and is important for the function of dendritic cells and T cells (Sun et al. 2011). The expression of this miRNA is deregulated in leukemia (Huang et al. 2009, Lv et al. 2012). By targeting on MLL-AF4 (Dou et al. 2013)or gp130 (Sonda et al. 2013), miR-142-3p prohibits cell proliferation and macrophage differentiation in leukemia and myelopoiesis. Our data provide another aspect of the important role miR-142-3p might play in the pathogenesis of human disease by targeting on GARP. Interestingly, in patients with RA, GARP expression negatively correlates with disease activity, whereas the expression of miR-142-3p positively correlates with disease activity. These observations may suggest an important evidence of Treg-specific functional association during disease development.

The SNP alleles, genotype and haplotype frequency in GARP 3'UTR region varied between RA and HC. Polymorphisms in the 3'UTR of a gene may enhance the disease risk by increasing the recognizing affinity of miRNA binding sites. For instance, the rs8126 T>C site in miR-184 binding site of *TNFAIP2* is identified to contribute to the risk with gastric cancer; several SNPs localized in the miRNA binding sites of APOL6 are associated with metabolic syndrome in Chinese Han population (Xu et al. 2013, Ye et al. 2013). Hereby, our findings brought a new concept to understand the diminished expression of GARP expression in patients with RA in the context of post-transcriptional regulation, although further investigations are yet required.

Taken together, we conclude that miR-142-3p expression in regulatory $CD25^+$ CD4 T cells might modulate the proliferative capacity of the cells and therefore interferers with disease pathogenesis. The SNPs in the GARP 3'UTR might associate with the risk of disease susceptibility.

4.3 Decreased expression of miR-146a and miR-155 in patients with RA

In the last part of the study, two additional miRNAs, miR-146a and miR-155, were assessed in $CD25^+$ CD4 T cells from patients with RA. We demonstrated a deregulated expression of miR-146a and miR-155. The altered expression of these two miRNAs may interfere cytokine

signaling pathway directly and result in an altered cytokine production pattern, which may contribute to the disease pathogenesis.

The expression of miR-146a and miR-155 were both attenuated in $CD25^+$ CD4 T cells from patients with RA as compared to healthy individuals. However, these two miRNAs showed different expression pattern in the context of CD4 T cells. The diminished expression of miR-146a was in a Treg-specific pattern, whereas the diminished expression of miR-155 can be observed in both $CD25^+$ CD4 T cells and $CD25^-$ CD4 T cells, suggesting their altered characteristic in RA. miR-146a and miR-155 have been reported to be widely expressed and involved in the controlling of innate and adaptive immune response (Rodriguez et al. 2007, Kawai and Akira 2010). miR-146a, by inhibiting the expression of TRAF6 and IRAK1, plays an important role in a negative feedback loop to dampen the downstream NF-κB activation and attenuate the expression of pro-inflammatory cytokines such as IL-6 and TNFα (Boldin et al. 2011, Zhao et al. 2011). miR-155 is involved in the NF-κB pathway by targeting on IKKε (Tili et al. 2007, Liang et al.). Based on the above reports, we therefore firstly investigated the effect of miR-146a and miR-155 in the regulation of NF-κB activity in $CD25^+$ CD4 T cells from RA. We observed elevated mRNA levels of TRAF6, IRAK1 and IKKε, however, no difference at the downstream NF-κB activity was detected. These data revealed that there might be other signaling pathways, which are targeted by miR-146a and miR-155 in human cells.

It has been reported that miR-146a can down-regulate the expression of STAT1 and play a crucial role in Tregs for mediating Th1 response (Lu et al. 2010). On the other hand, miR-155 accelerates the immune response by targeting on SHIP1 and SOCS1 (Androulidaki et al. 2009, O'Connell et al. 2009). In our human originated system, however, a fine correlation was observed between the expression levels of miR-146a and STAT1, but not between miR-155 and SOCS1. Further detailed investigation by stratifying patients groups according to disease activity indicated that patients with active disease possessed elevated level of STAT1 as a result of attenuated expression level of miR-146a; patients with low disease activity expressed comparable level of STAT1 as an effect of a similar level of miR-146a as compared to HC. In contrast, the expression of miR-155 in patients with both active disease and low disease activity was decreased as compared to HC, however, the sequential elevated expression of SOCS1 was only detected in patients with active disease, suggesting other mechanisms are involved in the controlling of SOCS1 expression in $CD25^+$ CD4 T cells from RA patients.

In vivo studies indicate that mice deficient in miR-146a have high disease susceptibility to collagen-induced arthritis suggesting a protective effect of this miRNA (Nakasa et al. 2011). Moreover, miR-155 is important for the clonal expansion of activated effector CD4 T cells by repressing B-cell integration cluster (BIC) and miR-155 deficient mice show failures in producing Th1 and Th17 cells in autoimmune inflammation (Rodriguez et al. 2007, Kurowska-Stolarska et al. 2011, Oertli et al. 2011). These published reports suggest contrary effects of miR-146a and miR-155 in immune response. Whereas miR-146a functions as an anti-inflammatory miRNA, miR-155 is rather a pro-inflammatory miRNA. In our hands, expression of miR-146a and miR-155 in patients with active disease showed similar contrary effects on their target genes expression. The diminished level of miR-146a led to an elevated level of STAT1 expression, thus might promote the cells towards a pro-inflammatory phenotype. In contrast, the reduced level of miR-155 resulted in an increased expression of SOCS1, which might protect the cell from inflammation. Moreover, interferences of miRNA biological function using miRNA mimics or antagomirs led to an opposite effect on cytokine production. Nevertheless, the overall phenotype of the $CD25^+$ CD4 T cells from patients with active disease was rather pro-inflammatory, supported by their elevated expression levels of pro-inflammatory cytokines, such as IL-2, IL-17, TNF and IFNγ. This could be further confirmed by the findings where we interfered with the biological activity of both miRNAs simultaneously. Hence, one may surmise that the resulting pro-inflammatory effect by reduced miR-146a expression augments the counteracting protecting effect by reduced miR-155 expression, leading to an overall pro-inflammatory phenotype of the cells in Tregs from RA.

The further evidence about the predominant effect of miR-146a over miR-155 was demonstrated in the correlation of their expression levels to clinical parameters. Only miR-146a expression level but not miR-155 was observed to be negatively correlated with disease activity score, DAS28. Interestingly, the expression of miR-146a was further inversely correlated with the parameters indicating local joint inflammation, e.g. TJC and SJC, but not with those indicating systemic inflammation, e.g. CRP and ESR. These results indicate that phenotype alternation by miR-146a was in particular important for local inflammation. Indeed, previously publication has reported that miR-146a prevented bone destruction although it was unsuccessful to completely amend inflammation (Nakasa et al. 2011). In patients with SLE, a decreased level of miR-146a is suggested to associate with kidney inflammation, but not with systemic inflammation (Tang et al. 2009).

Recent publication has revealed circulating miRNAs as biomarkers for disease diagnosis and prognosis (Grasedieck et al. 2013), especially in the study of human cancer (Kosaka et al. 2013). Circulating miRNA profiling in plasma from patients with SLE has demonstrated increased levels of miR-142-3p and miR-181a, and decreased levels of miR-106a, miR-17, miR-20a, miR-203, and miR-92a (Carlsen et al. 2013). A recent report by Filkova and colleagues has suggested that miR-16 and miR-223 as novel biomarkers for the disease outcome of early RA (Filkova et al. 2013). In our hands, we observed decreased level of miR-146a and miR-155 in patients with RA, although further investigations are required in order to provide more clear explanation for these observations.

Taken together, we conclude the altered expression of miR-146a and miR-155 in Tregs from RA patients might result in an altered cytokine production pattern of these cells, and thereby contribute to the pathogenesis of the disease. Moreover, in addition to their direct role in mediating Treg function, these two miRNAs might serve as potential biomarkers for disease diagnosis and prognosis.

Bibliography

Abbas, A. K., K. M. Murphy and A. Sher (1996). "Functional diversity of helper T lymphocytes." Nature **383**(6603): 787-793.

Acosta-Rodriguez, E. V., G. Napolitani, A. Lanzavecchia and F. Sallusto (2007). "Interleukins 1beta and 6 but not transforming growth factor-beta are essential for the differentiation of interleukin 17-producing human T helper cells." Nat Immunol **8**(9): 942-949.

Aletaha, D., T. Neogi, A. J. Silman, J. Funovits, D. T. Felson, C. O. Bingham, N. S. Birnbaum, G. R. Burmester, V. P. Bykerk, M. D. Cohen, B. Combe, K. H. Costenbader, M. Dougados, P. Emery, G. Ferraccioli, J. M. W. Hazes, K. Hobbs, T. W. J. Huizinga, A. Kavanaugh, J. Kay, T. K. Kvien, T. Laing, P. Mease, H. A. Menard, L. W. Moreland, R. L. Naden, T. Pincus, J. S. Smolen, E. Stanislawska-Biernat, D. Symmons, P. P. Tak, K. S. Upchurch, J. Vencovsky, F. Wolfe and G. Hawker (2010). "2010 Rheumatoid arthritis classification criteria: an American College of Rheumatology/European League Against Rheumatism collaborative initiative." Annals of the Rheumatic Diseases **69**(9): 1580-1588.

Androulidaki, A., D. Iliopoulos, A. Arranz, C. Doxaki, S. Schworer, V. Zacharioudaki, A. N. Margioris, P. N. Tsichlis and C. Tsatsanis (2009). "The kinase Akt1 controls macrophage response to lipopolysaccharide by regulating microRNAs." Immunity **31**(2): 220-231.

Annunziato, F., L. Cosmi, F. Liotta, E. Lazzeri, R. Manetti, V. Vanini, P. Romagnani, E. Maggi and S. Romagnani (2002). "Phenotype, localization, and mechanism of suppression of CD4(+)CD25(+) human thymocytes." J Exp Med **196**(3): 379-387.

Annunziato, F. and S. Romagnani (2009). "Heterogeneity of human effector CD4(+) T cells." Arthritis Research & Therapy **11**(6).

Arnett, F. C., S. M. Edworthy, D. A. Bloch, D. J. Mcshane, J. F. Fries, N. S. Cooper, L. A. Healey, S. R. Kaplan, M. H. Liang, H. S. Luthra, T. A. Medsger, D. M. Mitchell, D. H. Neustadt, R. S. Pinals, J. G. Schaller, J. T. Sharp, R. L. Wilder and G. G. Hunder (1988). "The American-Rheumatism-Association 1987 Revised Criteria for the Classification of Rheumatoid-Arthritis." Arthritis and Rheumatism **31**(3): 315-324.

Arroyo, J. D., J. R. Chevillet, E. M. Kroh, I. K. Ruf, C. C. Pritchard, D. F. Gibson, P. S. Mitchell, C. F. Bennett, E. L. Pogosova-Agadjanyan, D. L. Stirewalt, J. F. Tait and M. Tewari (2011). "Argonaute2 complexes carry a population of circulating microRNAs independent of vesicles in human plasma." Proc Natl Acad Sci U S A **108**(12): 5003-5008.

Asseman, C., S. Mauze, M. W. Leach, R. L. Coffman and F. Powrie (1999). "An essential role for interleukin 10 in the function of regulatory T cells that inhibit intestinal inflammation." Journal of Experimental Medicine **190**(7): 995-1003.

Bartel, D. P. (2009). "MicroRNAs: target recognition and regulatory functions." Cell **136**(2): 215-233.

Bayry, J., S. Siberil, F. Triebel, D. F. Tough and S. V. Kaveri (2007). "Rescuing CD4+CD25+ regulatory T-cell functions in rheumatoid arthritis by cytokine-targeted monoclonal antibody therapy." Drug Discov Today **12**(13-14): 548-552.

Beitzinger, M. and G. Meister (2011). "Experimental identification of microRNA targets by immunoprecipitation of Argonaute protein complexes." Methods Mol Biol **732**: 153-167.

Bentwich, I., A. Avniel, Y. Karov, R. Aharonov, S. Gilad, O. Barad, A. Barzilai, P. Einat, U. Einav, E. Meiri, E. Sharon, Y. Spector and Z. Bentwich (2005). "Identification of hundreds of conserved and nonconserved human microRNAs." Nat Genet **37**(7): 766-770.

Boldin, M. P., K. D. Taganov, D. S. Rao, L. Yang, J. L. Zhao, M. Kalwani, Y. Garcia-Flores, M. Luong, A. Devrekanli, J. Xu, G. Sun, J. Tay, P. S. Linsley and D. Baltimore (2011). "miR-146a is a significant brake on autoimmunity, myeloproliferation, and cancer in mice." J Exp Med **208**(6): 1189-1201.

Bradford, M. M. (1976). "A rapid and sensitive method for the quantitation of microgram quantities of protein utilizing the principle of protein-dye binding." Anal Biochem **72**: 248-254.

Brunkow, M. E., E. W. Jeffery, K. A. Hjerrild, B. Paeper, L. B. Clark, S. A. Yasayko, J. E. Wilkinson, D. Galas, S. F. Ziegler and F. Ramsdell (2001). "Disruption of a new forkhead/winged-helix protein, scurfin, results in the fatal lymphoproliferative disorder of the scurfy mouse." Nat Genet **27**(1): 68-73.

Burkhardt, H., J. R. Kalden and H. Schulze-Koops (2001). "Chicken and egg in autoimmunity and joint inflammation." Trends Immunol **22**(6): 291-293.

Carlsen, A. L., A. J. Schetter, C. T. Nielsen, C. Lood, S. Knudsen, A. Voss, C. C. Harris, T. Hellmark, M. Segelmark, S. Jacobsen, A. A. Bengtsson and N. H. H. Heegaard (2013). "Circulating MicroRNA Expression Profiles Associated With Systemic Lupus Erythematosus." Arthritis and Rheumatism **65**(5): 1324-1334.

Cascao, R., R. A. Moura, I. Perpetuo, H. Canhao, E. Vieira-Sousa, A. F. Mourao, A. M. Rodrigues, J. Polido-Pereira, M. V. Queiroz, H. S. Rosario, M. M. Souto-Carneiro, L. Graca and J. E. Fonseca (2010). "Identification of a cytokine network sustaining neutrophil and Th17 activation in untreated early rheumatoid arthritis." Arthritis Res Ther **12**(5): R196.

Chabaud, M., T. Aarvak, P. Garnero, J. B. Natvig and P. Miossec (2001). "Potential contribution of IL-17-producing Th(1)cells to defective repair activity in joint inflammation: partial correction with Th(2)-promoting conditions." Cytokine **13**(2): 113-118.

Chan, D. V., A. K. Somani, A. B. Young, J. V. Massari, J. Ohtola, H. Sugiyama, E. Garaczi, D. Babineau, K. D. Cooper and T. S. McCormick (2011). "Signal peptide cleavage is essential for surface expression of a regulatory T cell surface protein, leucine rich repeat containing 32 (LRRC32)." BMC Biochem **12**: 27.

Chen, C. Z., L. Li, H. F. Lodish and D. P. Bartel (2004). "MicroRNAs modulate hematopoietic lineage differentiation." Science **303**(5654): 83-86.

Chim, S. S., T. K. Shing, E. C. Hung, T. Y. Leung, T. K. Lau, R. W. Chiu and Y. M. Lo (2008). "Detection and characterization of placental microRNAs in maternal plasma." Clin Chem **54**(3): 482-490.

Chong, M. M. W., J. P. Rasmussen, A. Y. Rudensky and D. R. Littman (2008). "The RNAseIII enzyme Drosha is critical in T cells for preventing lethal inflammatory disease (vol 205, pg 2005, 2008)." Journal of Experimental Medicine **205**(10): 2449-2449.

Choy, E. (2012). "Understanding the dynamics: pathways involved in the pathogenesis of rheumatoid arthritis." Rheumatology (Oxford) **51 Suppl 5**: v3-11.

Cohen, S. M., J. Brennecke and A. Stark (2006). "Denoising feedback loops by thresholding--a new role for microRNAs." Genes Dev **20**(20): 2769-2772.

Collison, L. W., C. J. Workman, T. T. Kuo, K. Boyd, Y. Wang, K. M. Vignali, R. Cross, D. Sehy, R. S. Blumberg and D. A. A. Vignali (2007). "The inhibitory cytokine IL-35 contributes to regulatory T-cell function." Nature **450**(7169): 566-U519.

Cope, A. P., H. Schulze-Koops and M. Aringer (2007). "The central role of T cells in rheumatoid arthritis." Clin Exp Rheumatol **25**(5 Suppl 46): S4-11.

Cox, J. and M. Mann (2008). "MaxQuant enables high peptide identification rates, individualized p.p.b.-range mass accuracies and proteome-wide protein quantification." Nat Biotechnol **26**(12): 1367-1372.

Crowston, J. G., M. Salmon, P. T. Khaw and A. N. Akbar (1997). "T-lymphocyte-fibroblast interactions." Biochem Soc Trans **25**(2): 529-531.

Czech, B., C. D. Malone, R. Zhou, A. Stark, C. Schlingeheyde, M. Dus, N. Perrimon, M. Kellis, J. A. Wohlschlegel, R. Sachidanandam, G. J. Hannon and J. Brennecke (2008). "An endogenous small interfering RNA pathway in Drosophila." Nature **453**(7196): 798-802.

Dahl, R., J. C. Walsh, D. Lancki, P. Laslo, S. R. Iyer, H. Singh and M. C. Simon (2003). "Regulation of macrophage and neutrophil cell fates by the PU.1:C/EBPalpha ratio and granulocyte colony-stimulating factor." Nat Immunol **4**(10): 1029-1036.

Dai, R., Y. Zhang, D. Khan, B. Heid, D. Caudell, O. Crasta and S. A. Ahmed (2010). "Identification of a common lupus disease-associated microRNA expression pattern in three different murine models of lupus." PLoS One **5**(12): e14302.

Dardalhon, V., A. Awasthi, H. Kwon, G. Galileos, W. Gao, R. A. Sobel, M. Mitsdoerffer, T. B. Strom, W. Elyaman, I. C. Ho, S. Khoury, M. Oukka and V. K. Kuchroo (2008). "IL-4 inhibits TGF-beta-induced Foxp3+ T cells and, together with TGF-beta, generates IL-9+ IL-10+ Foxp3(-) effector T cells." Nat Immunol **9**(12): 1347-1355.

Dayan, C. M. and G. H. Daniels (1996). "Chronic autoimmune thyroiditis." N Engl J Med **335**(2): 99-107.

Debets, J. M., C. J. Van der Linden, I. E. Dieteren, J. F. Leeuwenberg and W. A. Buurman (1988). "Fc-receptor cross-linking induces rapid secretion of tumor necrosis factor (cachectin) by human peripheral blood monocytes." J Immunol **141**(4): 1197-1201.

Delprete, G. F., M. Decarli, M. Ricci and S. Romagnani (1991). "Helper Activity for Immunoglobulin-Synthesis of T-Helper Type-1 (Th1) and Th2 Human T-Cell Clones - the Help of Th1 Clones Is Limited by Their Cytolytic Capacity." Journal of Experimental Medicine **174**(4): 809-813.

Dou, L., J. Li, D. Zheng, Y. Li, X. Gao, C. Xu, L. Gao, L. Wang and L. Yu (2013). "MicroRNA-142-3p inhibits cell proliferation in human acute lymphoblastic leukemia by targeting the MLL-AF4 oncogene." Mol Biol Rep.

Du, C., C. Liu, J. Kang, G. Zhao, Z. Ye, S. Huang, Z. Li, Z. Wu and G. Pei (2009). "MicroRNA miR-326 regulates TH-17 differentiation and is associated with the pathogenesis of multiple sclerosis." Nat Immunol **10**(12): 1252-1259.

Dubois, C. M., M. H. Laprise, F. Blanchette, L. E. Gentry and R. Leduc (1995). "Processing of transforming growth factor beta 1 precursor by human furin convertase." J Biol Chem **270**(18): 10618-10624.

Duhen, T., R. Geiger, D. Jarrossay, A. Lanzavecchia and F. Sallusto (2009). "Production of

interleukin 22 but not interleukin 17 by a subset of human skin-homing memory T cells." Nat Immunol **10**(8): 857-863.

Edwards, J. P., H. Fujii, A. X. Zhou, J. Creemers, D. Unutmaz and E. M. Shevach (2013). "Regulation of the expression of GARP/latent TGF-beta1 complexes on mouse T cells and their role in regulatory T cell and Th17 differentiation." J Immunol **190**(11): 5506-5515.

Ehrenstein, M. R., J. G. Evans, A. Singh, S. Moore, G. Warnes, D. A. Isenberg and C. Mauri (2004). "Compromised function of regulatory T cells in rheumatoid arthritis and reversal by anti-TNFalpha therapy." J Exp Med **200**(3): 277-285.

Eulalio, A., E. Huntzinger, T. Nishihara, J. Rehwinkel, M. Fauser and E. Izaurralde (2009). "Deadenylation is a widespread effect of miRNA regulation." RNA **15**(1): 21-32.

Feuerer, M., J. A. Hill, K. Kretschmer, H. von Boehmer, D. Mathis and C. Benoist (2010). "Genomic definition of multiple ex vivo regulatory T cell subphenotypes." Proc Natl Acad Sci U S A **107**(13): 5919-5924.

Feuerer, M., J. A. Hill, D. Mathis and C. Benoist (2009). "Foxp3+ regulatory T cells: differentiation, specification, subphenotypes." Nat Immunol **10**(7): 689-695.

Filkova, M., B. Aradi, L. Senolt, C. Ospelt, S. Vettori, H. Mann, A. Filer, K. Raza, C. D. Buckley, M. Snow, J. Vencovsky, K. Pavelka, B. A. Michel, R. E. Gay, S. Gay and A. Jungel (2013). "Association of circulating miR-223 and miR-16 with disease activity in patients with early rheumatoid arthritis." Ann Rheum Dis.

Firestein, G. S. (2003). "Evolving concepts of rheumatoid arthritis." Nature **423**(6937): 356-361.

Flores-Borja, F., E. C. Jury, C. Mauri and M. R. Ehrenstein (2008). "Defects in CTLA-4 are associated with abnormal regulatory T cell function in rheumatoid arthritis." Proc Natl Acad Sci U S A **105**(49): 19396-19401.

Fontenot, J. D., J. P. Rasmussen, L. M. Williams, J. L. Dooley, A. G. Farr and A. Y. Rudensky (2005). "Regulatory T cell lineage specification by the forkhead transcription factor foxp3." Immunity **22**(3): 329-341.

Frazer, K. A., L. Pachter, A. Poliakov, E. M. Rubin and I. Dubchak (2004). "VISTA: computational tools for comparative genomics." Nucleic Acids Res **32**(Web Server issue): W273-279.

Frey, O., A. Reichel, K. Bonhagen, L. Morawietz, U. Rauchhaus and T. Kamradt (2010). "Regulatory T cells control the transition from acute into chronic inflammation in glucose-6-phosphate isomerase-induced arthritis." Annals of the Rheumatic Diseases **69**(8): 1511-1518.

Friedman, R. C., K. K. Farh, C. B. Burge and D. P. Bartel (2009). "Most mammalian mRNAs are conserved targets of microRNAs." Genome Res **19**(1): 92-105.

Fujimoto, M., S. Serada, M. Mihara, Y. Uchiyama, H. Yoshida, N. Koike, Y. Ohsugi, T. Nishikawa, B. Ripley, A. Kimura, T. Kishimoto and T. Naka (2008). "Interleukin-6 blockade suppresses autoimmune arthritis in mice by the inhibition of inflammatory Th17 responses." Arthritis Rheum **58**(12): 3710-3719.

Garchow, B. G., O. Bartulos Encinas, Y. T. Leung, P. Y. Tsao, R. A. Eisenberg, R. Caricchio, S. Obad, A. Petri, S. Kauppinen and M. Kiriakidou (2011). "Silencing of microRNA-21 in vivo ameliorates autoimmune splenomegaly in lupus mice." EMBO Mol Med **3**(10): 605-615.

Grasedieck, S., A. Sorrentino, C. Langer, C. Buske, H. Dohner, D. Mertens and F. Kuchenbauer (2013). "Circulating microRNAs in hematological diseases: principles, challenges, and perspectives." Blood **121**(25): 4977-4984.

Gregory, R. I., T. P. Chendrimada and R. Shiekhattar (2006). "MicroRNA biogenesis: isolation and characterization of the microprocessor complex." Methods Mol Biol **342**: 33-47.

Grossman, W. J., J. W. Verbsky, W. Barchet, M. Colonna, J. P. Atkinson and T. J. Ley (2004). "Human T regulatory cells can use the perforin pathway to cause autologous target cell death." Immunity **21**(4): 589-601.

Han, G. M., N. J. O'Neil-Andersen, R. B. Zurier and D. A. Lawrence (2008). "CD4+CD25high T cell numbers are enriched in the peripheral blood of patients with rheumatoid arthritis." Cell Immunol **253**(1-2): 92-101.

Harrington, L. E., R. D. Hatton, P. R. Mangan, H. Turner, T. L. Murphy, K. M. Murphy and C. T. Weaver (2005). "Interleukin 17-producing CD4(+) effector T cells develop via a lineage distinct from the T helper type 1 and 2 lineages." Nature Immunology **6**(11): 1123-1132.

Hasuwa, H., J. Ueda, M. Ikawa and M. Okabe (2013). "MiR-200b and miR-429 Function in Mouse Ovulation and Are Essential for Female Fertility." Science.

Haupt, S., Q. Zhou, S. Herrmann, H. Schulze-Koops and A. Skapenko (under preparation). "Treg-specific GARP expression is dependent on epigenetic modifications and Foxp3."

Hoeflich, K. P. and M. Ikura (2004). "Radixin: cytoskeletal adopter and signaling protein." Int J Biochem Cell Biol **36**(11): 2131-2136.

Huang, B., J. Zhao, Z. Lei, S. Shen, D. Li, G. X. Shen, G. M. Zhang and Z. H. Feng (2009). "miR-142-3p restricts cAMP production in CD4+CD25- T cells and CD4+CD25+ TREG cells by targeting AC9 mRNA." EMBO Rep **10**(2): 180-185.

Huntzinger, E. and E. Izaurralde (2011). "Gene silencing by microRNAs: contributions of translational repression and mRNA decay." Nature Reviews Genetics **12**(2): 99-110.

Iliopoulos, D., H. A. Hirsch and K. Struhl (2009). "An epigenetic switch involving NF-kappaB, Lin28, Let-7 MicroRNA, and IL6 links inflammation to cell transformation." Cell **139**(4): 693-706.

Infante-Duarte, C., H. F. Horton, M. C. Byrne and T. Kamradt (2000). "Microbial lipopeptides induce the production of IL-17 in Th cells." Journal of Immunology **165**(11): 6107-6115.

Iyer, A., E. Zurolo, A. Prabowo, K. Fluiter, W. G. M. Spliet, P. C. van Rijen, J. A. Gorter and E. Aronica (2012). "MicroRNA-146a: A Key Regulator of Astrocyte-Mediated Inflammatory Response." Plos One **7**(9).

Kawai, T. and S. Akira (2010). "The role of pattern-recognition receptors in innate immunity: update on Toll-like receptors." Nat Immunol **11**(5): 373-384.

Kawashiri, S. Y., A. Kawakami, A. Okada, T. Koga, M. Tamai, S. Yamasaki, H. Nakamura, T. Origuchi, H. Ida and K. Eguchi (2011). "CD4+CD25(high)C127(low/-) Treg Cell Frequency from Peripheral Blood Correlates with Disease Activity in Patients with Rheumatoid Arthritis." Journal of Rheumatology **38**(12): 2517-2521.

Kelchtermans, H., L. Geboes, T. Mitera, D. Huskens, G. Leclercq and P. Matthys (2009). "Activated CD4+CD25+ regulatory T cells inhibit osteoclastogenesis and collagen-induced

arthritis." Ann Rheum Dis **68**(5): 744-750.

Kinjyo, I., T. Hanada, K. Inagaki-Ohara, H. Mori, D. Aki, M. Ohishi, H. Yoshida, M. Kubo and A. Yoshimura (2002). "SOCS1/JAB is a negative regulator of LPS-induced macrophage activation." Immunity **17**(5): 583-591.

Kohlhaas, S., O. A. Garden, C. Scudamore, M. Turner, K. Okkenhaug and E. Vigorito (2009). "Cutting edge: the Foxp3 target miR-155 contributes to the development of regulatory T cells." J Immunol **182**(5): 2578-2582.

Korn, T., E. Bettelli, M. Oukka and V. K. Kuchroo (2009). "IL-17 and Th17 Cells." Annu Rev Immunol **27**: 485-517.

Kosaka, N., Y. Yoshioka, K. Hagiwara, N. Tominaga, T. Katsuda and T. Ochiya (2013). "Trash or Treasure: extracellular microRNAs and cell-to-cell communication." Front Genet **4**: 173.

Kotake, S. and N. Kamatani (2002). "The Role of IL-17 in Joint Destruction." Drug News Perspect **15**(1): 17-23.

Kozomara, A. and S. Griffiths-Jones (2011). "miRBase: integrating microRNA annotation and deep-sequencing data." Nucleic Acids Res **39**(Database issue): D152-157.

Krek, A., D. Grun, M. N. Poy, R. Wolf, L. Rosenberg, E. J. Epstein, P. MacMenamin, I. da Piedade, K. C. Gunsalus, M. Stoffel and N. Rajewsky (2005). "Combinatorial microRNA target predictions." Nat Genet **37**(5): 495-500.

Kryuchkova, P., A. Grishin, B. Eliseev, A. Karyagina, L. Frolova and E. Alkalaeva (2013). "Two-step model of stop codon recognition by eukaryotic release factor eRF1." Nucleic Acids Res **41**(8): 4573-4586.

Kurowska-Stolarska, M., S. Alivernini, L. E. Ballantine, D. L. Asquith, N. L. Millar, D. S. Gilchrist, J. Reilly, M. Ierna, A. R. Fraser, B. Stolarski, C. McSharry, A. J. Hueber, D. Baxter, J. Hunter, S. Gay, F. Y. Liew and I. B. McInnes (2011). "MicroRNA-155 as a proinflammatory regulator in clinical and experimental arthritis." Proceedings of the National Academy of Sciences of the United States of America **108**(27): 11193-11198.

Kurowska-Stolarska, M., S. Alivernini, L. E. Ballantine, D. L. Asquith, N. L. Millar, D. S. Gilchrist, J. Reilly, M. Ierna, A. R. Fraser, B. Stolarski, C. McSharry, A. J. Hueber, D. Baxter, J. Hunter, S. Gay, F. Y. Liew and I. B. McInnes (2011). "MicroRNA-155 as a proinflammatory regulator in clinical and experimental arthritis." Proc Natl Acad Sci U S A **108**(27): 11193-11198.

Lagos-Quintana, M., R. Rauhut, W. Lendeckel and T. Tuschl (2001). "Identification of novel genes coding for small expressed RNAs." Science **294**(5543): 853-858.

Lahl, K., C. Loddenkemper, C. Drouin, J. Freyer, J. Arnason, G. Eberl, A. Hamann, H. Wagner, J. Huehn and T. Sparwasser (2007). "Selective depletion of Foxp3+ regulatory T cells induces a scurfy-like disease." J Exp Med **204**(1): 57-63.

Lawrie, C. H., S. Gal, H. M. Dunlop, B. Pushkaran, A. P. Liggins, K. Pulford, A. H. Banham, F. Pezzella, J. Boultwood, J. S. Wainscoat, C. S. Hatton and A. L. Harris (2008). "Detection of elevated levels of tumour-associated microRNAs in serum of patients with diffuse large B-cell lymphoma." Br J Haematol **141**(5): 672-675.

Lee, Y., K. Jeon, J. T. Lee, S. Kim and V. N. Kim (2002). "MicroRNA maturation: stepwise

processing and subcellular localization." EMBO J **21**(17): 4663-4670.

Lee, Y., M. Kim, J. Han, K. H. Yeom, S. Lee, S. H. Baek and V. N. Kim (2004). "MicroRNA genes are transcribed by RNA polymerase II." EMBO J **23**(20): 4051-4060.

Lee, Y. H., Y. H. Rho, S. J. Choi, J. D. Ji, G. G. Song, S. K. Nath and J. B. Harley (2007). "The PTPN22 C1858T functional polymorphism and autoimmune diseases--a meta-analysis." Rheumatology (Oxford) **46**(1): 49-56.

Leipe, J., M. Grunke, C. Dechant, C. Reindl, U. Kerzendorf, H. Schulze-Koops and A. Skapenko (2010). "Role of Th17 cells in human autoimmune arthritis." Arthritis Rheum **62**(10): 2876-2885.

Leipe, J., M. A. Schramm, M. Grunke, M. Baeuerle, C. Dechant, A. P. Nigg, M. N. Witt, V. Vielhauer, C. S. Reindl, H. Schulze-Koops and A. Skapenko (2011). "Interleukin 22 serum levels are associated with radiographic progression in rheumatoid arthritis." Ann Rheum Dis **70**(8): 1453-1457.

Leipe, J., M. A. Schramm, I. Prots, H. Schulze-Koops and A. Skapenko (2014). "Increased Th17 cell frequency and poor clinical outcome in rheumatoid arthritis are associated with a genetic variant in the IL-4R gene, rs1805010." Arthritis Rheum.

Lewis, B. P., C. B. Burge and D. P. Bartel (2005). "Conserved seed pairing, often flanked by adenosines, indicates that thousands of human genes are microRNA targets." Cell **120**(1): 15-20.

Lewis, B. P., I. H. Shih, M. W. Jones-Rhoades, D. P. Bartel and C. B. Burge (2003). "Prediction of mammalian microRNA targets." Cell **115**(7): 787-798.

Li, J., Y. Wan, Q. Guo, L. Zou, J. Zhang, Y. Fang, J. Zhang, J. Zhang, X. Fu, H. Liu, L. Lu and Y. Wu (2010). "Altered microRNA expression profile with miR-146a upregulation in CD4+ T cells from patients with rheumatoid arthritis." Arthritis Res Ther **12**(3): R81.

Li, M. O., S. Sanjabi and R. A. Flavell (2006). "Transforming growth factor-beta controls development, homeostasis, and tolerance of T cells by regulatory T cell-dependent and -independent mechanisms." Immunity **25**(3): 455-471.

Liang, D., Y. Gao, X. Lin, Z. He, Q. Zhao, Q. Deng and K. Lan (2011). "A human herpesvirus miRNA attenuates interferon signaling and contributes to maintenance of viral latency by targeting IKKepsilon." Cell Res **21**(5): 793-806.

Liston, A., L. F. Lu, D. O'Carroll, A. Tarakhovsky and A. Y. Rudensky (2008). "Dicer-dependent microRNA pathway safeguards regulatory T cell function." J Exp Med **205**(9): 1993-2004.

Locksley, R. M. (2009). "Nine lives: plasticity among T helper cell subsets." J Exp Med **206**(8): 1643-1646.

Lu, L. F., M. P. Boldin, A. Chaudhry, L. L. Lin, K. D. Taganov, T. Hanada, A. Yoshimura, D. Baltimore and A. Y. Rudensky (2010). "Function of miR-146a in controlling Treg cell-mediated regulation of Th1 responses." Cell **142**(6): 914-929.

Lu, L. F., M. P. Boldin, A. Chaudhry, L. L. Lin, K. D. Taganov, T. Hanada, A. Yoshimura, D. Baltimore and A. Y. Rudensky (2010). "Function of miR-146a in Controlling Treg Cell-Mediated Regulation of Th1 Responses." Cell **142**(6): 914-929.

Lund, E. and J. E. Dahlberg (2006). "Substrate selectivity of exportin 5 and Dicer in the

biogenesis of microRNAs." Cold Spring Harb Symp Quant Biol **71**: 59-66.

Luo, X., W. Yang, D. Q. Ye, H. Cui, Y. Zhang, N. Hirankarn, X. Qian, Y. Tang, Y. L. Lau, N. de Vries, P. P. Tak, B. P. Tsao and N. Shen (2011). "A functional variant in microRNA-146a promoter modulates its expression and confers disease risk for systemic lupus erythematosus." PLoS Genet **7**(6): e1002128.

Lv, M., X. Zhang, H. Jia, D. Li, B. Zhang, H. Zhang, M. Hong, T. Jiang, Q. Jiang, J. Lu, X. Huang and B. Huang (2012). "An oncogenic role of miR-142-3p in human T-cell acute lymphoblastic leukemia (T-ALL) by targeting glucocorticoid receptor-alpha and cAMP/PKA pathways." Leukemia **26**(4): 769-777.

Ma, X., L. E. Becker Buscaglia, J. R. Barker and Y. Li (2011). "MicroRNAs in NF-kappaB signaling." J Mol Cell Biol **3**(3): 159-166.

MacGregor, A. J., H. Snieder, A. S. Rigby, M. Koskenvuo, J. Kaprio, K. Aho and A. J. Silman (2000). "Characterizing the quantitative genetic contribution to rheumatoid arthritis using data from twins." Arthritis Rheum **43**(1): 30-37.

Majithia, V. and S. A. Geraci (2007). "Rheumatoid arthritis: diagnosis and management." Am J Med **120**(11): 936-939.

Maragkakis, M., P. Alexiou, G. L. Papadopoulos, M. Reczko, T. Dalamagas, G. Giannopoulos, G. Goumas, E. Koukis, K. Kourtis, V. A. Simossis, P. Sethupathy, T. Vergoulis, N. Koziris, T. Sellis, P. Tsanakas and A. G. Hatzigeorgiou (2009). "Accurate microRNA target prediction correlates with protein repression levels." BMC Bioinformatics **10**: 295.

Matsuki, F., J. Saegusa, Y. Miyamoto, K. Misaki, Y. Miura, M. Kurosaka, S. Kumagai and A. Morinobu (2013). "CD45RA−Foxp3high activated/effector regulatory T cells in the CCR7+CD45RA–CD27+CD28+ central memory subset are decreased in peripheral blood from patients with rheumatoid arthritis." Biochemical and Biophysical Research Communications(0).

McInnes, I. B. and G. Schett (2007). "Cytokines in the pathogenesis of rheumatoid arthritis." Nat Rev Immunol **7**(6): 429-442.

Meier, J., V. Hovestadt, M. Zapatka, A. Pscherer, P. Lichter and M. Seiffert (2013). "Genome-wide identification of translationally inhibited and degraded miR-155 targets using RNA-interacting protein-IP." RNA Biol **10**(6): 1018-1030.

Meister, G., M. Landthaler, A. Patkaniowska, Y. Dorsett, G. Teng and T. Tuschl (2004). "Human Argonaute2 mediates RNA cleavage targeted by miRNAs and siRNAs." Mol Cell **15**(2): 185-197.

Miyara, M., Y. Yoshioka, A. Kitoh, T. Shima, K. Wing, A. Niwa, C. Parizot, C. Taflin, T. Heike, D. Valeyre, A. Mathian, T. Nakahata, T. Yamaguchi, T. Nomura, M. Ono, Z. Amoura, G. Gorochov and S. Sakaguchi (2009). "Functional Delineation and Differentiation Dynamics of Human CD4+ T Cells Expressing the FoxP3 Transcription Factor." Immunity **30**(6): 899-911.

Mosmann, T. R., H. Cherwinski, M. Bond and R. C. Coffman (1986). "Definition of 2 Types of Murine Helper Clone by Lymphokine Activity Profiles, Protein-Biosynthesis and B-Cell Helper Function." Journal of Cellular Biochemistry: 89-89.

Mourelatos, Z., J. Dostie, S. Paushkin, A. Sharma, B. Charroux, L. Abel, J. Rappsilber, M.

Mann and G. Dreyfuss (2002). "miRNPs: a novel class of ribonucleoproteins containing numerous microRNAs." Genes Dev **16**(6): 720-728.

Murchison, E. P. and G. J. Hannon (2004). "miRNAs on the move: miRNA biogenesis and the RNAi machinery." Curr Opin Cell Biol **16**(3): 223-229.

Murphy, K. P., C. A. Janeway, P. Travers, M. Walport, A. Mowat and C. T. Weaver (2012). Janeway's Immunobiology. London, Garland Science.

Nakae, S., A. Nambu, K. Sudo and Y. Iwakura (2003). "Suppression of immune induction of collagen-induced arthritis in IL-17-deficient mice." J Immunol **171**(11): 6173-6177.

Nakasa, T., S. Miyaki, A. Okubo, M. Hashimoto, K. Nishida, M. Ochi and H. Asahara (2008). "Expression of microRNA-146 in rheumatoid arthritis synovial tissue." Arthritis Rheum **58**(5): 1284-1292.

Nakasa, T., H. Shibuya, Y. Nagata, T. Niimoto and M. Ochi (2011). "The inhibitory effect of microRNA-146a expression on bone destruction in collagen-induced arthritis." Arthritis Rheum **63**(6): 1582-1590.

Nguyen, L. T., J. Jacobs, D. Mathis and C. Benoist (2007). "Where FoxP3-dependent regulatory T cells impinge on the development of inflammatory arthritis." Arthritis Rheum **56**(2): 509-520.

Nowak, E. C., C. T. Weaver, H. Turner, S. Begum-Haque, B. Becher, B. Schreiner, A. J. Coyle, L. H. Kasper and R. J. Noelle (2009). "IL-9 as a mediator of Th17-driven inflammatory disease." J Exp Med **206**(8): 1653-1660.

O'Connell, R. M., A. A. Chaudhuri, D. S. Rao and D. Baltimore (2009). "Inositol phosphatase SHIP1 is a primary target of miR-155." Proc Natl Acad Sci U S A **106**(17): 7113-7118.

O'Connell, R. M., D. Kahn, W. S. Gibson, J. L. Round, R. L. Scholz, A. A. Chaudhuri, M. E. Kahn, D. S. Rao and D. Baltimore (2010). "MicroRNA-155 promotes autoimmune inflammation by enhancing inflammatory T cell development." Immunity **33**(4): 607-619.

O'Connell, R. M., D. S. Rao and D. Baltimore (2012). "microRNA regulation of inflammatory responses." Annu Rev Immunol **30**: 295-312.

O'Neill, L. A., F. J. Sheedy and C. E. McCoy (2011). "MicroRNAs: the fine-tuners of Toll-like receptor signalling." Nat Rev Immunol **11**(3): 163-175.

Oertli, M., D. B. Engler, E. Kohler, M. Koch, T. F. Meyer and A. Muller (2011). "MicroRNA-155 Is Essential for the T Cell-Mediated Control of Helicobacter pylori Infection and for the Induction of Chronic Gastritis and Colitis." Journal of Immunology **187**(7): 3578-3586.

Oertli, M., D. B. Engler, E. Kohler, M. Koch, T. F. Meyer and A. Muller (2011). "MicroRNA-155 is essential for the T cell-mediated control of Helicobacter pylori infection and for the induction of chronic Gastritis and Colitis." J Immunol **187**(7): 3578-3586.

Ohkura, N., Y. Kitagawa and S. Sakaguchi (2013). "Development and maintenance of regulatory T cells." Immunity **38**(3): 414-423.

Ollendorff, V., T. Noguchi, O. deLapeyriere and D. Birnbaum (1994). "The GARP gene encodes a new member of the family of leucine-rich repeat-containing proteins." Cell Growth Differ **5**(2): 213-219.

Ollendorff, V., P. Szepetowski, M. G. Mattei, P. Gaudray and D. Birnbaum (1992). "New gene in the homologous human 11q13-q14 and mouse 7F chromosomal regions." Mamm Genome **2**(3): 195-200.

Orozco, G., B. Rueda and J. Martin (2006). "Genetic basis of rheumatoid arthritis." Biomed Pharmacother **60**(10): 656-662.

Pandiyan, P., L. Zheng, S. Ishihara, J. Reed and M. J. Lenardo (2007). "CD4+CD25+Foxp3+ regulatory T cells induce cytokine deprivation-mediated apoptosis of effector CD4+ T cells." Nat Immunol **8**(12): 1353-1362.

Park, H., Z. X. Li, X. O. Yang, S. H. Chang, R. Nurieva, Y. H. Wang, Y. Wang, L. Hood, Z. Zhu, Q. Tian and C. Dong (2005). "A distinct lineage of CD4 T cells regulates tissue inflammation by producing interleukin 17." Nature Immunology **6**(11): 1133-1141.

Patil, N. S., A. Pashine, M. P. Belmares, W. Liu, B. Kaneshiro, J. Rabinowitz, H. McConnell and E. D. Mellins (2001). "Rheumatoid arthritis (RA)-associated HLA-DR alleles form less stable complexes with class II-associated invariant chain peptide than non-RA-associated HLA-DR alleles." J Immunol **167**(12): 7157-7168.

Pauley, K. M., M. Satoh, A. L. Chan, M. R. Bubb, W. H. Reeves and E. K. Chan (2008). "Upregulated miR-146a expression in peripheral blood mononuclear cells from rheumatoid arthritis patients." Arthritis Res Ther **10**(4): R101.

Pesce, B., L. Soto, F. Sabugo, P. Wurmann, M. Cuchacovich, M. N. Lopez, P. H. Sotelo, M. C. Molina, J. C. Aguillon and D. Catalan (2013). "Effect of interleukin-6 receptor blockade on the balance between regulatory T cells and T helper type 17 cells in rheumatoid arthritis patients." Clinical and Experimental Immunology **171**(3): 237-242.

Pesu, M., W. T. Watford, L. Wei, L. Xu, I. Fuss, W. Strober, J. Andersson, E. M. Shevach, M. Quezado, N. Bouladoux, A. Roebroek, Y. Belkaid, J. Creemers and J. J. O'Shea (2008). "T-cell-expressed proprotein convertase furin is essential for maintenance of peripheral immune tolerance." Nature **455**(7210): 246-250.

Plenge, R. M., L. Padyukov, E. F. Remmers, S. Purcell, A. T. Lee, E. W. Karlson, F. Wolfe, D. L. Kastner, L. Alfredsson, D. Altshuler, P. K. Gregersen, L. Klareskog and J. D. Rioux (2005). "Replication of putative candidate-gene associations with rheumatoid arthritis in >4,000 samples from North America and Sweden: association of susceptibility with PTPN22, CTLA4, and PADI4." Am J Hum Genet **77**(6): 1044-1060.

Pratt, A. J. and I. J. MacRae (2009). "The RNA-induced silencing complex: a versatile gene-silencing machine." J Biol Chem **284**(27): 17897-17901.

Prevoo, M. L., M. A. van 't Hof, H. H. Kuper, M. A. van Leeuwen, L. B. van de Putte and P. L. van Riel (1995). "Modified disease activity scores that include twenty-eight-joint counts. Development and validation in a prospective longitudinal study of patients with rheumatoid arthritis." Arthritis Rheum **38**(1): 44-48.

Probst-Kepper, M., R. Balling and J. Buer (2010). "FOXP3: required but not sufficient. the role of GARP (LRRC32) as a safeguard of the regulatory phenotype." Curr Mol Med **10**(6): 533-539.

Probst-Kepper, M., R. Geffers, A. Kroger, N. Viegas, C. Erck, H. J. Hecht, H. Lunsdorf, R. Roubin, D. Moharregh-Khiabani, K. Wagner, F. Ocklenburg, A. Jeron, H. Garritsen, T. P. Arstila, E. Kekalainen, R. Balling, H. Hauser, J. Buer and S. Weiss (2009). "GARP: a key receptor controlling FOXP3 in human regulatory T cells." J Cell Mol Med **13**(9B): 3343-3357.

Prots, I., A. Skapenko, J. Wendler, S. Mattyasovszky, C. L. Yone, B. Spriewald, H. Burkhardt, R. Rau, J. R. Kalden, P. E. Lipsky and H. Schulze-Koops (2006). "Association of the IL4R single-nucleotide polymorphism I50V with rapidly erosive rheumatoid arthritis." Arthritis Rheum **54**(5): 1491-1500.

Rahman, A. and D. A. Isenberg (2008). "Systemic lupus erythematosus." N Engl J Med **358**(9): 929-939.

Ramming, A., D. Druzd, J. Leipe, H. Schulze-Koops and A. Skapenko (2012). "Maturation-related histone modifications in the PU.1 promoter regulate Th9-cell development." Blood **119**(20): 4665-4674.

Rana, T. M. (2007). "Illuminating the silence: understanding the structure and function of small RNAs." Nat Rev Mol Cell Biol **8**(1): 23-36.

Rodriguez, A., S. Griffiths-Jones, J. L. Ashurst and A. Bradley (2004). "Identification of mammalian microRNA host genes and transcription units." Genome Res **14**(10A): 1902-1910.

Rodriguez, A., E. Vigorito, S. Clare, M. V. Warren, P. Couttet, D. R. Soond, S. van Dongen, R. J. Grocock, P. P. Das, E. A. Miska, D. Vetrie, K. Okkenhaug, A. J. Enright, G. Dougan, M. Turner and A. Bradley (2007). "Requirement of bic/microRNA-155 for normal immune function." Science **316**(5824): 608-611.

Rodriguez-Pinto, D. (2005). "B cells as antigen presenting cells." Cell Immunol **238**(2): 67-75.

Romagnani, S. (2006). "Regulation of the T cell response." Clinical and Experimental Allergy **36**(11): 1357-1366.

Rosenberg, S. A. and P. E. Lipsky (1979). "Monocyte Dependence of Pokeweed Mitogen-Induced Differentiation of Immunoglobulin-Secreting Cells from Human Peripheral-Blood Mononuclear-Cells." Journal of Immunology **122**(3): 926-931.

Sakaguchi, S., N. Sakaguchi, M. Asano, M. Itoh and M. Toda (1995). "Immunologic self-tolerance maintained by activated T cells expressing IL-2 receptor alpha-chains (CD25). Breakdown of a single mechanism of self-tolerance causes various autoimmune diseases." J Immunol **155**(3): 1151-1164.

Schmidt, A., N. Oberle and P. H. Krammer (2012). "Molecular mechanisms of Treg-mediated T cell suppression." Frontiers in Immunology **3**.

Schulte, L. N., A. J. Westermann and J. Vogel (2013). "Differential activation and functional specialization of miR-146 and miR-155 in innate immune sensing." Nucleic Acids Research **41**(1): 542-553.

Schulze, W. X. and M. Mann (2004). "A novel proteomic screen for peptide-protein interactions." J Biol Chem **279**(11): 10756-10764.

Schulze-Koops, H. and J. R. Kalden (2001). "The balance of Th1/Th2 cytokines in rheumatoid arthritis." Best Pract Res Clin Rheumatol **15**(5): 677-691.

Schwartz, R. H. (1990). "A Cell-Culture Model for Lymphocyte-T Clonal Anergy." Science **248**(4961): 1349-1356.

Schwartz, R. H. (1992). "Costimulation of Lymphocytes-T - the Role of Cd28, Ctla-4, and B7/Bb1 in Interleukin-2 Production and Immunotherapy." Cell **71**(7): 1065-1068.

Seddiki, N., B. Santner-Nanan, J. Martinson, J. Zaunders, S. Sasson, A. Landay, M. Solomon,

W. Selby, S. I. Alexander, R. Nanan, A. Kelleher and B. Fazekas de St Groth (2006). "Expression of interleukin (IL)-2 and IL-7 receptors discriminates between human regulatory and activated T cells." J Exp Med **203**(7): 1693-1700.

Shabalina, S. A., A. Y. Ogurtsov, D. J. Lipman and A. S. Kondrashov (2003). "Patterns in interspecies similarity correlate with nucleotide composition in mammalian 3'UTRs." Nucleic Acids Res **31**(18): 5433-5439.

Sheedy, F. J., E. Palsson-McDermott, E. J. Hennessy, C. Martin, J. J. O'Leary, Q. Ruan, D. S. Johnson, Y. Chen and L. A. O'Neill (2010). "Negative regulation of TLR4 via targeting of the proinflammatory tumor suppressor PDCD4 by the microRNA miR-21." Nat Immunol **11**(2): 141-147.

Shimizu, J., S. Yamazaki, T. Takahashi, Y. Ishida and S. Sakaguchi (2002). "Stimulation of CD25(+)CD4(+) regulatory T cells through GITR breaks immunological self-tolerance." Nat Immunol **3**(2): 135-142.

Skapenko, A., J. Leipe, U. Niesner, K. Devriendt, R. Beetz, A. Radbruch, J. R. Kalden, P. E. Lipsky and H. Schulze-Koops (2004). "GATA-3 in human T cell helper type 2 development." J Exp Med **199**(3): 423-428.

Skapenko, A., P. E. Lipsky, H. G. Kraetsch, J. R. Kalden and H. Schulze-Koops (2001). "Antigen-independent Th2 cell differentiation by stimulation of CD28: regulation via IL-4 gene expression and mitogen-activated protein kinase activation." J Immunol **166**(7): 4283-4292.

Skapenko, A., J. Wendler, P. E. Lipsky, J. R. Kalden and H. Schulze-Koops (1999). "Altered memory T cell differentiation in patients with early rheumatoid arthritis." J Immunol **163**(1): 491-499.

Smith, S. H., M. H. Brown, D. Rowe, R. E. Callard and P. C. L. Beverley (1986). "Functional Subsets of Human Helper-Inducer Cells Defined by a New Monoclonal-Antibody, Uchl1." Immunology **58**(1): 63-70.

Smolen, J. S., D. Aletaha, M. Koeller, M. H. Weisman and P. Emery (2007). "New therapies for treatment of rheumatoid arthritis." Lancet **370**(9602): 1861-1874.

Sonda, N., F. Simonato, E. Peranzoni, B. Cali, S. Bortoluzzi, A. Bisognin, E. Wang, F. M. Marincola, L. Naldini, B. Gentner, C. Trautwein, S. D. Sackett, P. Zanovello, B. Molon and V. Bronte (2013). "miR-142-3p prevents macrophage differentiation during cancer-induced myelopoiesis." Immunity **38**(6): 1236-1249.

Stanczyk, J., D. M. Pedrioli, F. Brentano, O. Sanchez-Pernaute, C. Kolling, R. E. Gay, M. Detmar, S. Gay and D. Kyburz (2008). "Altered expression of MicroRNA in synovial fibroblasts and synovial tissue in rheumatoid arthritis." Arthritis Rheum **58**(4): 1001-1009.

Stark, A., J. Brennecke, N. Bushati, R. B. Russell and S. M. Cohen (2005). "Animal MicroRNAs confer robustness to gene expression and have a significant impact on 3'UTR evolution." Cell **123**(6): 1133-1146.

Staudt, V., E. Bothur, M. Klein, K. Lingnau, S. Reuter, N. Grebe, B. Gerlitzki, M. Hoffmann, A. Ulges, C. Taube, N. Dehzad, M. Becker, M. Stassen, A. Steinborn, M. Lohoff, H. Schild, E. Schmitt and T. Bopp (2010). "Interferon-regulatory factor 4 is essential for the developmental program of T helper 9 cells." Immunity **33**(2): 192-202.

Stittrich, A. B., C. Haftmann, E. Sgouroudis, A. A. Kuhl, A. N. Hegazy, I. Panse, R. Riedel,

M. Flossdorf, J. Dong, F. Fuhrmann, G. A. Heinz, Z. Fang, N. Li, U. Bissels, F. Hatam, A. Jahn, B. Hammoud, M. Matz, F. M. Schulze, R. Baumgrass, A. Bosio, H. J. Mollenkopf, J. Grun, A. Thiel, W. Chen, T. Hofer, C. Loddenkemper, M. Lohning, H. D. Chang, N. Rajewsky, A. Radbruch and M. F. Mashreghi (2010). "The microRNA miR-182 is induced by IL-2 and promotes clonal expansion of activated helper T lymphocytes." Nat Immunol **11**(11): 1057-1062.

Stockis, J., D. Colau, P. G. Coulie and S. Lucas (2009). "Membrane protein GARP is a receptor for latent TGF-beta on the surface of activated human Treg." Eur J Immunol **39**(12): 3315-3322.

Stockis, J., W. Fink, V. Francois, T. Connerotte, C. de Smet, L. Knoops, P. van der Bruggen, T. Boon, P. G. Coulie and S. Lucas (2009). "Comparison of stable human Treg and Th clones by transcriptional profiling." Eur J Immunol **39**(3): 869-882.

Sun, Y., S. Varambally, C. A. Maher, Q. Cao, P. Chockley, T. Toubai, C. Malter, E. Nieves, I. Tawara, Y. Wang, P. A. Ward, A. Chinnaiyan and P. Reddy (2011). "Targeting of microRNA-142-3p in dendritic cells regulates endotoxin-induced mortality." Blood **117**(23): 6172-6183.

Tang, Y., X. Luo, H. Cui, X. Ni, M. Yuan, Y. Guo, X. Huang, H. Zhou, N. de Vries, P. P. Tak, S. Chen and N. Shen (2009). "MicroRNA-146A contributes to abnormal activation of the type I interferon pathway in human lupus by targeting the key signaling proteins." Arthritis Rheum **60**(4): 1065-1075.

Thai, T. H., D. P. Calado, S. Casola, K. M. Ansel, C. Xiao, Y. Xue, A. Murphy, D. Frendewey, D. Valenzuela, J. L. Kutok, M. Schmidt-Supprian, N. Rajewsky, G. Yancopoulos, A. Rao and K. Rajewsky (2007). "Regulation of the germinal center response by microRNA-155." Science **316**(5824): 604-608.

Thornton, A. M. and E. M. Shevach (1998). "CD4(+)CD25(+) immunoregulatory T cells suppress polyclonal T cell activation in vitro by inhibiting interleukin 2 production." Journal of Experimental Medicine **188**(2): 287-296.

Tili, E., J. J. Michaille, A. Cimino, S. Costinean, C. D. Dumitru, B. Adair, M. Fabbri, H. Alder, C. G. Liu, G. A. Calin and C. M. Croce (2007). "Modulation of miR-155 and miR-125b levels following lipopolysaccharide/TNF-alpha stimulation and their possible roles in regulating the response to endotoxin shock." J Immunol **179**(8): 5082-5089.

Townsend, J. M., G. P. Fallon, J. D. Matthews, P. Smith, E. H. Jolin and N. A. McKenzie (2000). "IL-9-deficient mice establish fundamental roles for IL-9 in pulmonary mastocytosis and goblet cell hyperplasia but not T cell development." Immunity **13**(4): 573-583.

Tran, D. Q., J. Andersson, R. Wang, H. Ramsey, D. Unutmaz and E. M. Shevach (2009). "GARP (LRRC32) is essential for the surface expression of latent TGF-beta on platelets and activated FOXP3+ regulatory T cells." Proc Natl Acad Sci U S A **106**(32): 13445-13450.

Tran, D. Q., H. Ramsey and E. M. Shevach (2007). "Induction of FOXP3 expression in naive human CD4+FOXP3 T cells by T-cell receptor stimulation is transforming growth factor-beta dependent but does not confer a regulatory phenotype." Blood **110**(8): 2983-2990.

Trifari, S., C. D. Kaplan, E. H. Tran, N. K. Crellin and H. Spits (2009). "Identification of a human helper T cell population that has abundant production of interleukin 22 and is distinct from T(H)-17, T(H)1 and T(H)2 cells." Nat Immunol **10**(8): 864-871.

Valadi, H., K. Ekstrom, A. Bossios, M. Sjostrand, J. J. Lee and J. O. Lotvall (2007).

"Exosome-mediated transfer of mRNAs and microRNAs is a novel mechanism of genetic exchange between cells." Nat Cell Biol **9**(6): 654-659.

Valencia, X., G. Stephens, R. Goldbach-Mansky, M. Wilson, E. M. Shevach and P. E. Lipsky (2006). "TNF downmodulates the function of human CD4+CD25hi T-regulatory cells." Blood **108**(1): 253-261.

van Amelsfort, J. M., J. A. van Roon, M. Noordegraaf, K. M. Jacobs, J. W. Bijlsma, F. P. Lafeber and L. S. Taams (2007). "Proinflammatory mediator-induced reversal of CD4+,CD25+ regulatory T cell-mediated suppression in rheumatoid arthritis." Arthritis Rheum **56**(3): 732-742.

van der Graaff, W. L., A. P. Prins, T. M. Niers, B. A. Dijkmans and R. A. van Lier (1999). "Quantitation of interferon gamma- and interleukin-4-producing T cells in synovial fluid and peripheral blood of arthritis patients." Rheumatology (Oxford) **38**(3): 214-220.

Vang, T., M. Congia, M. D. Macis, L. Musumeci, V. Orru, P. Zavattari, K. Nika, L. Tautz, K. Tasken, F. Cucca, T. Mustelin and N. Bottini (2005). "Autoimmune-associated lymphoid tyrosine phosphatase is a gain-of-function variant." Nat Genet **37**(12): 1317-1319.

Veldhoen, M., C. Uyttenhove, J. van Snick, H. Helmby, A. Westendorf, J. Buer, B. Martin, C. Wilhelm and B. Stockinger (2008). "Transforming growth factor-beta 'reprograms' the differentiation of T helper 2 cells and promotes an interleukin 9-producing subset." Nat Immunol **9**(12): 1341-1346.

Vickers, K. C., B. T. Palmisano, B. M. Shoucri, R. D. Shamburek and A. T. Remaley (2011). "MicroRNAs are transported in plasma and delivered to recipient cells by high-density lipoproteins." Nat Cell Biol **13**(4): 423-433.

Vignali, D. A., L. W. Collison and C. J. Workman (2008). "How regulatory T cells work." Nat Rev Immunol **8**(7): 523-532.

Volpe, E., N. Servant, R. Zollinger, S. I. Bogiatzi, P. Hupe, E. Barillot and V. Soumelis (2008). "A critical function for transforming growth factor-beta, interleukin 23 and proinflammatory cytokines in driving and modulating human T(H)-17 responses." Nat Immunol **9**(6): 650-657.

Wan, Y. Y. and R. A. Flavell (2008). "TGF-beta and regulatory T cell in immunity and autoimmunity." J Clin Immunol **28**(6): 647-659.

Wang, G., B. C. H. Kwan, F. M. M. Lai, K. M. Chow, P. K. T. Li and C. C. Szeto (2011). "Elevated levels of miR-146a and miR-155 in kidney biopsy and urine from patients with IgA nephropathy." Disease Markers **30**(4): 171-179.

Wang, R., L. Kozhaya, F. Mercer, A. Khaitan, H. Fujii and D. Unutmaz (2009). "Expression of GARP selectively identifies activated human FOXP3+ regulatory T cells." Proc Natl Acad Sci U S A **106**(32): 13439-13444.

Wang, R., Q. Wan, L. Kozhaya, H. Fujii and D. Unutmaz (2008). "Identification of a regulatory T cell specific cell surface molecule that mediates suppressive signals and induces Foxp3 expression." PLoS One **3**(7): e2705.

Wang, R., J. Zhu, X. Dong, M. Shi, C. Lu and T. A. Springer (2012). "GARP regulates the bioavailability and activation of TGFbeta." Mol Biol Cell **23**(6): 1129-1139.

Wang, Y., J. Gu, J. A. Roth, M. A. Hildebrandt, S. M. Lippman, Y. Ye, J. D. Minna and X.

Wu (2013). "Pathway-based serum microRNA profiling and survival in patients with advanced stage non-small cell lung cancer." Cancer Res **73**(15): 4801-4809.

Williams, A. E. (2008). "Functional aspects of animal microRNAs." Cell Mol Life Sci **65**(4): 545-562.

Wilson, N. J., K. Boniface, J. R. Chan, B. S. McKenzie, W. M. Blumenschein, J. D. Mattson, B. Basham, K. Smith, T. Chen, F. Morel, J. C. Lecron, R. A. Kastelein, D. J. Cua, T. K. McClanahan, E. P. Bowman and R. de Waal Malefyt (2007). "Development, cytokine profile and function of human interleukin 17-producing helper T cells." Nat Immunol **8**(9): 950-957.

Winter, J., S. Jung, S. Keller, R. I. Gregory and S. Diederichs (2009). "Many roads to maturity: microRNA biogenesis pathways and their regulation." Nat Cell Biol **11**(3): 228-234.

Wong, L. E., Y. Li, S. Pillay, L. Frolova and K. Pervushin (2012). "Selectivity of stop codon recognition in translation termination is modulated by multiple conformations of GTS loop in eRF1." Nucleic Acids Res **40**(12): 5751-5765.

Xu, Y., H. Ma, H. Yu, Z. Liu, L. E. Wang, D. Tan, R. Muddasani, V. Lu, J. A. Ajani, Y. Wang and Q. Wei (2013). "The miR-184 binding-site rs8126 T>C polymorphism in TNFAIP2 is associated with risk of gastric cancer." PLoS One **8**(5): e64973.

Yago, T., Y. Nanke, M. Kawamoto, T. Furuya, T. Kobashigawa, N. Kamatani and S. Kotake (2007). "IL-23 induces human osteoclastogenesis via IL-17 in vitro, and anti-IL-23 antibody attenuates collagen-induced arthritis in rats." Arthritis Res Ther **9**(5): R96.

Yang, L., D. E. Anderson, C. Baecher-Allan, W. D. Hastings, E. Bettelli, M. Oukka, V. K. Kuchroo and D. A. Hafler (2008). "IL-21 and TGF-beta are required for differentiation of human T(H)17 cells." Nature **454**(7202): 350-352.

Ye, Q., X. Zhao, K. Xu, Q. Li, J. Cheng, Y. Gao, J. Du, H. Shi and L. Zhou (2013). "Polymorphisms in lipid metabolism related miRNA binding sites and risk of metabolic syndrome." Gene **528**(2): 132-138.

Zenewicz, L. A., G. D. Yancopoulos, D. M. Valenzuela, A. J. Murphy, M. Karow and R. A. Flavell (2007). "Interleukin-22 but not interleukin-17 provides protection to hepatocytes during acute liver inflammation." Immunity **27**(4): 647-659.

Zernecke, A., K. Bidzhekov, H. Noels, E. Shagdarsuren, L. Gan, B. Denecke, M. Hristov, T. Koppel, M. N. Jahantigh, E. Lutgens, S. Wang, E. N. Olson, A. Schober and C. Weber (2009). "Delivery of microRNA-126 by apoptotic bodies induces CXCL12-dependent vascular protection." Sci Signal **2**(100): ra81.

Zhao, J. L., D. S. Rao, M. P. Boldin, K. D. Taganov, R. M. O'Connell and D. Baltimore (2011). "NF-kappaB dysregulation in microRNA-146a-deficient mice drives the development of myeloid malignancies." Proc Natl Acad Sci U S A **108**(22): 9184-9189.

Acknowledgements

I would like to acknowledge Prof. Dr. Hendrik Schulze-Koops for giving me the chance to perform my PhD thesis in Germany, for the support and guidance through the whole project and for the nice working conditions with the chance to participate in national and international scientific meetings.

I am grateful to PD Dr. Alla Skapenko for supervising me, for providing me with excellent scientific and tenchnical guidance, for the helpful revision of my dissertation and the manuscripts and for encouraging me to become a scientific researcher.

I thank Prof. Dr. Stefen Endres and Grako 1202 for providing the financial support, PD Dr. Susanne Krauss-Etschmann and PD Dr. Robert Besch to help me to coordinate a nice life with science. My special thanks to Prof. Dr. Gerhard Metze and his wife Dr. Yao Lin for their generous help.

I am very grateful to all blood donors for providing me research materials. Thanks to the nurses (especially Christine Strasser) and all colleagues from the Division of Rheumatology and Clinical Immunology in Munich for helping me to get patient samples.

I would like to thank Sonja Haupt and Johannes Kreuzer for the helpful discussions and for the generation of excellent data, which led to the final publication of these data.

I am grateful to the present and past lab members, first of all to Dr. Iryna Prots and Dr. Andreas Ramming for their friendship and their support; to Dr. Jan Leipe for all the nice discussions; and to my soccer group- Andreas, Clemens, Lena and Markus. I am also thankful to Christine Schnabel, Wenke Barkey and Nicole Kirsch for the expert technical assistance, especially Christine! Thanks to all colleagues for your help and for the nice working atmosphere: Alma Markl, Andreas Ramming, Andriy Samokhin, Clemens Küpper, Christine Schnabel, Elfried Kilger (especially for her kind help in dealing with administration), Fausto Pirronello, Iryna Prots, Jan Leipe, Johannes Kreuzer, Katja Thümmler, Lena Vockentanz, Margarete Wüllner, Markus Schramm, Nicole Kirsch, Simon Hermann, Sonja Haupt and Wenke Barkey.

My special thanks to my best friend Clemens Küpper for his precious friendship, his help in reviewing this dissertation and his encouragement in learning German. I am grateful to him

and his familly for never getting annoyed to answer all of our stupid questions. I thank Beibei Cao (**曹北北**), Moli Wan (**万茉莉**) and Zhixin Liu (**刘志鑫**) for their valuable friendship and for all the holiday time we spent together.

I want to thank especially my husband Shunting Cao for his love, his encouragement, his patience and tolerance, without whom I would have never succeeded in performing this PhD. And my sincerest thanks to my parents and my relatives for their permanent support, encouragement and affection.

感谢我的顺艇， 我的父母和我的亲人们， 感谢你们长久以来的爱、包容、 支持和鼓励。